

UNIVERSITY OF OKLAHOMA
GRADUATE COLLEGE

DISTRIBUTED ENERGY FEEDBACK CONTROL FOR DEMAND RESPONSE
OPERATIONS IN COMMERCIAL HVAC SYSTEMS

A THESIS

SUBMITTED TO THE GRADUATE FACULTY

in partial fulfillment of the requirements for the

Degree of

MASTER OF SCIENCE

By
Rodney Hurt
Norman, Oklahoma
2021

DISTRIBUTED ENERGY FEEDBACK CONTROL FOR DEMAND RESPONSE
OPERATIONS IN COMMERCIAL HVAC SYSTEMS

A THESIS APPROVED FOR THE
SCHOOL OF AEROSPACE AND MECHANICAL ENGINEERING

BY THE COMMITTEE CONSISTING OF

Dr. Li Song, Chair

Dr. Jie Cai

Dr. Hamidreza Shabgard

© Copyright by Rodney Hurt 2021
All Rights Reserved.

Acknowledgements

Many people have helped me throughout my master's education journey that I would like to acknowledge. First, I would like to thank Professor Li Song for mentoring and teaching me through this process. She has spent countless hours helping me since I joined the lab in 2019. I've been pushed to grow my technical skills and knowledge and to grow as a person. I've been given the opportunity to be a part of and learn from multiple research projects. She even encouraged me to be a teaching assistant which is something that I never thought I would do. I would not have made it this far in my education without her support.

I would also like to thank Professor Farrokh Mistree. He has mentored me in multiple courses and encouraged me to join the Graduate Student Community. I was eventually nominated as the Co-Chair of the GSC. This experience really broadened my horizons as I met other students from around the world and worked together in the GSC.

Lastly, I would like to thank my family and friends. They have kept me sane during this journey. They have all been there for problems that I ran into both in my education and in life. I wouldn't be here in my education without the help and support of many people. Thank you to everyone who helped me over the years, including those that are not explicitly mentioned here.

Contents

| | |
|--|-----|
| Acknowledgements..... | iv |
| Contents..... | v |
| List of Figures | vii |
| List of Tables | ix |
| Nomenclature | x |
| Abstract..... | xi |
| Chapter 1 Introduction..... | 12 |
| 1.1 Research Rationale..... | 18 |
| 1.2 Proposed Solution and Research Questions | 20 |
| 1.3 Thesis Overview | 22 |
| Chapter 2 Review of State of the Art | 24 |
| 2.1 Methods for Determination of New Space Air Temperature Set Point..... | 25 |
| 2.2 Methods for mitigation of comfort losses | 26 |
| 2.3 Inconsistent load profile..... | 29 |
| 2.4 Closing remarks | 31 |
| Chapter 3 Identification of System and Operating Parameters..... | 32 |
| 3.1 Overview of Thermal Systems in Buildings | 32 |
| 3.2 Operation of Air-Handling Unit and Terminal Devices | 34 |
| 3.3 Experimental Test Bed | 38 |
| 3.4 System Modeling..... | 45 |
| 3.4.1 Thermal Zone Modeling using 3R3C Technique | 53 |
| 3.4.2 Modeling Terminal Box Operation | 62 |
| 3.4.3 Modeling AHU operation..... | 64 |
| Chapter 4 Energy-feedback control analysis through simulation and experimentation..... | 76 |
| 4.1 Energy-feedback control compared with conventional temperature set point adjustment control | 76 |
| 4.1.1 Demand control by using temperature reset adjustments | 76 |
| 4.1.2 Energy Demand Respond (EDR) using energy-feedback control for the cooling coil | 78 |
| 4.2 Simulation and result analysis..... | 83 |

| | | |
|------------|--|-----|
| 4.3 | Experimental result comparison | 92 |
| Chapter 5 | Integration of Transactive Control and Coordination | 102 |
| 5.1 | Overview of Transactive Control and Coordination Operation | 102 |
| 5.2 | Application of TCC in EDR Control..... | 104 |
| 5.2.1 | Bid Pricing | 104 |
| 5.2.2 | Bid Quantity | 107 |
| 5.2.3 | TCC Market Agent..... | 112 |
| 5.2.4 | TCC Operation..... | 115 |
| 5.3 | Simulation results of EDR+TCC and EDR Comparison..... | 117 |
| 5.4 | Simulation Results Under Different Scenarios of EDR+TCC Operation..... | 122 |
| 5.4.1 | Category 1 – Maximum Supply Airflow Switch from the lowest to highest priority zone | 123 |
| 5.4.2 | Category 2 – Different Desired Temperature for Different Zones | 124 |
| 5.4.3 | Category 3 – Different Comfort Bands for Different Zones..... | 127 |
| Chapter 6 | Concluding Remarks..... | 130 |
| 6.1 | Future Work | 131 |
| 6.1.1 | Scale up EDR+TCC | 131 |
| 6.1.2 | Validate EDR+TCC Experimentally | 131 |
| 6.1.3 | Investigate Limitations of EDR+TCC..... | 132 |
| References | | 134 |
| Appendix | | 138 |

List of Figures

| | |
|--|-----|
| Figure 1-1: U.S. Electricity consumption by end-use sector [1]..... | 12 |
| Figure 1-2: CAISO Electricity Duck Curve [2]..... | 14 |
| Figure 1-3: Commercial Electricity Consumption by End Use [6]..... | 16 |
| Figure 1-4: Demand-side energy management strategies [8]..... | 18 |
| Figure 2-1: Conceptual diagram of demand savings from temperature setpoint reset [7] | 30 |
| Figure 3-1: Sources of heat gain in thermal zone [13]..... | 33 |
| Figure 3-2: Basic air handling unit diagram | 36 |
| Figure 3-3: Engineering Laboratory building floorplan..... | 39 |
| Figure 3-4: IECC United States climate zone map..... | 40 |
| Figure 3-5: Engineering Lab Building Layout | 41 |
| Figure 3-6: AHU used for Experiments | 42 |
| Figure 3-7: Building Automation System | 43 |
| Figure 3-8: Additional Building Automation System MNL800 Controller | 43 |
| Figure 3-9: Ultrasonic flowmeter | 44 |
| Figure 3-10: Ultrasonic flowmeter transducer setup | 44 |
| Figure 3-11: Steady state thermal circuit | 47 |
| Figure 3-12: Electrical RC circuit diagram | 49 |
| Figure 3-13: RC circuit, current pathways identified | 51 |
| Figure 3-14: 1R1C Thermal Circuit | 52 |
| Figure 3-15: 3R3C model..... | 55 |
| Figure 3-16: Model of Thermal Zones..... | 59 |
| Figure 3-17: Envelope RC Model..... | 60 |
| Figure 3-18: VAV Control Diagram..... | 64 |
| Figure 3-19: Supply Air Fan Model..... | 66 |
| Figure 3-20: single node cooling coil thermal circuit..... | 68 |
| Figure 3-21: Discretized cooling coil diagram | 73 |
| Figure 4-1: EDR Control Sequences | 82 |
| Figure 4-2: Simulation Inputs based on Time of Day..... | 84 |
| Figure 4-3: Energy Demand Response Simulation Temperatures..... | 87 |
| Figure 4-4: Setpoint Reset Simulation Temperatures | 88 |
| Figure 4-5: Setpoint Reset, EDR Temperature Comparison | 89 |
| Figure 4-6: SP Reset, EDR Cooling Coil Load Comparison..... | 91 |
| Figure 4-7: Zone Temperature Reset Test | 94 |
| Figure 4-8: Energy Demand Response Control, Experimental Temperature Response..... | 95 |
| Figure 4-9: EDR and Setpoint Reset Temperature Response Comparison for Zone F | 97 |
| Figure 4-10: EDR and Setpoint Reset Temperature Response Comparison for Zone E | 98 |
| Figure 4-11: Experimental Cooling Coil Load Profile | 99 |
| Figure 5-1: Illustration of single commodity market inside a commercial building [41]..... | 103 |
| Figure 5-2: Illustration of multiple commodity markets inside a commercial building [41] | 104 |

Figure 5-3: Bid Price Curve [42] 105
Figure 5-4: Bid Pricing Test 107
Figure 5-5: Bid Quantity Comparison 112
Figure 5-6: TCC Uncongested Sample Market Agent [42] 113
Figure 5-7: TCC Congested Market Agent [42] 114
Figure 5-8: Cleared price at bidding agent [42] 115
Figure 5-9: TCC Market operation [42] 116
Figure 5-10: EDR+TCC Temperature Response of all Zones 118
Figure 5-11: EDR+TCC and EDR Temperature Comparison 119
Figure 5-12: EDR+TCC Cooling Coil Load Comparison 121
Figure 5-13: EDR+TCC Category 1 Temperature Response 124
Figure 5-14: EDR+TCC Category 2 Temperature Response 126
Figure 5-15: EDR+TCC Category 3 Temperature Response 128

List of Tables

| | |
|--|-----|
| Table 1-1: Control strategy qualitative comparison | 21 |
| Table 2-1: ASHRAE Limits on Temperature Drifts and Ramps (ASHRAE-55-2010) [24] | 29 |
| Table 3-1: Conduction heat flux variable definitions..... | 47 |
| Table 3-2: 3R3C Variable Definitions | 55 |
| Table 3-3: Model Envelope Materials..... | 61 |
| Table 3-4: Model RC Values | 61 |
| Table 3-5: cooling coil model variable descriptions | 68 |
| Table 4-1: Simulation maximum zone flowrate..... | 85 |
| Table 4-2: Simulation Zone Temperature Setpoints..... | 88 |
| Table 4-3: Zone Temperature Setpoints for Reset Test..... | 93 |
| Table 4-4: Maximum zone temperature experimental results | 96 |
| Table 5-1:TCC Bidding Parameters | 105 |
| Table 5-2: TCC Simulation K values..... | 118 |
| Table 5-3: 3-day cooling coil load | 121 |
| Table 5-4:EDR+TCC Test Conditions..... | 123 |
| Table 5-5: EDR+TCC Category 1 Test Conditions | 123 |
| Table 5-6: EDR+TCC Category 2 Test Conditions | 125 |
| Table 5-7:EDR+TCC Category 2 Results..... | 127 |
| Table 5-8: EDR+TCC Category 3 Test Conditions | 127 |
| Table 5-9: EDR+TCC Category 3 Results..... | 128 |

Nomenclature

| | |
|-----------------------------|---|
| AHU | <i>Air Handling Unit</i> |
| ASHRAE | <i>American Society of Heating, Refrigeration, and Air-Conditioning Engineers</i> |
| BAS | <i>Building Automation System</i> |
| BTU | <i>British Thermal Unit</i> |
| C | <i>Capacitance (thermal and/or electrical)</i> |
| CAISO | <i>California Independent System Operator</i> |
| CHW | <i>Chiller Water</i> |
| cp | <i>Specific heat at constant pressure</i> |
| EDR | <i>Energy Demand Response</i> |
| HVAC | <i>Heating, Ventilation, and Air Conditioning</i> |
| IAQ | <i>Indoor Air Quality</i> |
| KCL | <i>Kirchhoff's Current Law</i> |
| KVL | <i>Kirchhoff's Voltage Law</i> |
| kWh | <i>kilowatt hour</i> |
| m | <i>Mass</i> |
| \dot{m} | <i>Mass flow rate</i> |
| MA | <i>Mixing Air or mixed air</i> |
| MBTU | <i>equivalent to one-thousand (1,000) BTU</i> |
| MMBTU | <i>equivalent to one-million (1,000,000) BTU</i> |
| OA | <i>Outdoor Air</i> |
| ODE | <i>Ordinary Differential Equation</i> |
| PI | <i>Proportional-Integral (with respect to feedback control)</i> |
| PID | <i>Proportional-Integral-Derivative (with respect to feedback control)</i> |
| PNNL | <i>Pacific Northwest National Laboratory</i> |
| PV | <i>Photovoltaic</i> |
| Q | <i>Volumetric flowrate</i> |
| R | <i>Resistance or Resistor</i> |
| RA | <i>Return Air</i> |
| RC | <i>Resistor-Capacitor</i> |
| RH | <i>Relative Humidity</i> |
| SA | <i>Supply Air</i> |
| SP, sp | <i>Set point</i> |
| T | <i>Temperature</i> |
| TCC | <i>Transactive Control and Coordination</i> |
| TOU | <i>Time of Use</i> |
| V | <i>Voltage</i> |
| VAV | <i>Variable Air Volume</i> |
| VFD | <i>Variable Frequency Drive</i> |
| VOC | <i>Volatile Organic Compound</i> |

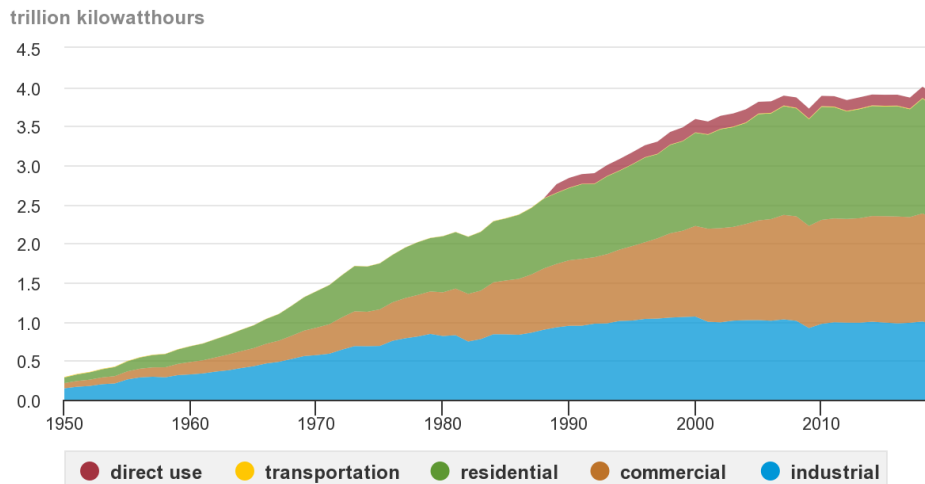
Abstract

The goal of this thesis is to identify methods to control a commercial Heating, Ventilation, and Air Conditioning (HVAC) system that results in precise control of the cooling coil load and the ability to prioritize the comfort of certain zones. The state of the art method of zone temperature setpoint adjustments is introduced and the weaknesses are identified. Temporarily resetting the zone temperature setpoints shows the capacity to significantly reduce the cooling coil load, but the load is not controlled precisely. The setpoint reset method is compared through simulation and experimentation to the proposed solutions of Energy Demand Response control (EDR) and Transactive Control and Coordination (TCC) integrated with EDR control. A model of the system that captures the relevant behaviors was developed to test each of the control strategies under different scenarios. Through simulation it was found that EDR control can precisely regulate the cooling coil load but does not provide any way to prioritize the zones. EDR combined with TCC precisely controls the cooling coil load and allows for the comfort of specific zones to be prioritized. The setpoint reset and EDR control strategies were validated experimentally on a multizone variable air volume air handling unit. The cooling coil load during a period of setpoint reset was experimentally found to vary between 1.1 ± 0.4 refrigeration tons. The cooling coil load under EDR control was regulated between 1.1 ± 0.1 refrigeration tons. Future areas of study have been identified, which includes using a virtual flow meter for EDR control and increasing the scale of EDR+TCC implementation.

Chapter 1 Introduction

Throughout the United States and the rest of the world, energy consumption is steadily increasing. Energy consumption in all forms may be rising, but electricity consumption specifically is growing and presents certain risks. The total electricity consumption in the United States reached 3.8 trillion kWh in 2020. This consists of the end use by all sectors including residential, commercial, industrial, transportation, and direct use. The consumption is up from only 0.29 trillion kWh in 1950. [1] The historical electricity consumption by end-use sector is shown in Figure 1-1. It can be seen that electricity use by all sectors is increasing and that the most impactful sectors are residential, commercial, and industrial. The electricity consumption of the commercial sector made up approximately 35% of the total electricity sales in the United States. The residential sector and industrial sector cover 39% and 25% of the electricity sales, respectively [1].

U.S. electricity retail sales to major end-use sectors and electricity direct use by all sectors, 1950-2019



Source: U.S. Energy Information Administration, *Monthly Energy Review*, Table 7.6, July 2020

Figure 1-1: U.S. Electricity consumption by end-use sector [1]

It is not fair to claim that this growth in electricity consumption is necessarily a bad thing. Growth in this way is an expected outcome as more and more devices become connected to the grid and communities gain access to electricity. However, continued growth in electricity consumption requires pause for certain considerations such as: Can electricity production keep up with the growing consumption? Can the current electrical grid handle the growing consumption? Is the total electricity consumption the only concern moving forward?

It is true that the total electricity consumption is a concern. As more devices are connected, the total electricity demand will continue to grow and must be offset through increased generation. Many electricity providers are working to meet this demand by utilizing renewable energy sources like solar photovoltaic (PV) farms. Electricity generation from renewable sources is great but also brings about new complications. Considering solar farms, operation is shut down at night and can be affected by environmental factors like cloud cover. Peak solar generation occurs early to mid-afternoon when electricity demand is relatively stable. During peak solar generation, some generators may need to be shut down to prevent over-generation and damage to the system. In the early evening, there is double blow to the system as solar generation begins to reduce and the demand increases. This combination creates a massive ramp in the net load that must be met through alternative generation methods [2, 3]. The net load, normal load minus PV and wind generation, can be seen in Figure 1-2. The “belly” or dip in the duck curve is becoming increasingly pronounced each year. This results in an intensive load ramp and peak that must be met.

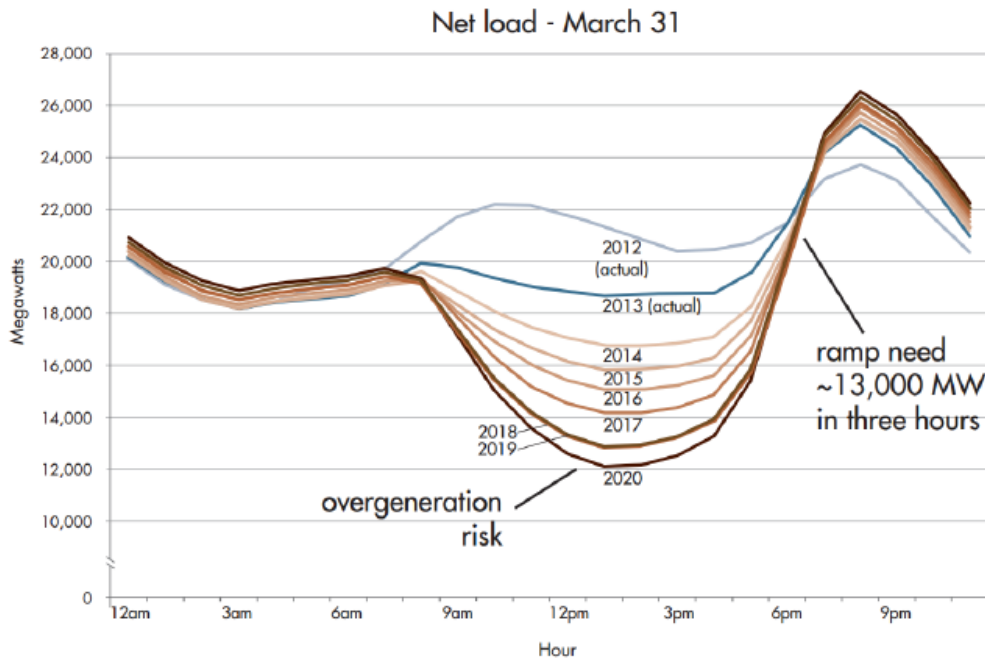


Figure 1-2: CAISO Electricity Duck Curve [2]

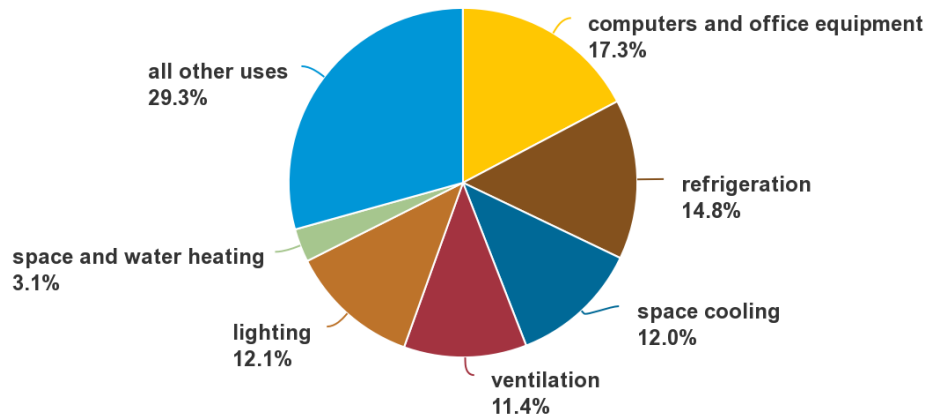
The leading proposals to reduce the risks associated with the duck curve are “flattening” and “fattening” the curve. Fattening the curve will increase the dip by allowing for more solar generation and reduced generation from other sources. Much of this approach relies on the providers to allow non-solar generation to be reduced and requires that the load forecast can predict the net load ramp. The alternative is to flatten the duck curve. Flattening requires reducing the peak load and increasing the load during the dip. With load shifting, electricity can be consumed, and energy can be stored during the low load period and released for use during the peak time [3].

Many electricity providers are attempting to flatten the duck curve by incentivizing consumption outside of the peak time or disincentivizing electricity consumption during peak time. Electricity use is generally disincentivized by introducing a tariff or by increasing the cost during peak hours. This is often referred to as Time of Use (TOU) rates or Peak Hours Pricing. The

time range of peak hours, to be referred to as “peak hours”, is set to diminish the effects of the net load ramp intensity and net load peak. Peak hours may or may not be constant as the net load profile can change due to seasonal changes or other operational changes. For example, California ISO has proposed four TOU rates, Super-peak, peak, super off-peak, and off-peak to address different levels of grid risk [4]. OGE Energy Corporation, a local utility provider, holds peak hours weekdays from 2PM to 7PM. The pricing rate during and outside of peak hours are 0.22 \$/kWh and 0.05 \$/kWh respectively [5]. Different regions may require unique peak hours to achieve the maximum benefits.

Not all devices can contribute to load shifting because the energy from some devices is not easily storable. For example, building lighting could be turned on earlier or at night but will still need to follow occupants’ needs. Electricity is consumed in commercial buildings by multiple devices as indicated by Figure 1-3. Many of these devices like computers operate under direct user interaction. Others add or remove heat from the building. Space heating, cooling, and ventilation account for approximately 25% of electricity consumed in all commercial buildings [6]. Heat is a form of energy that can be stored in multiple ways such as sensible heat in the thermal mass of the building.

U.S. commercial sector electricity consumption by major end uses, 2020



Source: U.S. Energy Information Administration, *Annual Energy Outlook, 2021*, Table 5, February 2021

Figure 1-3: Commercial Electricity Consumption by End Use [6]

Heating, ventilation, and air conditioning (HVAC) systems make up a significant portion of the total electricity consumption and are not required to operate at a specific level like computers. Energy from the HVAC systems can also be stored in the existing structure through heating or cooling. These factors make the HVAC system a prime contender for load management [7, 8]. A report from The Office of Energy Efficiency and Renewable Energy considered four demand-side energy management strategies as given below [8]. The load behavior is also shown in Figure 1-4.

1. **“Efficiency:** the ongoing reduction in energy use while providing the same or improved level of building function.
2. **Load Shed:** the ability to reduce electricity use for a short time period and typically on short notice. Shedding is typically dispatched during peak demand periods and during emergencies.

3. **Load Shift:** the ability to change the timing of electricity use. In some situations, a shift may lead to changing the amount of electricity that is consumed. Load shift in the *GEB Technical Report Series* focuses on intentional, planned shifting for reasons such as minimizing demand during peak periods, taking advantage of the cheapest electricity prices, or reducing the need for renewable curtailment. For some technologies, there are times when a load shed can lead to some level of load shifting.
4. **Modulate:** the ability to balance power supply/demand or reactive power draw/supply autonomously (within seconds to sub seconds) in response to a signal from the grid operator during the dispatch period.
5. **Generate:** the ability to generate electricity for on-site consumption and even dispatch electricity to the grid in response to a signal from the grid. Batteries are often included in this discussion, as they improve the process of dispatching such generated power.”

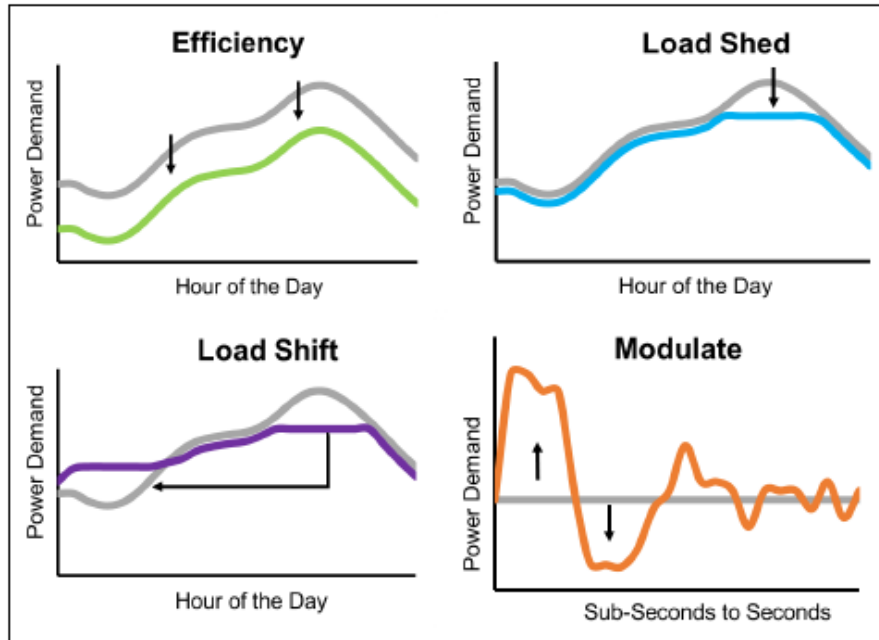


Figure 1-4: Demand-side energy management strategies [8]

The Modulating and Generating categories will not be considered as they are less likely to be intentionally affected by the HVAC system or building thermal dynamics. Each of these energy management strategies has unique benefits and tradeoffs that can be explored. For example, improving the system efficiency often requires that the system be retrofitted or replaced. Load shifting and load shedding can both be accomplished in some capacity through HVAC control changes. Load shedding simply eliminates a portion of the load, while load shifting moves a portion of the load from one time to another [8]. This work will primarily focus on load shedding of the HVAC system.

1.1 Research Rationale

The peak load during and after peak hours must be mitigated. Electricity is consumed by a variety of devices and systems, but HVAC systems are a major contributor to the building load. The HVAC system uses electricity for many processes, but not all components make a significant

impact. The HVAC type under consideration will be a commercial system with a chilled water cooling coil.

This type of HVAC system has multiple levels that each have some electricity consuming components. The major areas that will be considered are at the air handling unit (AHU) level and chiller level. The AHU is responsible for distributing cool, dry air to all of the zones in the building. The chiller must remove heat from the chiller water after it is used by the AHU. Each level has major components that greatly affect the building load and control components that do not impact the building load in a significant way.

The supply air fan is generally the primary electricity consuming device in the AHU. This drives the conditioned air to building zones by converting electricity to air movement. The other element in the AHU that must be considered is the cooling coil. The cooling coil does not directly consume electricity but is responsible for transferring heat from the air to the chiller water. The water is then cycled back to the chiller where the heat must be removed. Therefore, electricity consumption may be reduced by operating the supply air fan at a lower speed or by limiting the amount of heat removed by the cooling coil.

The state of the art method of shifting HVAC electricity consumption is by resetting the zone temperature setpoints for some period of time. A setpoint adjustment to a higher temperature causes a series of events that leads to a load reduction. First, the terminal box damper of the specific zone will close and reduce supply air into the zone so that the new setpoint can be achieved. All specified zones will result in a reduction of the total supply air flow. This lower flowrate results in both less heat entering the chiller water through the cooling coil and less electricity consumed by the supply air fan.

The combination of reduced supply air fan speed and cooling coil load significantly impact the electricity consumption while the strategy is active. However, the cooling coil load, and thus, the electricity consumption cannot be controlled precisely. It is difficult to estimate to what level the setpoint reset will affect the electricity use. Additionally, this method will not strictly control the cooling coil load or supply air fan operation. The cooling coil load will initially drop significantly but will begin to rise as the zones reach the new setpoints.

1.2 Proposed Solution and Research Questions










The goal of this work can be separated into two distinct parts. First, the cooling coil load must be precisely controlled for the duration of the specified time. Second, the system must be able to prioritize certain zones in the building. This does not mean that some zones are simply neglected but not all zones will require the same level of comfort.

The proposed solution consists of two major components to reach both goals. A form of direct load control that will be known as energy demand response (EDR) control will be used to precisely manage the cooling coil load. This requires reassigning levels of importance for certain operating parameters in the AHU. The cooling coil load is the primary concern, and the zone temperatures are treated as a secondary concern. This control strategy by itself will regulate the cooling coil load; however, it does not offer any way to prioritize any zones.

The second piece of the proposed solution is to integrate Transactive Control and Coordination (TCC) into the control strategy. TCC is a control method developed by Pacific Northwest National Laboratory (PNNL). TCC allows each zone to bid for cooling from the AHU based on its need. The cool air can then be distributed to all zones by using the bids. TCC can also limit the cooling coil load, but it may not be controlled with the required level of accuracy.

The combination of these two strategies will allow for both goals to be achieved. Although, each strategy brings about unique tradeoffs. A qualitative comparison of relevant parameters and tradeoffs is given in Table 1-1. For example, each method requires that the zone temperatures increase to reduce the cooling coil load, but this compromised temperature may be inconsistent. However, compromised temperature can be strictly enforced with the setpoint reset method. The other two control methods will result in a compromised zone temperature that may not be desired.

Table 1-1: Control strategy qualitative comparison

| | Compromised Temperature Control | Precise Load Control | Zone Prioritization |
|-----------------------|---|--|---|
| Setpoint Reset |  |  |  |
| EDR |  |  |  |
| EDR combined with TCC |  |  |  |

The main research questions reside in understanding what unique benefits and tradeoffs of each control strategy can offer that may be necessary in different scenarios. To answer the main research question, the following research questions need to be addressed in this thesis:

1. What are the necessary parameters to quantify the benefits and tradeoffs of control strategies?
2. How should the system components be defined and the dynamics modeled to conduct control performance analysis?
3. How should experimental procedures be designed to validate the simulation results?
4. What operation scenarios should be considered for performance validation?

1.3 Thesis Overview

The broad research objective of this thesis is to develop and test a method to limit the cooling coil load that address the shortcomings of the state-of-the-art strategy. The produced outcome must be able to precisely control the cooling coil load and provide a way to prioritize the comfort of certain zones. Specific objectives include identifying the cause of the shortcomings, creating a model that captures relevant system behaviors, validating the proposed method by comparing the developed control method to the current methods, and identifying future work on the topic. The structure of this thesis is summarized as follows:

Chapter One serves as an introduction into the background of the problem, namely the growing peak electricity demand. The state-of-the-art method of load control and the proposed solutions to improve upon the current strategy are also established.

Chapter Two serves as a literature review of the state-of-the-art control method. It provides the details and shortcomings of the current control method.

Chapter Three is primarily the development of the model used for all simulations. The experimental test bed and set up are also introduced.

Chapter Four covers the test conditions and results, both simulated and experimental, of the setpoint reset tests and the energy demand response tests.

Chapter Five introduces Transactive Control and Coordination and integrates it with energy demand response control. The simulated results and analysis of EDR+TCC operation are included in this chapter.

Chapter Six serves as the concluding remarks of the thesis. The major takeaways from each of the control methods are covered, and potential future work is also established.

Chapter 2 Review of State of the Art

One of the leading state of the art methods to reduce cooling coil load and in turn the electricity demand is by raising the zone temperature setpoints in the building [7, 9]. The sequence of operations that are induced with this strategy can be simplified to the following summary. Once the temperature setpoint is reset to a higher value, the terminal box damper will begin to close. The reduced damper position result in less cool, dry air being supplied into the room. As the room temperature approaches the new setpoint, the damper will open and modulate to maintain the zone temperature. A higher zone temperature will result in slightly less heat entering the zone that must be removed by conditioned air. Reduced air into the zones will cause less supply air to be needed and a lower cooling coil load. Some of the studies in the area of set point reset to reduce the load can be found in [7, 10, 11, 9]. Although the space air temperature reset can result in load reduction in general, three major operational challenges are identified:

- 1)** The space air temperature reset usually does not provide a precise load reduction, i.e., it is difficult to relate the degrees of temperature rise to the percentage of load reduction.
- 2)** Mitigation methods for comfort loss do not effectively consider the potential provided by different preferences in different thermal zones.
- 3)** The load profile is inconsistent using the space air temperature reset.

2.1 Methods for Determination of New Space Air Temperature Set Point

When using space air temperature reset to manipulate the load reductions, the first challenge is to define the new space air temperature set point. It needs to satisfy the load reduction purpose and maintain a certain level of comfort.

A majority of the studies set the adjusted space air temperature setpoints a few degrees higher than the ones in normal operation uniformly through a global reset command in building automation system (BAS) to obtain a load reduction. However, the magnitude of the load reduction using this strategy is not a directly controlled amount. The magnitude of the load reduction is hard to calculate due to the complexity of the system and likely will not be constant because of dynamic loads in the building. It was noted that, "It is often difficult to estimate the demand savings achieved by HVAC strategies, because the building's HVAC electric load is dynamic and sensitive to weather conditions, occupancy, and other factors." [7] Additionally, it has been observed that the temperature and load responses are affected by factors such as the time of day and weather conditions. The demand response potentials decrease when the outdoor air temperature is less than 75°F or when the load exceeds the HVAC system capacity [12].

Some studies adopted models to predict the new space air temperature set point based on a load reduction goal. For example, a representative building model was developed in eQUEST to study the effects of different setpoint adjustments on the cooling load [12]. However, a highly detailed model would likely require a unique model for each building or a set of representative buildings and would not be feasible for real-time calculations. Many studies utilize RC models to predict the temperature dynamics, predict the cooling load, and determine a new setpoint. RC

models can provide a reasonable representation of the system, but this requires accurate determination of the R and C values. The values could be calculated based on the building structure and materials. They could also be calculated using parameter estimation techniques [13]. Aside from detailed simulations and RC models, the temperature and load can be predicted with “gray-box” or “black-box” models [14, 15]. These are broadly data driven models that calculate an output based the probability from measured data. The accuracy of the model and the challenge of running a complex model for real-time control can present a challenge for precise load management.

2.2 Methods for mitigation of comfort losses

The more common strategy is to attenuate the comfort compromise is by precooling. The basic concept of precooling is to overcool the zone before peak hours, then allow the zone temperature to rise slightly during peak hours [16]. This shifts a portion of the load that would occur during peak hours to the time leading up to peak hours. The zone temperatures should remain comfortable for the occupants because of the temperature decreasing before rising.

Precooling is a popular strategy to reduce the load during peak hours and still maintain reasonable levels of comfort. However, the issue lies in determining what the setpoint should be throughout the day. This has been approached in numerous ways from rule-based strategies to optimized control and model predictive control. Even a simple rule-based method will still require some insight to achieve the most effective outcome. A building with an undersized cooling system may take longer to precool than one with an oversized system. Rule-based precooling strategies have shown to be effective in reducing the peak load and load during peak hours [17, 16]. A set of rule-based precooling tests were conducted by Xu et Al. and found to reduce chiller

power by 80-100% during peak hours when precooling was initiated prior to peak hours [16]. The efficacy of rule-based strategies was also validated experimentally. It was found to reduce the load of zones during occupied hours by 23% compared to a night setup where the setpoint was increased during unoccupied hours [18].

There is also a significant amount of research going into precooling strategies that implement Model Predictive Control (MPC). Lee et Al. predicted a peak load reduction of 30% in a demand limiting period while still maintaining comfortable conditions. The strategy was also implemented on site and resulted in a 30% reduction of the peak cooling load compared to the same building operating under standard conditions [9]. A higher level MPC study with solar PV panels and electrical storage found an electricity demand reduction of 23% even when these extra devices were unused [19].

Wang et al. investigated the formulation of an appropriate model and optimal precooling in residential buildings. This was compared to two rule-based strategies and found that the optimal control was much better at preventing peak hours operation, and that in some scenarios it may be more efficient to precool early in the day instead of directly before peak hours [13, 20]. Multiple studies also found that there can be significant cost savings in commercial buildings through optimal control when the demand is increased at night with the energy to be stored for later use [21, 22].

If precooling is not viable for the system, the setpoint reset could also be initiated at the onset of peak hours. This would entail raising the setpoint only at the start of peak hours. This strategy will primarily result in load shedding but a portion of the load during peak hours to the time after peak hours when the reset is released, and the system returns to the initial conditions

[8]. This method is less common because it may increase the likelihood that occupants become uncomfortable. The reset setpoint may need to be higher than if precooling were used if the system is to remain below the same load. This method would be more likely to be used when there is not ample notice to plan for precooling, such as during a grid emergency when the demand must be immediately reduced [8]. This setpoint reset strategy has been explored by Cai et al. and found that this strategy will result in some amount of load shedding as well as load shifting. They found that “an average of 1.6% daily energy savings can be achieved with 5°F increase in set point.” In regard to reducing the peak demand during peak hours, this method is more effective during mild outdoor conditions [10].

The value chosen for the new temperature setpoint may not be accepted by all occupants. The temperature chosen for the reset is likely to change depending on the required level of energy demand reduction, so occupant comfort may vary day to day. A detailed review of the effects of an increased setpoint adjustment on thermal comfort has been conducted by Aghniaey and Lawrence [23]. The study included the effects on human comfort of operating the system at a higher setpoint and the discomfort caused by temperature drift. They found increased discomfort of occupants “especially for temperatures higher than [82.4°F]” The discomfort caused by temperature ramp will usually be minimized if the temperature increase is slow enough and the cycling rate is maintained [23]. The values vary between studies but follow these general assertions. ASHRAE also provides a guideline of temperature drift as given in Table 2-1 [24]. These temperature drift effects will be important in determining the acceptability of the proposed load reduction solution.

Table 2-1: ASHRAE Limits on Temperature Drifts and Ramps (ASHRAE-55-2010) [24]

| Time Period, h | 0.25 | 0.5 | 1 | 2 | 4 |
|--|-------------|------------|-----------|-----------|-----------|
| Maximum Operative Temperature Change Allowed, °C (°F) | 1.1 (2.0) | 1.7 (3.0) | 2.2 (4.0) | 2.8 (5.0) | 3.3 (6.0) |

2.3 Inconsistent load profile

Due to the complexity of the sequence of operations and physical limitations of the system, the cooling load profile will not be consistent throughout the active time. The model-based study by Lee et Al. found the peak cooling load could be reduced by as much as 30% during peak hours when a precooling strategy was implemented. Although the ideal scenario during peak hours would be a constant cooling load, the study noted that “The actual load profile was not flat due to imperfect building modeling and weather predictions” [9]. This variable cooling coil load profile is a primary characteristic of setpoint reset operation that needs to be addressed.

The demand reduction behavior has been defined by Motegi et Al. as two components, steady-state savings, and transient savings. The steady state savings are a result of less heat entering a zone once the temperature has increased. The transient savings are caused by the effects of the thermal mass and the control device dynamics. A conceptual diagram of the demand reduction, in which the zone temperature setpoint is increased from 72° to 75°F, was developed by Motegi et Al. is given as Figure 2-1 [7]. It can be noted that the transient savings are a much greater magnitude than the steady state savings. However, the transient savings are diminished once the zone temperature reaches the adjusted setpoint in about 30 minutes, usually much shorter than required peak hours. Savings analogous to the steady state savings in this figure have been studied Roussac et Al. The standard operating setpoints were all increased by a specific amount resulting in a decrease in total energy consumption [25].

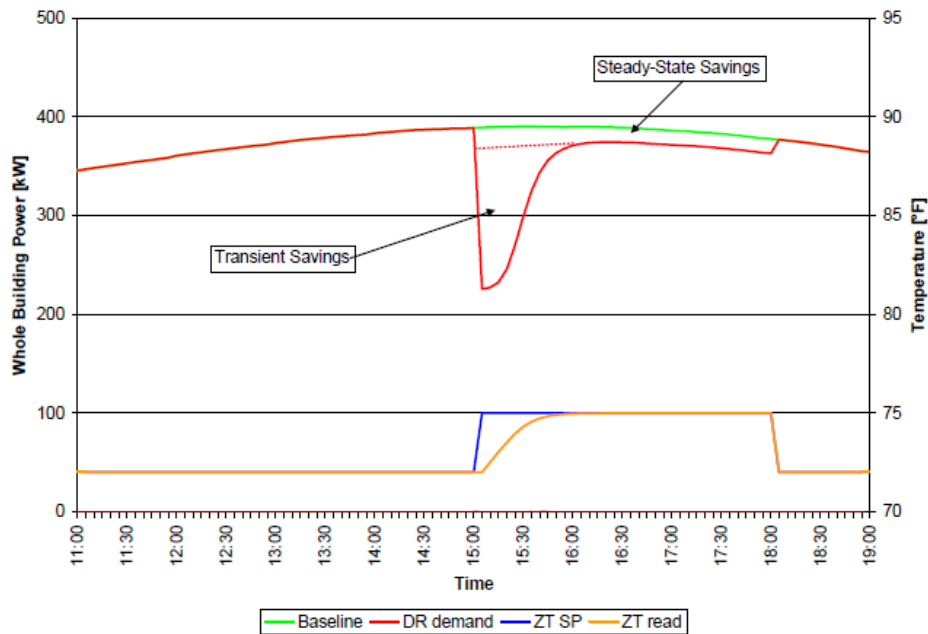


Figure 2-1: Conceptual diagram of demand savings from temperature setpoint reset [7]

The load variation that occurs when the temperature reaches a new setpoint has been coined as “load rebound” by Candanedo et Al. This load variation is a result of the system dynamics. Once a new setpoint is initiated, the system will reduce cooling into the zone and the temperature will rise. The system must then act to stop the temperature rise and maintain the temperature at the new setpoint. If the temperature reaches the setpoint more quickly, the load variation is likely to be larger [26]. A load increase during a setpoint reset period was also observed by Cai et Al. A “demand restrike” or increase in peak demand after a setpoint reset reached magnitudes of up to 6.3% [10].

The cooling load can be reduced by increasing the zone temperature setpoints, but this strategy does not address all concerns. The cooling coil load is reduced but is not modulated precisely. The load is greatly reduced during the transient response. The steady state load during the setpoint reset operation is still reduced from standard operation but is not constant and can

be affected by external factors. For example, Increased occupancy could cause the load to rise beyond desired levels. The cooling load should be precisely maintained while still allowing some level of prioritization between zones.

2.4 Closing remarks

Temperature setpoint adjustment is a valid method of reducing the cooling coil load but has some important characteristics. It is a widely applicable strategy, and a simple, rule-based approach can be implemented on most building automation systems with little effort. A temperature reset in each zone specifically can be scheduled by the building manager on most systems, which allows for some level of temperature prioritization between zones. Methods that are not rule-based are generally much more difficult to implement. They often require model calibration from the user and/or time to train certain parameters. With most control methods, the cooling coil load will not be constant. There is a load variation as the temperatures reach the adjusted setpoint and load variation due to dynamics in the zone load. For example, there may be changes in internal gain due to occupancy or more heat may enter through the envelope due to changes in cloud cover. Therefore, there is a need for a load shedding method that can quickly and precisely control the amount of load to be reduced while maintaining maximum comfort for critical zones by effectively redistributing the limited resources.

Chapter 3 Identification of System and Operating Parameters

Topics in this chapter will include identifying the relevant components in the HVAC and building energy systems and how these systems operate. The system operations in question range from the thermal zone up to the air handling unit and chiller. The primary focus will be the operation and modeling of the system and components under normal operation. Normal operation is defined as such that the system will operate within its bounds and prioritize human comfort.

3.1 Overview of Thermal Systems in Buildings

First, the role of the thermal zone must be understood. The thermal zone in regard to the building comfort system is an area that is heated or cooled to maintain comfort or other environmental factors. Generally, this will be a room or rooms that are occupied by people. Other spaces could be heated and cooled as well, such as server rooms, green houses, or any area that requires temperature and humidity control. In order to maintain comfort, the HVAC system must be able to remove the heat and water vapor entering the zone.

The largest environmental factor affecting human comfort in the thermal zone is the temperature. The humidity in the zone must also be considered but is often treated as a secondary concern for human comfort. Eight common sources of heat gain into a thermal zone are marked in Figure 3-1. The heat transfer into the zone will be distinguished as heat passing through the envelope and heat from internal gains in the zone. Heat through the envelope, from electronics, lighting, and people provide sensible heat to the zone. This heat will result in a

temperature increase to some extent. Latent heat will be introduced into the zone by people as they exhale water vapor and by infiltration to some extent [13].

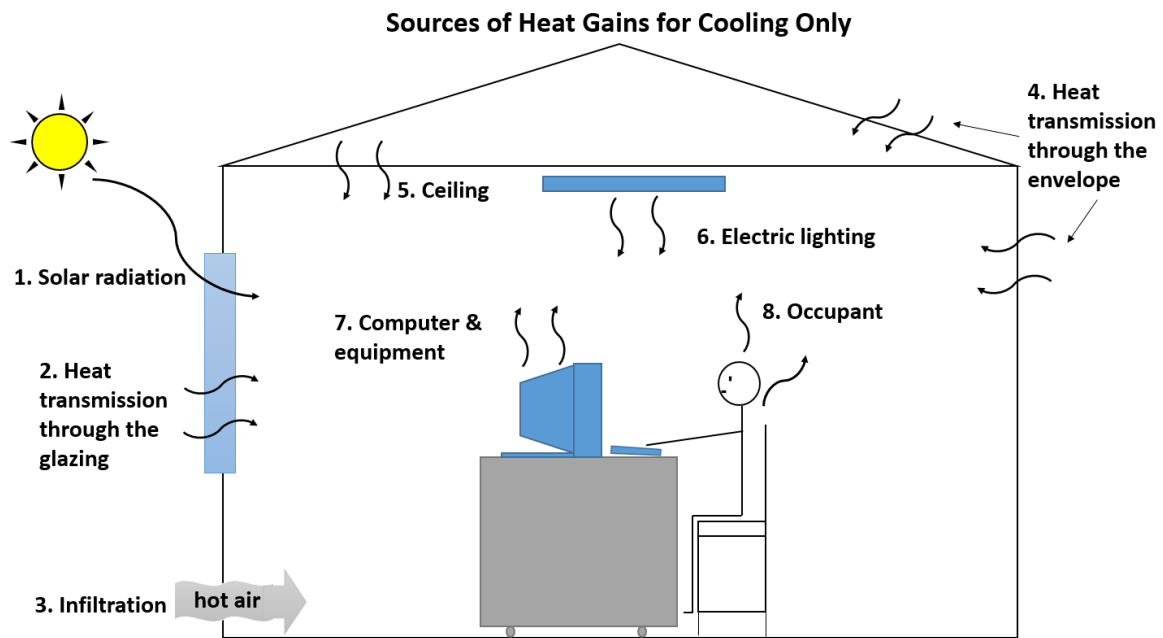


Figure 3-1: Sources of heat gain in thermal zone [13]

Heat entering into the zone through the envelope has three heat transfer modes. Heat can enter the zone by conduction combined with convection through the solid components and by radiation through the windows. Each of these can vary drastically between different buildings and are greatly affected by the building materials and even slightly by the desired conditions. For example, increasing the insulation in the walls and ceiling will reduce the amount of heat transferred through the envelope. Building with bricks instead of wood frame and siding will change the thermal capacitance and shift the thermal load. Increasing the room temperature would reduce the heat transfer into the zone because of a smaller temperature difference driving that heat transfer. The heat transfer into the zone will be affected by many factors leading to somewhat unique operation between buildings [13, 27].

Heat transfer into the zone can also occur due to internal gains. Convective effects of internal gains will result in heat being directly transferred into the zone from the source. For example, a 1 kW heater in a room would add nearly the entire kilowatt directly to the air in that room. Aside from heat transfer into the air through convection, thermal capacitance and radiation can also be considered. When a light is turned on, some heat directly enters the air through convection. The rest of the heat will enter the environment through radiation and be slowly released into the air over time.

Heat from all internal sources may either be sensible or latent. Common sources of sensible heat include lighting, electronics, and even sedentary people at an approximate rate of 250 Btu/hr. These heat sources will raise the temperature and enthalpy of the air without affecting the humidity in the zone. Other sources will be latent heat as from people, humidifiers, or anything increasing the humidity. Sedentary people like those working in an office generate latent heat at a rate of 200 Btu/hr [27]. Latent heat sources will increase the enthalpy of the air by increasing the humidity. All of the heat transferred into the zone must be removed by supplying cool, dry air in order to maintain the comfort conditions in the room.

A combination of experimental tests and simulation have been used to understand the behavior of the system. In the following subsections in Chapter 3, the component model of the thermal system for this research will be introduced.

3.2 Operation of Air-Handling Unit and Terminal Devices

The air handling unit is a complex system that must meet numerous objectives. The most basic requirement of the AHU can be reduced to its main function. The AHU must provide cool, dry air to all of the zones. Multiple other requirements arise to meet this function. A basic air

handling unit diagram is given as Figure 3-2, which is used to illustrate the main components in common AHUs. Figure 3-2 will be used to briefly introduce the main parts of the AHU. Moving from left to right on the diagram, the first components seen are the inlets and dampers for outdoor air and return air. Next is the filtering section and preheat coil. Lastly, the cooling coil and supply air fan are reached, which are the final components in the AHU before the supply air is routed through ducts and terminal boxes to all of the thermal zones served by the AHU.

A simplified sequence of operations of the AHU can be viewed in the same order. Air is brought into the AHU from both the return air and the outdoor air. The ratio of each is controlled by modulating the return air (RA) damper and outdoor air (OA) damper positions. The outdoor air and return air are mixed in the mixing chamber. Next, the air is filtered before reaching any heat exchangers or other equipment that could be damaged by air contaminants. The preheat coil is used to bring the air into safe operating conditions during periods of extreme cold weather. The cooling coil is used to bring the supply air (SA) to the desired conditions, typically at 55 degrees Fahrenheit. This air temperature is modulated through the use of a chiller water control valve. The position of this valve affects the chiller water flow rate, which will then affect the supply air temperature. Lastly, in draw-through AHUs, the supply air fan provides the pressure difference to drive the airflow.

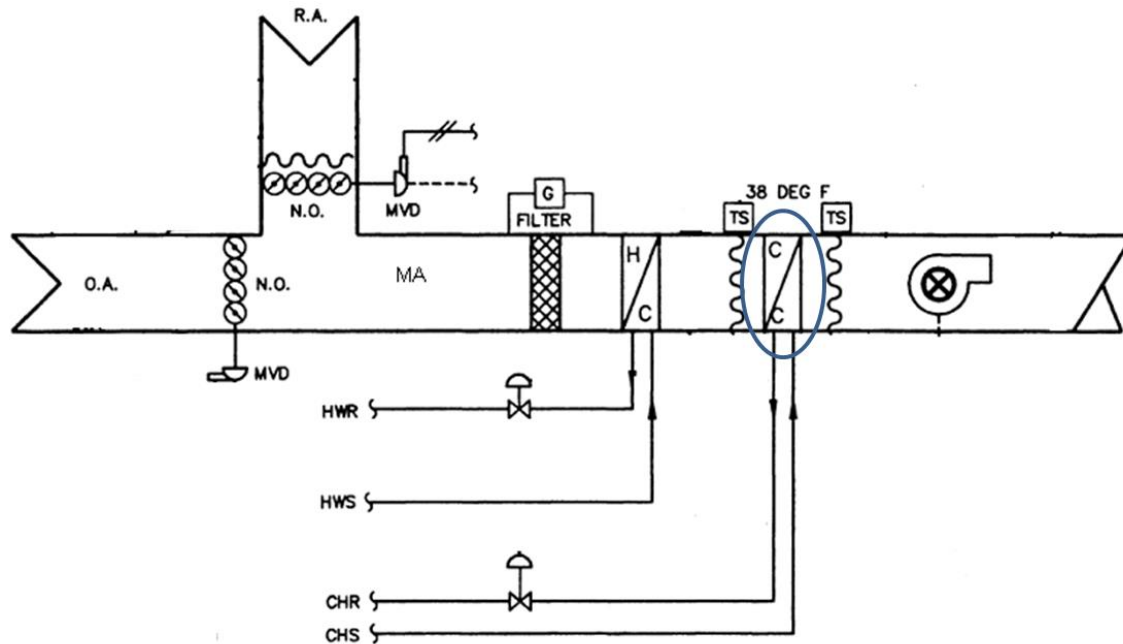


Figure 3-2: Basic air handling unit diagram

The operation of the outdoor air damper and return air damper can become a very in-depth topic in some circumstances. The most significant reason that outdoor air is required is to preserve the indoor air quality (IAQ) by diluting the polluted air with fresh, outdoor air. The outdoor air requirements for reasons of IAQ are dictated by ASHRAE 62.1. The pollutants are primarily those which present health risks to humans such as carbon dioxide and volatile organic compounds (VOCs). The introduction of outdoor air into the system can also be used to pressurize the building. Slight building pressurization reduces infiltration of hot humid air from outside. Generally speaking, the outdoor airflow rate will be at the minimum during cooling season. The temperature and enthalpy of the outdoor air are usually higher than that of the return air, so a higher outdoor airflow rate would result in more energy into the system that would need to be removed by the cooling coil. The other scenario is economizer operation in which the outdoor airflow rate is increased or even used completely when the OA enthalpy is less than that of the

return air. All experiments were conducted during cooling season when economizer operation would not be a factor.

Next, the filter and preheat coil are reached. The function of the filter is intuitive but very important. The filter will remove particulate matter from the air before reaching other components that could be damaged. These contaminants are primarily dust particles that would otherwise get caught in the heat exchangers. If too much contamination were to build up on a heat exchanger, known as fouling, the effectiveness would be greatly reduced [28]. Filter quality can vary widely even to the point of particles down to the size of airborne viruses. There is, however, a tradeoff. A filter that is capable of removing smaller particles may result in a larger pressure drop [29]. A filter that capable of removing small contaminants will need to be replaced on a regular basis. If the filter is heavily contaminated, the fan operation may be impacted significantly [30].

The basic function of the preheat coil is to increase the temperature of the filtered mixing air so that downstream components are not damaged. This is primarily only used during periods of extremely cold outdoor air temperature where the cold air could cause freezing or damage to the cooling coil.

The air then reaches the cooling coil, which is responsible for cooling the hot, humid mixing air to supply air conditions. The operation may be fully dry cooling in which temperature is reduced and no moisture is removed from the air or have wet cooling that reduces temperature and humidity. The controlled variable is the supply air temperature. Regardless of wet cooling or dry cooling the supply air temperature is maintained at 55° Fahrenheit. The temperature is maintained through the use of a PID control loop with the chiller water control valve. Simply put,

if the measured supply air temperature is higher than the setpoint, then the controller will signal the valve to open. If the measured supply air temperature is lower than the setpoint, then the controller will signal the chiller water valve to close.

Finally, the supply air fan provides the pressure rise that moves the supply airflow. Supply air fans may run at a constant speed or a variable speed through the use of a VFD. On a variable speed system, the actual fan speed is controlled based on the duct static pressure. This duct static pressure is measured a distance downstream, usually two-thirds of the of the distance to the furthest terminal box. Maintaining a positive duct static pressure downstream ensures that there will be ample airflow for all zones. In variable air volume (VAV) systems, such as in the engineering lab, the airflow rate into each zone is modulated by a damper in the terminal box. This damper position is used to maintain the zone air temperature at the setpoint by utilizing another PID control loop [27].

3.3 Experimental Test Bed

All experiments were conducted on the same test building. The test unit is a portion of the Engineering Laboratory Building on the University of Oklahoma – Norman Campus. The portion of the building used for experiments is served by one AHU and consists of seven thermal zones. The building is comprised of both interior and exterior zones, resulting in a wider range of operating conditions. The building zones are also served by terminal boxes of multiple sizes with unique maximum airflow rates. A floorplan layout of the experimental zones in the Engineering Laboratory building are given as Figure 3-3.

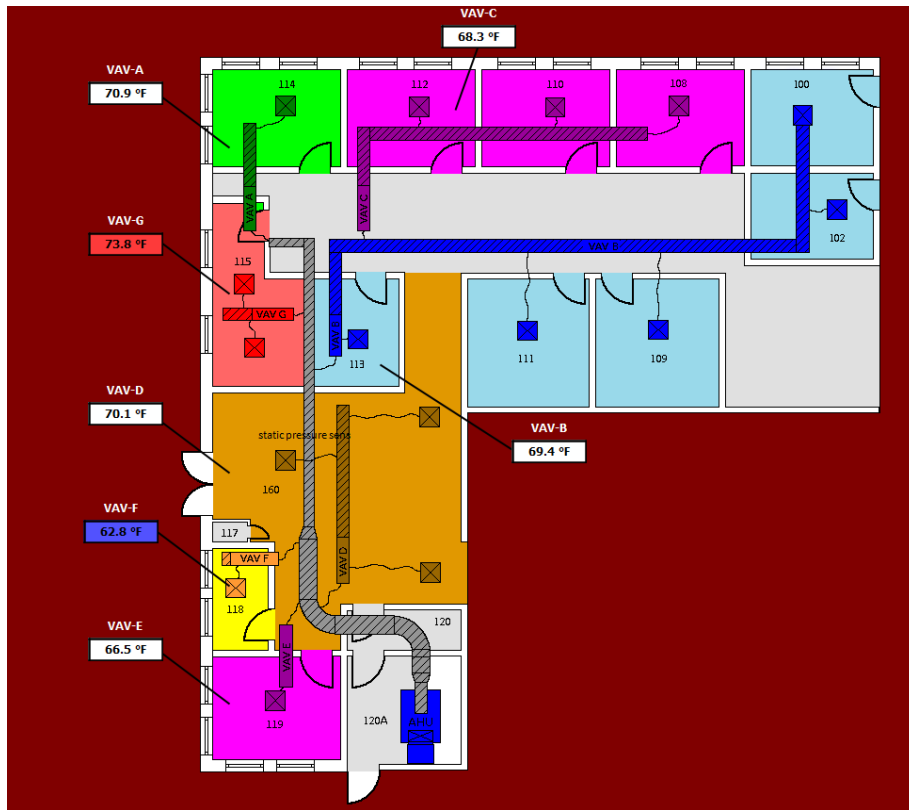


Figure 3-3: Engineering Laboratory building floorplan

The University of Oklahoma Norman Campus is located in the International Energy Conservation Code (IECC) climate zone 3A [31]. The United States climate zones are shown in Figure 3-4. This indicates that the test building is in a climate zone with a consistent cooling season. The abundant cooling season allows for more opportunity or experiments.

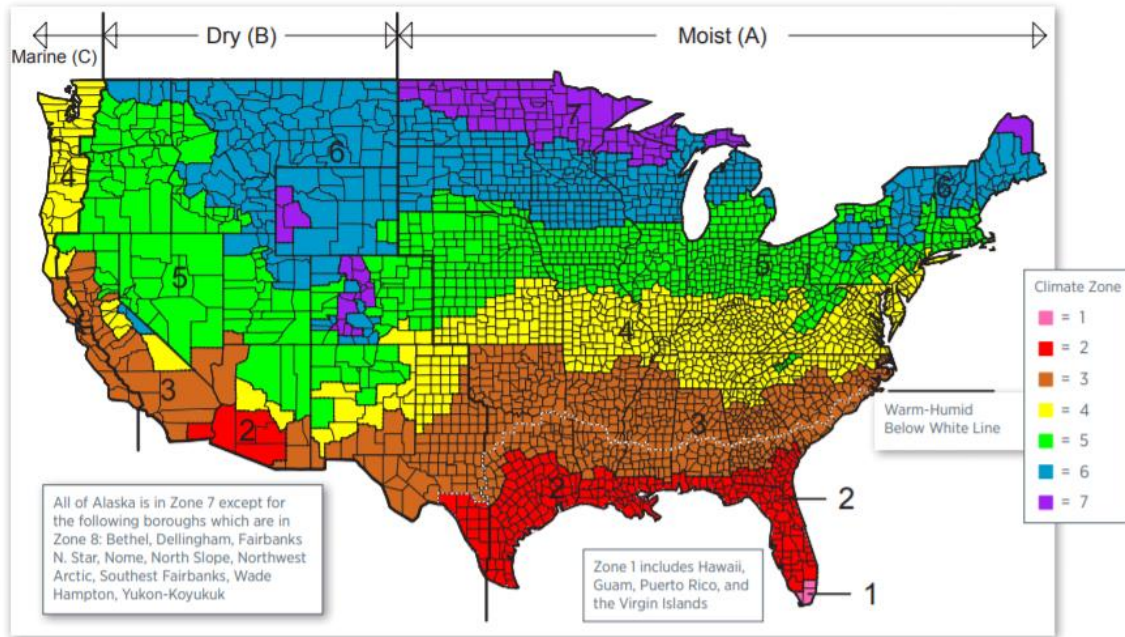


Figure 3-4: IECC United States climate zone map

The test building is served by two air handling units, but experiments are only conducted on the portion of the building served by one AHU. This section of the building contains seven thermal zones, labeled A through G on Figure 3-5. The thermal zones in the experimental area offer a range of operating conditions. There are interior zones and those with at least one exterior wall. The exterior zones also do not all share the same direction. For example, zone C has a north facing exterior wall, and zones G and F have a west facing exterior wall. There are multiple, unique thermal zones in the experimental test building to offer a range of operating conditions.

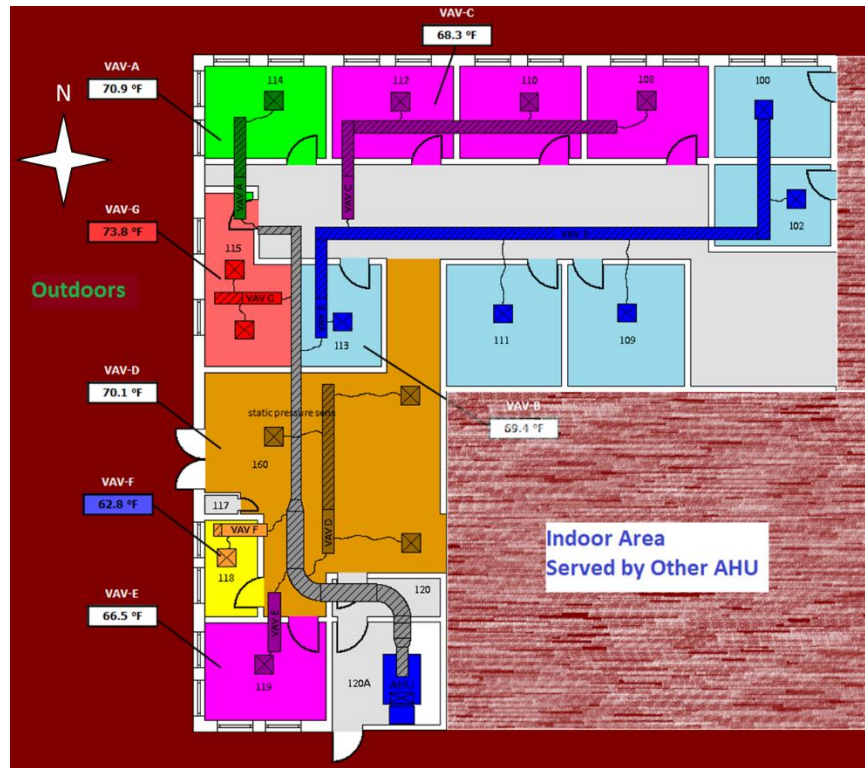


Figure 3-5: Engineering Lab Building Layout

The seven thermal zones are served by an 8-ton, single duct AHU. The air is cooled through the use of a chilled water cooling coil. Chiller water is provided to the AHU from a central chiller plant. The supply air temperature is maintained by modulating the chiller water flowrate through the use of an electronically actuated control valve. On the air side, the supply air fan speed is adjusted by a PI control loop to maintain the duct static pressure. The supply air fan speed is regulated through the use of a variable frequency drive (VFD). This air handling unit can be seen in Figure 3-6. Certain components important to this work are highlighted in the figure. The cooling coil location and chiller water control valve are marked by blue. The supply air fan location is in the AHU section behind the red circle. The green area marks the air mixing chamber, where the return air and outdoor air meet before entering the rest of the AHU.

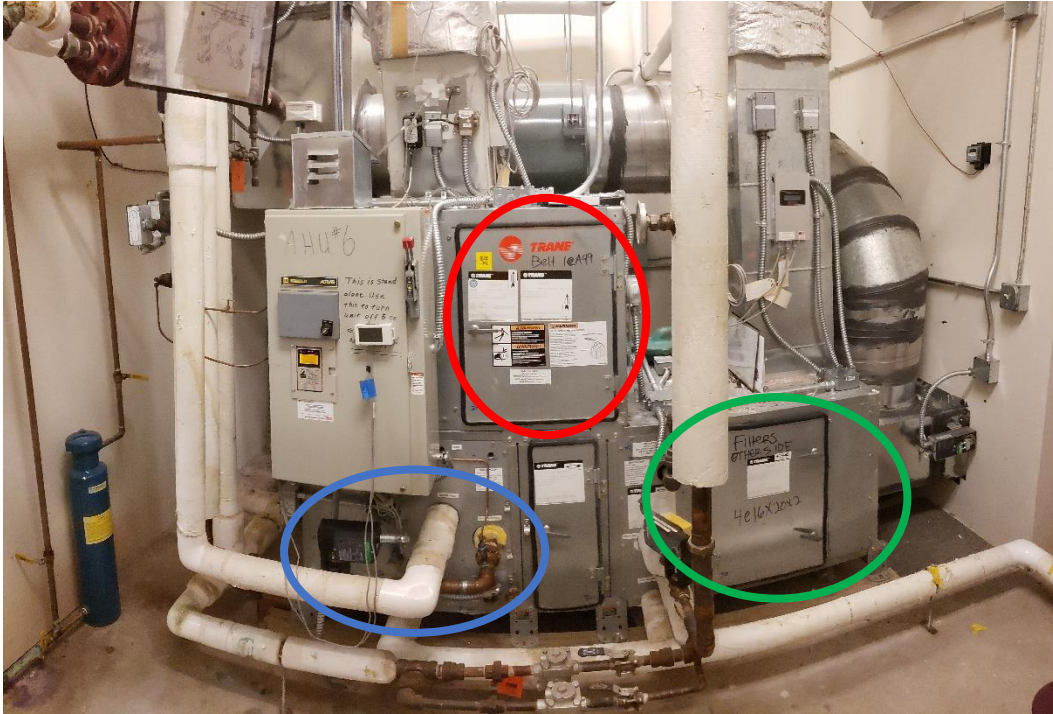


Figure 3-6: AHU used for Experiments

The Building Automation System (BAS) uses Invensys software and hardware. All control processes are completed by a set of Schneider MNL-800 controllers. These controllers allow for some flexibility in the control sequence but are still representative of the limitations of most commercial systems. They are capable of basic mathematics, feedback loops, scheduling, and other simple operations [32]. These controllers are not capable of some complex calculations or algorithms that are at the forefront of some research areas. The system records and archives most data points at one-minute increments. Additional data loggers were installed for all tests conducted to measure necessary data at a rate of one sample per second. The control system hardware can be seen in Figure 3-7 and Figure 3-8. The controller in Figure 3-8 was installed to conduct experiments on the system without the need to continuously update the program on the primary controllers. It also allowed for controls to be implemented where inputs would otherwise be separated.

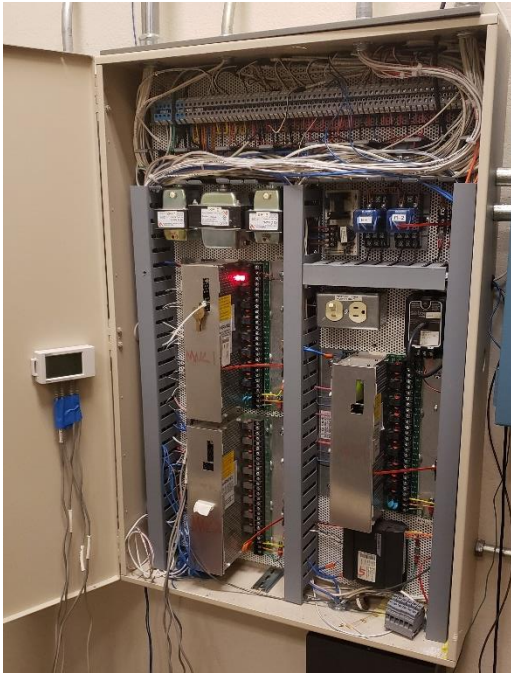


Figure 3-7: Building Automation System



Figure 3-8: Additional Building Automation System MNL800 Controller

Most measurements were taken from sensors and meters that were already in place for system operation. For example, the supply air temperature is already measured by the system and is used as the input to the PI loop that controls the chiller water valve. This decision was made so that the recorded values were the same as the values being used by the control loops. If additional sensors were to be added, there may be some bias or offset between recorded values and control input values.

The only major component that needed to be installed was the chiller water flow meter. The output of this meter was still shared by the control software and the data logger. Due to certain system constraints, the flow meter had to be noninvasive. The system could not be shut down and disassembled to install an in-line flow meter. For this reason, an ultrasonic flow meter was chosen. The ultrasonic flowmeter is installed on the outside of a rigid pipe and does not

require any system downtime. The flow meter setup used for these experiments can be seen in Figure 3-9 and Figure 3-10.

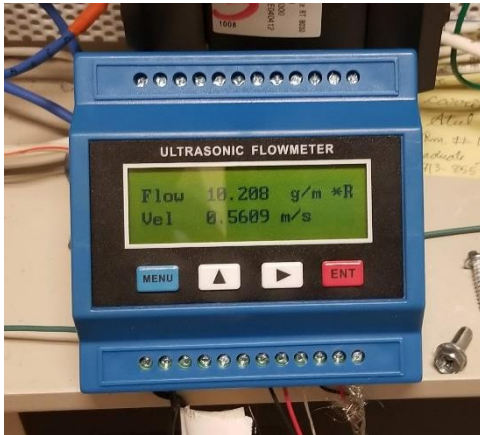


Figure 3-9: Ultrasonic flowmeter

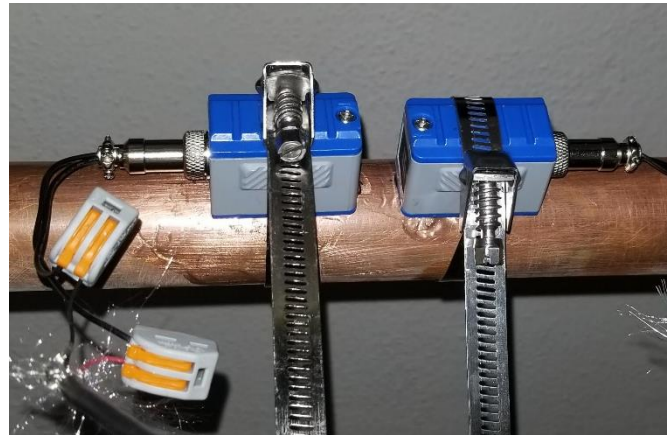


Figure 3-10: Ultrasonic flowmeter transducer setup

One of the main downsides of ultrasonic flow meters is that they can be inherently susceptible to noise. In order to combat the effects of this noise, a type of digital filter in the control software was used. The filter process can be seen in Equation 3.1. This essentially reduces the amount that a measured variable can change between measurements. This strategy removes most noise that could decrease the stability of the control loop while maintaining a reasonable approximation of the measured value.

$$\text{output} = \text{previous output} + [\text{filter constant} * (\text{present input} - \text{previous output})] \quad (3.1)$$

The other concern with ultrasonic flowmeters is that the accuracy is reduced at very low flow velocities. This concern could be neglected because the experiments were conducted during the cooling season when the chiller water flowrate was high.

Experimental tests are crucial but bring about certain limitations. There are many factors in experiments that cannot be controlled. For example, the outdoor air temperature cannot be adjusted to be constant or to follow a perfect pattern. This brings about the need for a reliable

model in which many unique scenarios can be tested. A certain control strategy may show promise during a hot summer day, but is it still beneficial on a mild summer day? It is also important to recognize that the experiments and simulated results can be used to build off each other. Creating and using a model is necessary and complementary to the observations made through experimentation.

3.4 System Modeling

Alongside experimental work, modeling and simulation were used to verify and improve the results. The simulation environment was built up using primarily physics-based models. The choice to build custom models instead utilizing a commercially available software was made largely due to the lack of certain freedoms in the commercial software. Most dynamics of the physical systems can be represented very well by sets of ordinary differential equations (ODEs). Representing the system through sets of ODEs also allows for robust solutions.

The first set of models to discuss will be for the thermal zone and envelope. Modeling these are crucial to creating behavior similar to a real system. Before going into the details of the specific modeling technique used, it is important understand how the system behaves and how the model is expected to behave. The boundaries and scope of the system must also be well defined. For example, when considering the thermal zone, do we only care about the air in the zone? Do we treat the zone and envelope as a control volume? one important behavior that needs to be captured is the effects of the outdoor air temperature on the envelope and the air in the zone. It must also be known how air conditioning and internal gains affect the behavior of the zone and envelope.

The 3R2C (3-Resistor-2-capacitor) modeling technique was used to represent the envelope plus a 1R1C model to represent the thermal zone [33]. This method relies on the heat transfer concept of the thermal circuit. The thermal circuit is used to relate the transfer of heat directly to electrical circuits. This allows many of the same solution techniques of electrical circuits to be used for the thermal zone and envelope model. Steady state results could be determined by implementing a thermal circuit with only resistance. Since the major concern of this work relies on the building dynamics, capacitors are incorporated into the thermal circuit. It is known that some heat transfer in the building will be stored in the envelope, and some will result in a direct temperature change.

An electrical circuit will be used to introduce the concepts necessary to solve the analogous thermal circuit. The dynamic behavior that we expect to see in a thermal zone will be represented by an R-C circuit. Direct correlations can be drawn between components and variables in electrical circuits and in thermal circuits. If heat transfer via conduction is considered, given by Fourier's Law in Equation 3.2 with definitions in Table 3-1, it can be asserted that the temperature difference is the driving force of heat transfer [34]. The temperature difference is analogous to the voltage (V) difference in an electrical circuit which is the driving force of the current (I). The thermal resistance is equivalent to electrical resistance as both impede the "flow" of heat or electrical current. The final analogous components are the thermal capacitance of the building and electrical capacitors. Capacitors in both the electrical and thermal circuits represent an energy storage component that introduce thermal inertia dynamics into the results.

$$q'' = -k\nabla T \quad (3.2)$$

Table 3-1: Conduction heat flux variable definitions

| Parameter | Description |
|------------|----------------------|
| q'' | Heat flux |
| k | Thermal Conductivity |
| ∇T | Temperature Gradient |

Again, from Fourier's Law, it can be noted that the temperature difference or temperature gradient is the driving force of the heat transfer. From this, it can be asserted that a larger temperature difference, with all other factors kept constant, will result in a greater heat transfer rate. A steady state thermal circuit is given by Figure 3-11. It can be seen in this circuit that there are three resistors and no capacitors. This implies that the heat transfer is in steady state because heat cannot be stored in this system. If heat moves from left to right, when T_1 is greater than T_4 , the heat transfer rate must be the same at all points. The heat flowing through R_1 must be the same as the heat flowing through R_2 and R_3 . Since the resistors cannot store energy, it also follows that the heat entering one resistor must be the same as the heat exiting that same resistor. This observation can be equated to Kirchoff's Current Law in Electrical circuits which states that, "the algebraic sum of all the currents at any node in a circuit equals zero." [35] With this relationship, we can solve for the heat transfer rate or unknown temperatures using the techniques derived from Ohm's Law in electrical circuits. The equations that represent this system are shown by Equations 3.3-3.5.

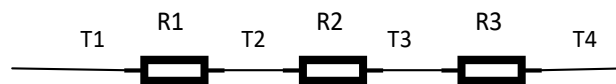


Figure 3-11: Steady state thermal circuit

$$V = IR \quad (3.3)$$

$$I = \frac{V}{R} \quad (3.4)$$

$$q'' = \frac{\Delta T}{R} \quad (3.5)$$

For example, if T_1 , T_4 , and the resistance values are known, the heat transfer rate could be calculated. This could then be used to calculate the temperatures T_2 and T_3 . This calculation is demonstrated below in Equations 3.6-3.9. While parts of this solution may seem trivial, it is valuable to recognize how techniques generally used in electrical circuit solutions can be utilized for thermal circuits. If this thermal circuit were to be used to represent a building wall with known materials, then the heat transfer and temperature gradient through the wall could be calculated.

$$q'' = \frac{T_1 - T_4}{R_1 + R_2 + R_3} \quad (3.6)$$

$$T_1 - T_2 = q'' * R_1 \quad (3.7)$$

$$T_2 = T_1 - (q'' * R_1) \quad (3.8)$$

$$T_2 = T_1 - \frac{(T_1 - T_4) * R_1}{R_1 + R_2 + R_3} \quad (3.9)$$

The resistance in a thermal circuit can also be correlated to resistance in electrical circuits. In an electrical circuit, “resistance is the capacity of materials to impede the flow of current or ... the flow of electric charge” [35]. In the analogous thermal circuit, the thermal resistance can be viewed as the capacity of the material to resist heat transfer. The thermal resistance for 1-D heat transfer per unit area due to conduction through an isotropic material can be calculated using the relationship given by Equation 3.11, where Δx is the material thickness and k is the material thermal conductivity. Due to the relationship between the thermal resistance and heat transfer, a couple of notable conclusions can be made [34]. As thermal conductivity increases, thermal resistance decreases and heat transfer increases. As the material thickness increases, the

resistance also increases. This resistance value is dependent on the material and the geometry but can be a major consideration in building design. For example, if the insulation material in a building can be replaced with a material where the conductivity is reduced, then the heat transfer through the envelope will also be reduced.

$$R = \frac{\Delta x}{k} \quad (3.10)$$

The final major component introduced into the model of the envelope and zone is the capacitor. A capacitor in electrical circuits is a component that is able to store electrical charge, which is crucial to modeling the behavior of the physical system. Figure 3-12 is a diagram of a simple RC circuit that is equivalent to the 1R1C model used for the thermal circuit. Incorporating the capacitor into the circuit allows for the time response of the system to be viewed. Thermal capacitance behaves in the same way, except by storing heat instead of electrical charge. From the simple RC circuit, if we know certain values, then the other values can be calculated using techniques derived from Kirchhoff's Laws. For example, if V_1 , R_1 , and C_1 are known, then V_2 can be calculated.

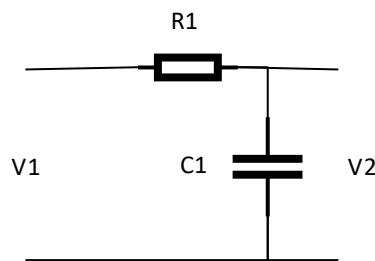


Figure 3-12: Electrical RC circuit diagram

Again, the voltage in the electrical circuit is analogous to temperature, electrical resistance to thermal resistance, and now the electrical capacitor is related thermal capacitance in the system. The thermal capacitance is based on the material density and specific heat and can

be calculated using Equation 3.11. It is introduced to represent the temperature dynamics of a specific node [36]. In a way, the thermal capacitance represents the node's resistance to temperature change for a given heat input. This behavior can be broken down by observing example units of thermal capacitance such as Btu per Fahrenheit (Btu/F) or Joules per Kelvin (J/K). Simply put, the thermal capacitance is the amount of heat required to raise the temperature of that node or section by a specific amount. So, a mass with a larger thermal capacitance will require more heat transfer before the temperature significantly changes.

$$C = mc_p = \rho Vc_p \quad (3.11)$$

Since the thermal parameters (temperature, thermal resistance, etc.) have been directly correlated to their electrical counterparts, the circuit can be solved. The thermal 1R1C model could represent some mass with heat being transferred into it from a surrounding fluid of known temperature. If the temperature of the mass is desired, then it can be determined from the surrounding temperature, resistance, and capacitance. One major assumption made in this step is that for a given capacitance, the temperature is the same throughout. Therefore, the temperature of some mass represented by a capacitor will be more of an average temperature through the mass. To solve for V_2 , or the temperature of the example mass, the first step will involve Kirchhoff's Voltage Law (KVL). KVL states, "The algebraic sum of all the voltages around any closed path in a circuit equals zero." [35] It can be noted that there are two loops in this circuit, as indicated by Figure 3-13.

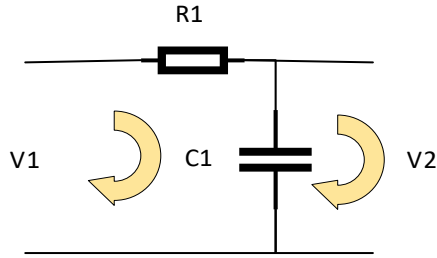


Figure 3-13: RC circuit, current pathways identified

Based on the two loops for current to flow through, two sets of equations can be derived to represent the voltage for each component.

$$V1 - V_{R1} - V_{C1} = 0 \quad (3.12)$$

$$-V_{C1} + V2 = 0 \quad (3.13)$$

This formulation is true, but it does not give us much information and more unknown parameters. The only voltage that is known from the beginning is V1. Using Ohm's law, the voltage across the resistor R1 can be determined in terms of current and resistance. It is known that the voltage across the capacitor C1 is equal to V2, where V2 is the value to be solved for.

$$V2 = V_{C1} \quad (3.14)$$

$$V_{C1} = V1 - V_{R1} \quad (3.15)$$

$$V2 = V1 - V_{R1} \quad (3.16)$$

$$V2 = V1 - R1 * I_{R1} \quad (3.17)$$

This is slightly better because we likely know the resistance value, but there is now a new unknown parameter. This reformulation introduces the current through the resistor as a new unknown to be calculated for. This may seem to be moving away from desired value can be approached by using KCL. Current cannot flow through the path of V2 because it is open, thus the relationship of Equation 3.19 can be asserted.

$$I_{R1} - I_{C1} = 0 \quad (3.18)$$

$$I_{C1} = I_{R1} \quad (3.19)$$

The current through the capacitor can be determined based on the capacitance and the rate of change of the voltage. This is the point at which dynamics are truly introduced into the solution. The current through the capacitor, more accurately the displacement current, can be calculated from Equation 3.20.

$$I_{C1} = C1 * \frac{dV_{C1}}{dt} \quad (3.20)$$

With the current now expressed as known parameters, V2 can be solved for.

$$V2 = V1 - (R1 * C1) \frac{dV2}{dt} \quad (3.21)$$

This is not technically an exact solution but is the ordinary differential form of the RC circuit. However, it shows how the dynamics are introduced into the system by the capacitors to store charge or the thermal capacitance to store heat. An exact solution for this simple system can be calculated, but for more complex systems, numerical solutions will prove necessary. Before getting into the techniques used for the complex system, this system will be reformulated as a thermal circuit given by Figure 3-14.

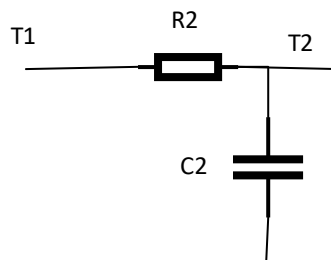


Figure 3-14: 1R1C Thermal Circuit

To reiterate, voltage is equivalent to temperature, resistance to thermal resistance, electrical capacitance to thermal capacitance, and electrical current to heat transfer rate. Therefore, the temperature at node T2 can be determined from Equations 3.22 and 3.23.

$$T2 = T1 - (R1 * C1) \frac{dT2}{dt} \quad (3.22)$$

$$\frac{dT2}{dt} = \frac{T1 - T2}{R1 * C1} \quad (3.23)$$

This formulation gives us an understanding of how the temperature T2 will behave with time. As a type of reality check, the behavior under different conditions should be considered. If T1 is greater than T2, then $\frac{dT2}{dt}$ will be positive, indicating that the temperature T2 will increase. This is exactly what is expected from a physical system. The heat will flow from the point of higher temperature to the point of lower temperature. The temperature at the lower point will also increase as heat transfer into the node occurs. Additionally, if the resistance R1 increases, the rate of temperature change at T2 will decrease. This is expected too as the resistance will affect the heat transfer rate into the node which slows the rate that the temperature will increase. Lastly, the capacitance of the node affects how quickly the temperature will change. If the mass or specific heat is greater, then temperature will change more slowly.

3.4.1 Thermal Zone Modeling using 3R3C Technique

The thermal system of a building envelope and thermal zone is much more complicated than what can be represented by a simple RC circuit (1R1C). Therefore, a suitable model for each must be used. It is necessary to first know what is needed from the model. An incredibly complex model that yields very precise results could be used to represent the system, but this complexity comes at a cost. The system must be solvable and capture the most important behaviors. When modelling the thermal zone, the average air temperature is crucial to calculate. The air temperature is how the airflow through the terminal box is controlled and is crucial for human comfort. For this study, the air temperature is arguably the most important factor calculate, but in order to do this, the status of the envelope must also be known.

In order to determine heat transfer between the wall and the air in the zone, the convection coefficient and temperature difference must be known. The temperature difference here that matters is the difference between the bulk air temperature and the interior wall surface temperature. This same requirement can be said about the exterior wall. It can be asserted that in order to calculate the air temperature dynamics in the zone, the heat entering the zone must be known. In order to know the heat entering the zone through the envelope, the heat transfer rate through the wall must be known. To know the heat transfer rate through the wall caused by the temperature difference, both of the surface temperatures should be known.

Since the thermal capacitance is used to introduce the temperature dynamics, there should be three capacitors in the thermal circuit. One capacitor is needed for the zone air temperature, one for the interior surface temperature, and one for the exterior surface temperature. Additionally, it is known that there is some impedance to heat transfer in the system. Heat does not flow freely at an infinitely large rate. There should be thermal resistance to convection between the zone air and interior wall surface. This is also true for the outdoor air and exterior wall surface [36, 33]. There should also be resistance to conduction through the wall. Most structures are not made out of a single material so the thermal resistance in the wall may vary, but the total resistance can be calculated and used because the temperature of the inside of the wall is not a consideration. The model that meets all of these criteria is given below by Figure 3-15 with notations in Table 3-2.

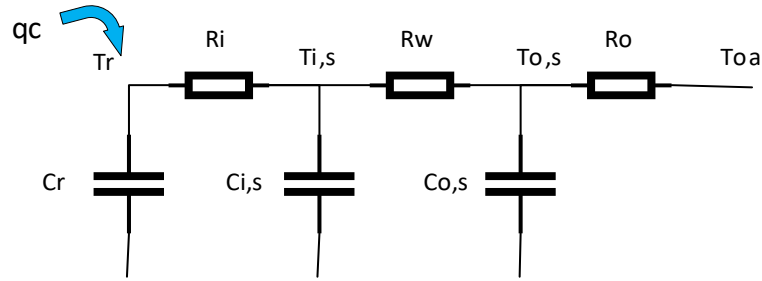


Figure 3-15: 3R3C model

Table 3-2: 3R3C Variable Definitions

| Variable | Description |
|------------------------|--|
| Tr | Zone air temperature |
| T_{i,s} | Wall interior surface temperature |
| To,s | Wall exterior surface temperature |
| R_i | Interior surface convection resistance |
| R_w | Wall conduction resistance |
| R_o | exterior surface convection resistance |
| Cr | Zone air capacitance |
| C_{i,s} | Wall interior surface capacitance |
| C_{o,s} | Wall exterior surface capacitance |
| qc | Direct heat transfer (due to heating or cooling) |

It should be noted that the wall temperature is split into two sections, interior surface and exterior surface. Again, this so that the heat transfer between the wall and the surrounding air, either zone air or outdoor air, can be calculated for the system. One fundamental reason for this is that heat transfer in the system is not immediate. It takes time for the mass to heat up and reach equilibrium with the surrounding temperature. additionally, in a physical system, both surfaces of a wall would rarely be at the same temperature. This could happen in some circumstances but is unlikely, especially during cooling season.

There is also a term “qc” in the model formulation. This term represents heat directly added or removed from the air due to the convective effects of internal gains and the HVAC

system. The term is critical to simulating the AC operation. It is known that the temperature is maintained in a zone (during cooling season) by supplying cool dry air. The sensible cooling rate is affected by the supply airflow rate into the zone and the difference between the supply air temperature and zone air temperature.

The complexity of this model has increased significantly from the 1R1C model and will require solving a set of equations. There should be one ordinary differential equation for each capacitor introduced into the model, three total for this model. The heat transfer rate at each node changes based on the temperature dynamics at that node and surrounding nodes. Nodes with a larger capacitance could prolong a higher heat transfer rate or be taken advantage of through techniques like precooling. The complexity also increases slightly due to the consideration of internal gains and cooling. Based on this revised model, the set of governing equations can be determined and are given by Equation 3.24.

$$\begin{aligned}
 C_r \frac{dT_r}{dt} &= \frac{T_{i,s} - T_r}{R_i} + q \\
 C_{i,s} \frac{dT_{i,s}}{dt} &= \frac{T_{o,s} - T_{i,s}}{R_w} + \frac{T_r - T_{i,s}}{R_i} \\
 C_{o,s} \frac{dT_{o,s}}{dt} &= \frac{T_{oa} - T_{o,s}}{R_o} + \frac{T_{i,s} - T_{o,s}}{R_w}
 \end{aligned} \tag{3.24}$$

The set of differential equations will be solved numerically. Since the system in this formulation is linear, a state-space model will be utilized. The set of Equations will be reorganized to be placed into state-space formulation in Equation 3.25.

$$\begin{aligned}
\frac{dT_r}{dt} &= \frac{1}{C_r R_i} T_{i,s} - \frac{1}{C_r R_i} T_r + \frac{1}{C_r} q \\
\frac{dT_{i,s}}{dt} &= \frac{1}{C_{i,s} R_w} T_{o,s} - \left(\frac{1}{C_{i,s} R_w} + \frac{1}{C_{i,s} R_i} \right) T_{i,s} + \frac{1}{C_{i,s} R_i} T_r \\
\frac{dT_{o,s}}{dt} &= - \left(\frac{1}{C_{o,s} R_o} + \frac{1}{C_{o,s} R_w} \right) T_{o,s} + \frac{1}{C_{o,s} R_w} T_{i,s} + \frac{1}{C_{o,s} R_o} T_{oa}
\end{aligned} \tag{3.25}$$

The standard state-space formulation is given by Equation 3.26, where x is the state variable or set of variables being solved for, \dot{x} is the derivative of x with respect to time (equivalent to $\frac{dx}{dt}$), u is a single input or vector of inputs, and A and B are matrices that define the system. Equation 3.27 is the output Equation where y is the output of the system.

$$\dot{x} = Ax + Bu \tag{3.26}$$

$$y = Cx + Du \tag{3.27}$$

The state variables must be solved for. The inputs, given by u , are independent of the state variables in the system. In the case of this model, the input variables are outdoor air temperature and heat into the zone. Therefore, the state-space model can be developed as Equation 3.28.

$$\begin{aligned}
\begin{bmatrix} \frac{dT_r}{dt} \\ \frac{dT_{i,s}}{dt} \\ \frac{dT_{o,s}}{dt} \end{bmatrix} &= \begin{bmatrix} -\frac{1}{C_r R_i} & \frac{1}{C_r R_i} & 0 \\ \frac{1}{C_{i,s} R_i} & -\left(\frac{1}{C_{i,s} R_w} + \frac{1}{C_{i,s} R_i} \right) & \frac{1}{C_{i,s} R_w} \\ 0 & \frac{1}{C_{o,s} R_w} & -\left(\frac{1}{C_{o,s} R_o} + \frac{1}{C_{o,s} R_w} \right) \end{bmatrix} \begin{bmatrix} T_r \\ T_{i,s} \\ T_{o,s} \end{bmatrix} + \\
&\quad \begin{bmatrix} \frac{1}{C_r} & 0 \\ 0 & 0 \\ 0 & \frac{1}{C_{o,s} R_o} \end{bmatrix} \begin{bmatrix} q \\ T_{oa} \end{bmatrix}
\end{aligned} \tag{3.28}$$

The rate of cooling, as in kW or Btu/h, is not a directly controlled variable on physical systems. For residential systems, the controlled variable would be the AC status, either on or off. Thus, residential cooling often can be assumed to be a constant cooling rate. However, in a commercial system, this assumption would not be valid. The cooling rate will change on a VAV system, such as the system used by the experimental test bed, by adjusting the supply airflow rate into the zone. It is assumed that the supply air flow rate and return airflow rate for each zone are equal during operation. The mass of the air in the zone remains constant. Based on the energy balance and this assumption, the cooling rate can be determined by Equation 3.29. This can then be simplified further based on the volumetric flowrate of the supply air, given by Equation 3.30. This simplification was made because the volumetric flowrate, in cubic feet per minute (cfm), is measured on many systems.

$$q_{cool} = \dot{m}_{air} c_{p,air} (T_{sa} - T_{zone}) \quad (3.29)$$

$$q_{cool} = 1.1 * Q_{sa}[cfm] * (T_{sa} - T_{zone}) \quad (3.30)$$

This relationship can then be inserted back into the governing Equations, as given by Equation 3.31. This substitution makes the system nonlinear but allows for a variable cooling rate to be applied to the zone. This is a critical behavior because the supply airflow rate varies in many systems and most importantly on the experimental test bed.

$$\begin{aligned} \frac{dT_r}{dt} &= \frac{1}{C_r R_i} T_{i,s} - \left(\frac{1}{C_r R_i} + \frac{1.1 Q_{sa}}{C_r} \right) T_r + \frac{1}{C_r} q_{ig} + \frac{1.1 Q_{sa}}{C_r} T_{sa} \\ \frac{dT_{i,s}}{dt} &= \frac{1}{C_i R_w} T_{o,s} - \left(\frac{1}{C_i R_w} + \frac{1}{C_i R_i} \right) T_{i,s} + \frac{1}{C_i R_i} T_r \\ \frac{dT_{o,s}}{dt} &= - \left(\frac{1}{C_o R_o} + \frac{1}{C_o R_w} \right) T_{o,s} + \frac{1}{C_o R_w} T_{i,s} + \frac{1}{C_o R_o} T_{oa} \end{aligned} \quad (3.31)$$

The nonlinearity introduced through the cooling substitution inhibits solving the set of Equations using traditional linear techniques. However, since the system is solved numerically, it

will still be represented by a state-space model. This new model is given by Equation 3.32. In a sense, the system will be linearized at each time step and then solved for that time step. At time step the A matrix and B matrix are each calculated based on the current operating conditions.

$$\begin{bmatrix} \frac{dT_r}{dt} \\ \frac{dT_{i,s}}{dt} \\ \frac{dT_{o,s}}{dt} \end{bmatrix} = \begin{bmatrix} -\left(\frac{1}{C_r R_i} + \frac{1.1 Q_{sa}}{C_r}\right) & \frac{1}{C_r R_i} & 0 \\ \frac{1}{C_{i,s} R_i} & -\left(\frac{1}{C_{i,s} R_w} + \frac{1}{C_{i,s} R_i}\right) & \frac{1}{C_{i,s} R_w} \\ 0 & \frac{1}{C_{o,s} R_w} & -\left(\frac{1}{C_{o,s} R_o} + \frac{1}{C_{o,s} R_w}\right) \end{bmatrix} \begin{bmatrix} T_r \\ T_{i,s} \\ T_{o,s} \end{bmatrix} + \begin{bmatrix} \frac{1}{C_r} & 0 & \frac{1.1 Q_{sa}}{C_r} \\ 0 & 0 & 0 \\ 0 & \frac{1}{C_{o,s} R_o} & 0 \end{bmatrix} \begin{bmatrix} q_{i,g} \\ T_{oa} \\ T_{sa} \end{bmatrix} \quad (3.32)$$

The modeling parameters were chosen based on the properties of physical systems. The modeled consists of three thermal zones named as Zone A, Zone B, and Zone C. The zones are identical in size and structure. The thermal zones are 30'x30'x9'. no walls are shared between zones. So, each zone is surrounded by outdoor air. The basic layout of the thermal zones is given by Figure 3-16.

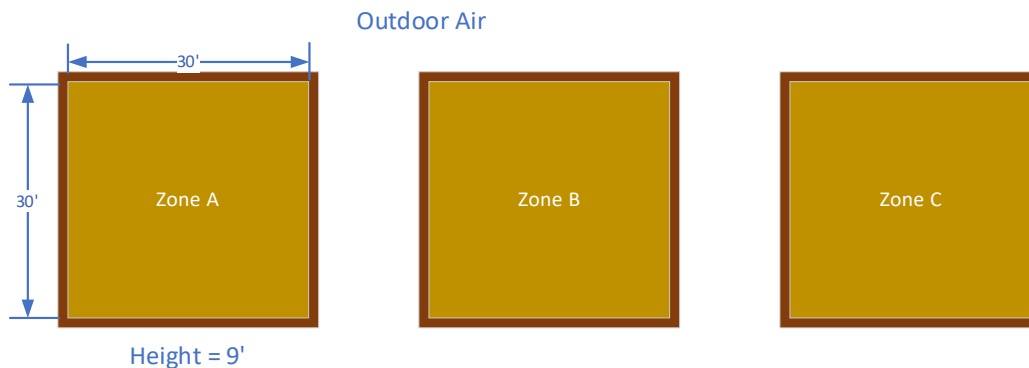


Figure 3-16: Model of Thermal Zones

It is assumed that heat can transfer through all 4 walls, the floor, and the ceiling. Therefore, the area of the envelope for each zone is 2880 ft². Based on the envelope area and

structure materials, the thermal resistance can be calculated. The walls are composed of three layers. From the interior to exterior, the layers are drywall, lightweight fiberglass insulation, and brick. This structure can be seen in Figure 3-17.

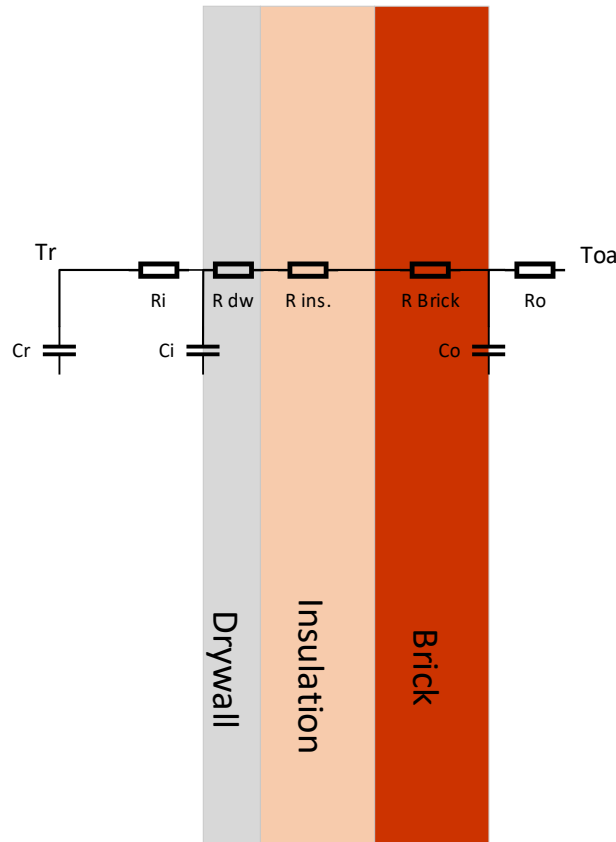


Figure 3-17: Envelope RC Model

The resistance and capacitance values can be determined using standard material properties, given in Table 3-3 [27]. The thermal resistance for heat transfer through conduction is a function of the structure geometry and the conductivity. The thermal capacitance is a function of the mass and specific heat of the material. The mass of each component can be determined from the geometry and density. For example, the volume of the thermal zone 8100 ft³. The mass of the air can be calculated using the average density.

Table 3-3: Model Envelope Materials

| Structure | Cp | Density | Conductivity | Thickness | Resistance |
|-----------------------------------|-----------|---------------------|------------------------------|------------------|---------------------------|
| | Btu/lbm-F | lbm/ft ³ | Btu-in/hr-ft ² -F | inch | Ft ² -f-hr/Btu |
| Outside air resistance(A0) | | | | | 0.1255 |
| Brick (A2) | 0.22 | 125 | 9.24 | 4 | |
| Insulation(B15) | 0.201 | 5.7 | 0.3 | 6 | |
| Lightweight concrete (C14) | 0.2 | 40 | 1.2 | 4 | |
| Inside air resistance(E0) | | | | | 0.687 |

The capacitance values must be separated in some way. It is known that there are two temperature dynamics that must be tracked, which are each represented by a capacitor. There are numerous ways that each capacitance value of the wall structure could be determined. One method is to determine the total capacitance of all components of the wall structure, then treat each capacitance as a fraction of the total. So, if there are two capacitors in the model, each will be half of the total capacitance. This method is generally better suited to a structure in which the materials have similar capacitance or density and specific heat values.

The capacitance values of the wall for this model were calculated by separating the materials. The capacitor representing the interior portion was determined by the capacitance of only the lightweight concrete. The capacitor representing the exterior section of the wall was chosen to be the capacitance of both the brick layer and the insulation layer. The resistance and capacitance values used for the models are shown in Table 3-4.

Table 3-4: Model RC Values

| Parameter | Value |
|------------------|---------------------|
| Ri | 8.56 E-01 [F-s/Btu] |
| Rw | 5.31 E-01 [F-s/Btu] |
| Ro | 3.13 E-01 [F-s/Btu] |
| Ci | 7.68 E+03 [Btu/F] |
| Co | 2.80 E+04 [Btu/F] |
| Cr | 1.05 E+02 [Btu/F] |

With the resistance and capacitance values determined, the system can be modeled. These values are used in both the state of the art model and models using the proposed control strategies. It is desired to see how the behavior of the system changes by adjusting control methods, not by changing the materials.

3.4.2 Modeling Terminal Box Operation

Moving up one layer from the thermal zone and envelope, the variable air volume operation of the terminal box is reached. Based on the last formulation of the thermal zone and envelope state-space model, the supply airflow rate into the zone has become increasingly important. The system is fairly complex like most systems in buildings but can be reduced down to the most important behaviors that need to be present.

The airflow rate into the zone, both on a physical system and in the model, is controlled through the use of a proportional-integral (PI) controller. This is a reference tracking controller based on the zone temperature. The goal is to reduce the error between the measured zone temperature and the zone setpoint. If the zone temperature is higher than the setpoint, then the terminal box damper will open further allowing more cold air into the zone. Conversely, if the zone temperature is lower than the setpoint, then the damper will close to reduce the airflow into the zone. The controller will continuously signal the terminal box to open and close to reduce the zone temperature error.

One behavior that must be captured is the delay or lag in the damper operation. An improperly tuned controller could signal for the damper to rapidly open and close, but that does not necessarily mean the damper would fully open or close instantaneously. For example, the

VAV actuators in the EL building have a drive time of 300 seconds. This means that it takes 5 minutes for the damper to move from the fully closed position to the fully open position. If the damper velocity is constant through its range, then the actual position of the damper can be represented by a first order system. A time constant of 60 seconds will be used for this system because it takes 5 time constants for a first order system to settle within 99.3% from a step response [37].

The airflow rate through the terminal box on a true system is complex and dependent on fluid principles. The exact behavior down to the level of airflow rate fluctuations due to pressure changes or slight variations in fan speed is not necessary. The important requirements are that the desired airflow rate based on the PI controller output is available and a realistic lag is placed on this value to prevent the system dynamics from becoming unreasonably fast. The control diagram for this scenario is given by Figure 3-18. In this, certain limitations are placed to increase the accuracy of the behavior. The output of the controller is saturated between the minimum value (30%) and the maximum (100%). This represents the minimum supply air flow rate as required by ASHRAE Standard 62 [38]. The gain of the first order transfer function represents the maximum flow rate into the zone, and the time constant is based on the actuator drive time.

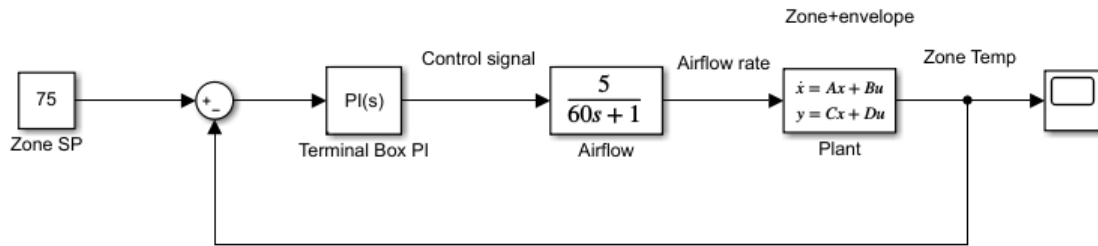


Figure 3-18: VAV Control Diagram

If Figure 3-18 is followed from start to finish (left to right), the error is calculated based on the reference and zone temperature output from the state-space model. The PI controller uses this error to calculate a new output or desired airflow rate percentage. The desired airflow moves to the transfer function that outputs the actual airflow rate for the model. The plant is simplified in this diagram but represents the thermal zone and envelope. The new zone temperature is calculated, and the process starts over with a new error into the controller.

3.4.3 Modeling AHU operation

Following the air distribution, the air handling unit is the next layer up from the terminal box operation. The air handling unit as a whole introduces many complex operations but some are not relevant to this work. There are operations of two components in the AHU that must be captured by the model, the change in airflow rate caused by the supply air fan and the dynamics of the cooling coil and associated components. As seen in Figure 3-2, many components aside from the cooling coil and supply air fan are required for true operation of the AHU. The main outcomes of this work will rely on the cooling coil load or the heat transfer rate of the cooling coil, so not all components are necessary to the model. The simulation period is assumed to be during cooling season so the preheat coil will not be used. It is also assumed that the conditions

of the air entering the cooling coil are known. If all of these parameters are known, then the effects of the filter and RA/OA dampers are not necessary to calculate.

The supply air fan provides the driving force that moves cool, dry air to all of the zones. The fan in a physical system moves the air by providing a pressure rise that will overcome the pressure losses due to friction, fittings, and components like the terminal boxes. The objective of the model supply air fan is to meet the total desired airflow rate from all zones, as discussed in the terminal box operation section. The behavior that should be captured by the model is the delay of the actual supply airflow rate approaching the desired airflow rate. The terminal box desired flow rate increasing quickly that does not mean the supply air fan can adjust instantaneously. The actual supply air flow rate in the model is calculated by a PI controller with the reference as the total desired supply airflow rate from all zones.

A simplified supply air fan model was chosen to capture the relevant behavior with a reasonable level of complexity. High complexity supply air fan and air distribution models would require the calculations of the pressure changes throughout the system. The main behavior that needs to be captured in this study is how the supply air flowrate changes with respect to time and controller input. This was captured by using a PI controller and a first order transfer function. The input to the controller is the error between the current supply air flowrate and the total desired flowrate from all zones. The controller tuning creates dynamics like the physical system controller, and the transfer function introduces the delay in the fan speed and flowrate change. This control loop is given in Figure 3-19.

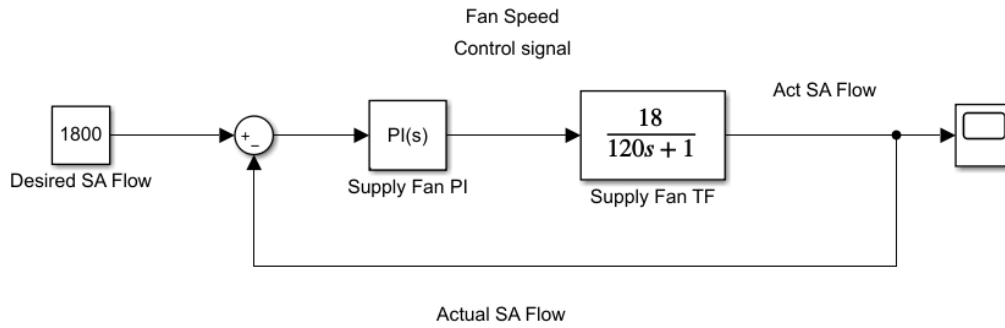


Figure 3-19: Supply Air Fan Model

The cooling coil operation is more complex to solve and capture the necessary behaviors. The basic function of the cooling coil is to remove heat from the mixing air so that the supply air reaches proper operating conditions. The supply air temperature is actually controlled by modulating the chiller water control valve. By adjusting the chiller water flow rate, the cooling coil heat transfer rate will change resulting in a change in supply air temperature. The behaviors that must be captured in the cooling coil model are that the exiting supply air and chiller water temperatures can be calculated, the heat transfer rate is affected by the flow rate of both the chiller water and supply air, and each part of the heat exchanger has some thermal dynamics. For example, on a given cooling coil, increasing the chiller water flowrate while keeping all other parameters constant would decrease the exiting air temperature. This exiting air temperature change would not be instantaneous. It will take a small amount of time for the heat exchanger surface temperature to change and time for the air temperature in the final section of the coil to change.

Again, the most important outcome of the cooling coil model is to understand the load behavior over the simulation time. the actual magnitude of the cooling coil load is useful, but

even more important is how this load changes as other factors change. How does the cooling coil load change as supply airflow rate increases? Even deeper, how does the cooling coil load change as outdoor air temperature changes or as the zone temperature setpoint is adjusted? Due to the considerations listed, the cooling coil model is discretized and in dry cooling operation.

The basic framework of the cooling coil model can be viewed similarly to the 3R3C model used for the thermal zone and envelope. An overly simplified version in which the cooling coil is treated as only one discrete section is given by Figure 3-20 to introduce the basic concepts. In this cooling coil, there are two or three points of interest in which the temperature is desired. The temperature of the water leaving the coil, the temperature of the air, and the cooling coil surface temperature. The entering conditions of both the air and the chiller water are known in this model.

From heat exchanger operation and drawing from Figure 3-20, certain broad assertions can be made. In an air-to-water heat exchanger in operation, there is some heat transfer due to convection between the water and the material of the actual heat exchanger. There is also some heat transfer due to convection between the heat exchanger material and the air. The heat transfer pathway is represented by the resistors. There is some flow of the fluids in the heat exchanger. It is an open system with mass entering and exiting the control volume. Again, the temperature at each node does not change instantaneously, represented by a capacitor. The total heat transfer rate will change as the flow rate of either fluid changes. The heat transfer rate changes both due to the mass flow rate fluctuating directly and because the convection coefficient will change as the fluid velocity changes. The basic formulation of this cooling coil

model is based on the discrete model proposed by Zhou [39]. The chiller water and coil are each represented by differential equations, but the resistance value is determined in a different way.

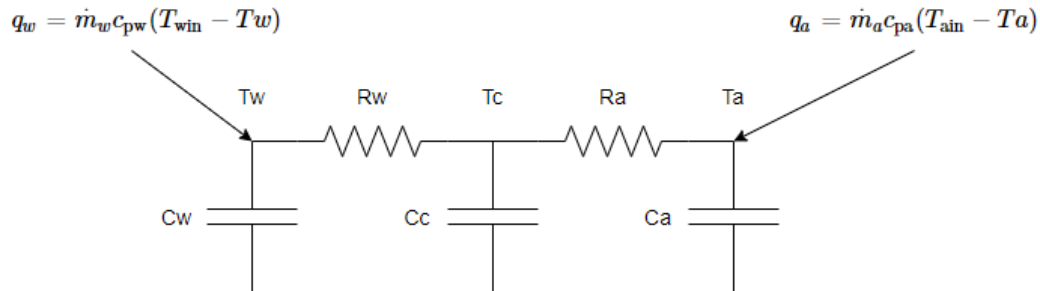


Figure 3-20: single node cooling coil thermal circuit

The dynamics of this cooling coil can be represented by a set of differential Equations much like the thermal zone and envelope. The governing equations for this single node cooling coil are given by Equations 3.33, where variable descriptions are given in Table 3-5.

$$\begin{aligned}
 C_w \frac{dT_w}{dt} &= \frac{T_c - T_w}{R_w} + \dot{m}_w c_{p,w} (T_{w,in} - T_w) \\
 C_c \frac{dT_c}{dt} &= \frac{T_w - T_c}{R_w} + \frac{T_a - T_c}{R_a} \\
 C_a \frac{dT_a}{dt} &= \frac{T_c - T_a}{R_a} + \dot{m}_a c_{p,a} (T_{a,in} - T_a)
 \end{aligned}
 \tag{3.33}$$

Table 3-5: cooling coil model variable descriptions

| Variable | Description |
|-------------|--|
| $T_{w, in}$ | Water inlet temperature |
| T_w | Bulk water temperature (assumed to be exiting temperature) |
| T_c | Coil temperature |
| T_a | Air temperature (assumed to be exiting temperature) |
| $T_{a, in}$ | Air inlet temperature |
| R_w | Water side resistance |
| R_a | Air side resistance |
| C_w | Water capacitance |
| C_c | Coil capacitance |
| C_a | Air capacitance |

A simple reality check can be conducted based on these governing equations. Looking at the equation for water temperature, if the coil temperature is higher than the water temperature, then the exiting water temperature will increase due to the convection, as expected. If the mass flow rate of the water increases and $T_{w,in}$ is less than T_w , then the exiting water temperature will decrease. More cold water entering the system with other parameters held constant should decrease the exiting the water temperature. The same observations can be made about the air side node. Heat transfer to and from the cooling coil material is only due to convection, which is expected because that mass does not change.

The resistance which represents convection in the model is expected to change as fluid velocity changes. This fluid velocity will change as the mass flowrate or volumetric flowrate changes. On a system with a constant cross-sectional area, the fluid velocity will change linearly with mass and volumetric flowrates. The relationship between volumetric and mass flow rates and fluid velocity are given by Equations 3.34 and 3.35.

$$Q = AV \quad (3.34)$$

$$\dot{m} = \rho AV \quad (3.35)$$

The basic idea of how these resistance values will be determined is to calculate the resistance values at some known conditions, then adjust the resistance based on the fluid velocity. Dimensions and heat exchanger effectiveness at known conditions for the model are based on cooling coil in the experimental test building. It is an 8-ton cooling coil and with a design chiller water temperature difference of 12° F. The initial resistance values are calculated from the

design conditions of this cooling coil. The resistance due to convection is the inverse of the convection coefficient as given by Equation 3.36.

$$R_{conv} = \frac{1}{h_{conv}} \quad (3.36)$$

The convection coefficient can be corrected based on an understanding of the Nusselt number for a particular heat exchanger. The relationship between the Nusselt number and convection coefficient is given by the following Equations 3.37 and 3.38.

$$Nu = \frac{hA}{k} \quad (3.37)$$

$$h = \frac{Nuk}{A} \quad (3.38)$$

The chiller water in the cooling coil flows through a series of tubes. During cooling season, when the cooling coil load is high, the chiller water flow will likely be turbulent. This due to the higher water flow rate required during high cooling periods and the small diameter of the tubes. Based on this assumption, the Dittus-Boelter Equation given by Equation 3.39 can be used to calculate the Nusselt number for the chiller water [34].

$$Nu_D = 0.023Re_D^{0.8}Pr^{0.4} \quad (3.39)$$

The convection coefficient correlation for the airflow side can be determined through Equation 3.40, which is the Nusselt number correlation for a flow across a bank of tubes [34].

$$Nu_D = 0.40Re_D^{0.6}Pr^{0.36} \left(\frac{Pr}{Pr_s} \right)^{\frac{1}{4}} \quad (3.40)$$

Since the convection coefficient values at design conditions are already known, these correlations will be used to correct the resistance values. The convection coefficient for the water side is corrected by comparing the Nusselt number at current conditions to that at design

conditions. The relationship is given in the following Equation 3.41, where Nu is the current Nusselt number and Nu' is at design conditions.

$$\frac{Nu}{Nu'} = \frac{h}{h'} = \left(\frac{Re}{Re'}\right)^{0.8} = \left(\frac{V}{V'}\right)^{0.8} = \left(\frac{Q/A}{Q'/A}\right)^{0.8} = \left(\frac{Q}{Q'}\right)^{0.8} \quad (3.41)$$

The correction of the convection coefficient can be reduced to terms of only the fluid velocity. Since the cross-sectional area in the tube is constant over time, the relationship can also be made in terms of the flowrate. This can be useful in comparing the model to a physical system as many design values are in terms of the flowrate, not velocity. Additionally, the Prandtl number will cancel out in the correction because it is based on the fluid material properties. The corrected resistance value 'R' for the chiller water side convection can then be determined by Equation 3.42.

$$R_{water} = R'_{water} \left(\frac{Q}{Q'}\right)^{0.8} \quad (3.42)$$

The air side resistance can also be corrected with the appropriate correlation, given by Equations 3.43 and 3.44.

$$\frac{Nu}{Nu'} = \frac{h}{h'} = \left(\frac{Q}{Q'}\right)^{0.6} \quad (3.43)$$

$$R_{air} = R'_{air} \left(\frac{Q}{Q'}\right)^{0.6} \quad (3.44)$$

A basic model of the cooling coil has been introduced including a method to correct the resistance values, but there has been a major simplification. Treating the cooling coil as one node will force the temperature difference driving the heat transfer to either use the entering or exiting temperatures of the fluids. This is a poor assumption because the temperature difference would not be consistent across the entire coil. For example, a parallel flow heat exchanger would

have the greatest temperature difference where both fluids enter and the smallest temperature difference at the exiting location. The temperature difference that causes heat transfer is not the same at every location.

The assumption that the cooling coil can be represented by a single section will significantly impact the accuracy and behavior of the model. The cooling coil model will be discretized into multiple sections to provide a range of temperatures and increase the accuracy of the solution. The cooling coil will be split into 'N' discrete sections. The coil will be treated as a counter flow heat exchanger, where fluids enter from opposite nodes or sections. The chiller water will enter through the first node and exits from node 'N'. The air moves in the opposite direction, entering node 'N' and exiting from the first node. The discretized cooling coil model is shown as Figure 3-21. In this figure, the discrete sections range from 1 to 'N' with section 'i' being the index for all sections in between.

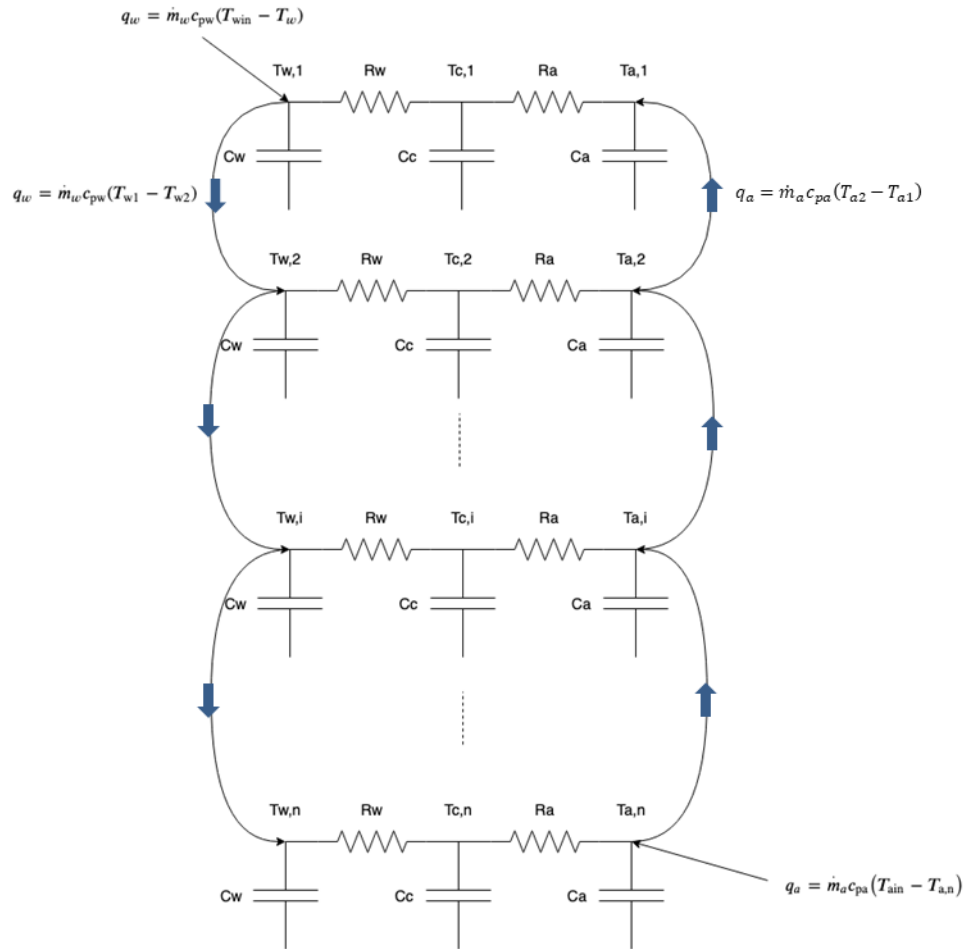


Figure 3-21: Discretized cooling coil diagram

This formulation of the cooling coil allows for a range of temperature differences to be incorporated into the model. This allows for unique heat transfer rates to be calculated based on the temperatures of each fluid at each node. The desired outcome of this model is to be able to determine the exiting temperatures of each fluid, air and chiller water, and to determine the total heat transfer rate or cooling coil load. The exiting fluid temperatures are considered to be equivalent to the fluid temperature at the final node before the fluid exits. So, the exiting chiller water temperature is $T_{w,n}$ and the supply air temperature is $T_{a,1}$. This system is represented by Equations 3.45-3.47., shown below.

$$\begin{aligned}
\frac{dT_{w1}}{dt} &= -\left(\frac{1}{C_w R_w} + \frac{\dot{m}_w c_{p,w}}{C_w}\right) T_{w1} + \frac{1}{C_w R_w} T_{c1} + \frac{\dot{m}_w c_{p,w}}{C_w} T_{w,in} \\
\frac{dT_{c1}}{dt} &= \frac{1}{C_c R_w} T_{w1} + \left(\frac{-1}{C_c R_w} + \frac{-1}{C_c R_a}\right) T_{c1} + \frac{1}{C_c R_a} T_{a1} \\
\frac{dT_{a1}}{dt} &= \frac{1}{C_a R_a} T_{c1} + \left(\frac{-1}{C_c R_a} + \frac{-\dot{m}_a c_{p,a}}{C_a}\right) T_{a1} + \frac{\dot{m}_a c_{p,a}}{C_a} T_{a2}
\end{aligned} \tag{3.45}$$

⋮

$$\begin{aligned}
\frac{dT_{w,i}}{dt} &= -\left(\frac{1}{C_w R_w} + \frac{\dot{m}_w c_{p,w}}{C_w}\right) T_{w,i} + \frac{1}{C_w R_w} T_{c,i} + \frac{\dot{m}_w c_{p,w}}{C_w} T_{w,i-1} \\
\frac{dT_{c,i}}{dt} &= \frac{1}{C_c R_w} T_{w,i} + \left(\frac{-1}{C_c R_w} + \frac{-1}{C_c R_a}\right) T_{c,i} + \frac{1}{C_c R_a} T_{a,i} \\
\frac{dT_{a,i}}{dt} &= \frac{1}{C_a R_a} T_{c,i} + \left(\frac{-1}{C_c R_a} + \frac{-\dot{m}_a c_{p,a}}{C_a}\right) T_{a,i} + \frac{\dot{m}_a c_{p,a}}{C_a} T_{a,i+1}
\end{aligned} \tag{3.46}$$

⋮

$$\begin{aligned}
\frac{dT_{w,n}}{dt} &= -\left(\frac{1}{C_w R_w} + \frac{\dot{m}_w c_{p,w}}{C_w}\right) T_{w,n} + \frac{1}{C_w R_w} T_{c,n} + \frac{\dot{m}_w c_{p,w}}{C_w} T_{w,n-1} \\
\frac{dT_{c,n}}{dt} &= \frac{1}{C_c R_w} T_{w,n} + \left(\frac{-1}{C_c R_w} + \frac{-1}{C_c R_a}\right) T_{c,n} + \frac{1}{C_c R_a} T_{a,n} \\
\frac{dT_{a,n}}{dt} &= \frac{1}{C_a R_a} T_{c,n} + \left(\frac{-1}{C_c R_a} + \frac{-\dot{m}_a c_{p,a}}{C_a}\right) T_{a,n} + \frac{\dot{m}_a c_{p,a}}{C_a} T_{a,in}
\end{aligned} \tag{3.47}$$

This formulation is easily scalable to reach the desired level of accuracy. The coil could be split into any number of nodes. Overall, more nodes will increase the accuracy of the model, but that comes at a computational cost. Each section has a set of three equations that must be solved. The A matrix representing this coil will be of size $[3n \times 3n]$ where n is the number of sections in the coil. The solution for this work requires enough accuracy that operational changes are verifiable and can be captured. The coil has been separated into ten sections for this simulation.

The cooling coil is the final major component that needs to be modeled so that the simulated behaviors represent the physical system. The complete system behavior can now be captured with acceptable models of necessary components and subsystems.

The cooling coil was separated into ten sections to introduce a sufficient temperature distribution. The resistance values were chosen such that the supply air temperature could be maintained at peak load conditions with a chiller water flowrate of 12 gallons per minute. Additionally, the resistance values were set so that the chiller water temperature difference across the cooling coil at design conditions was 12°F. The material parameters were chosen so that the simulated cooling coil had similar characteristics to a physical coil of the same size. These range from the total mass of chiller water in the coil to the material of the coil being aluminum.

Chapter 4 Energy-feedback control analysis through simulation and experimentation

4.1 Energy-feedback control compared with conventional temperature set point adjustment control

4.1.1 Demand control by using temperature reset adjustments

The primary desired objective is to reduce and control the cooling coil load in a predictable and repeatable way. This could be done for multiple reasons such as to reduce the cost effects of peak hours or time of use (TOU) rates. First, the state of the art method and necessary background information will be introduced. If one wishes to reduce the cooling load in a zone, then the heat entering the zone must be reduced. This could be accomplished in multiple ways. The most obvious may be to reduce internal gains in the zone. However, this may not be possible in many circumstances. If an office building is considered, the internal gains could come from computers, lighting, and people among other sources. These heat sources cannot just be removed while routine office work continues. The people need to be able to see and work. The heat entering the zone through the envelope must also be considered. Based on 3R2C envelope model or the physical system is considered, it is known that the temperature difference between the zone air and outdoor air is the driving force behind heat transfer through the envelope. Unfortunately, the outdoor air temperature is not something that can be controlled. However, the zone air temperature can be controlled by adjusting the zone air temperature setpoint. During cooling season, this reduced temperature difference will result in a lower heat transfer rate through the envelope.

The cooling loads in all zones will contribute to the cooling coil load. If the load in a zone increases, then the amount of cool, dry air supplied to that room must also increase in order to

maintain the comfort conditions in the zone. As conditioned air entering the zone increases, the supply air flowrate must also increase. The supply air conditions are known to be 55°F, as required by ASHRAE Standard 90.1, and 90-95% RH [40]. Therefore, the cooling coil load will increase by increasing the supply air flowrate if the entering air and supply air conditions are maintained by modulating the chiller water control valve. This provides the necessary context for the current method of reducing cooling coil load and overall building load. The cooling coil load can be reduced by increasing the zone temperature setpoints throughout the building.

The amount of supply air needed to maintain a certain zone air temperature will reduce as the zone temperature setpoint increases and the system dynamics reach steady state. This is an expected response as less heat is transferred into the zone through the envelope. However, there is another response in the cooling load that should be acknowledged. If the zone temperature setpoint is increased by some amount, then the terminal box damper will begin to close until the zone temperature reaches the new setpoint. During this time, the amount of air entering the zone will be greatly reduced and could even reach the minimum flow limit. As the zone air temperature increases to the new setpoint, the cooling coil load due to this zone will decrease dramatically. The total cooling coil load can be reduced considerably for a limited time if multiple zones served by an AHU experience a zone temperature setpoint reset. However, as the zones heat up and pass the new setpoint, the damper will begin to open again. Then the cooling coil load due to these zones will also begin to increase.

The sharp decrease in cooling load at the onset of a zone temperature setpoint reset may not be ideal in all scenarios but can be useful under some circumstances. The zone temperature reset could prevent failure in a scenario where the building is approaching a hard limit in power

consumption. This dynamic behavior also brings about certain drawbacks. As the dampers begin to open to maintain the new zone temperature setpoint, the load increases. The load will still be less than the original load but will not be controlled precisely. This brings about a tradeoff between precise zone temperature control or precise load control. Therefore, the studied energy-feedback control in this thesis is a means to provide precise load control when load demand becomes the first priority.

4.1.2 Energy Demand Respond (EDR) using energy-feedback control for the cooling coil

Instead of adjusting the zone temperature conditions, the cooling coil load is directly controlled throughout the duration of EDR operation. This operating mode is used to address the previous concern of imprecise load control. However, it also brings about new compromises that must be considered. If the load is to be precisely controlled, then a tradeoff must be made somewhere. The load cannot simply be reduced while still fully meeting comfort levels. During EDR control, human comfort in the affected thermal zones is essentially treated as a secondary concern with the primary concern being the cooling coil load.

All of this is not to say that human comfort does not matter at all. The requirement to choose between cooling coil load and accurate temperature control just indicates that operating constraints and needs will change at times. If it were the case that human comfort was unimportant, then the most effective way to reduce HVAC power consumption would be to simply disable all operation, which is not a feasible solution in most scenarios. This introduces the requirement to choose a cooling coil load that is sufficiently reduced but is still enough to keep people safe or comfortable.

In order to understand how energy demand response control is implemented, it is important to remember how certain components operate under normal conditions. First, the supply air temperature must be maintained at 55°F [40]. This is done by modulating the chiller water valve position, which in turn, alters the chiller water flow rate. Next, the supply air fan speed is adjusted to maintain a certain duct static pressure. The positive duct static pressure ensures that each zone receives ample supply airflow. These two control loops work together to provide enough cool, dry air to maintain desired conditions in the thermal zone.

If the cooling coil load is to be precisely maintained, then one of these two constraints must be given up. This decision is not necessarily straightforward, as each requirement has important justifications for existing. To start, the supply air temperature must be maintained because the cool air is what will actually maintain the desired conditions in the thermal zones. If the supply air temperature increases by too much, then the thermal zone temperature could not be maintained. A slight increase in supply air temperature could be offset by increasing the supply air flowrate, but this introduces even more concerns. It may not be feasible to increase the supply air flowrate would increase for all zones based on the fan limitations. The increase in fan power could also be considered in this scenario. Increasing the fan power will not only directly increase the total power consumption but will also increase the cooling coil load as the heat generated by the fan must still be removed. Additionally, an increase in the supply air temperature will result in less moisture being removed from the air during wet or partial-wet cooling. This could introduce problems as the zone humidity increases beyond reasonable levels.

The other constraint that may be given up is the duct static pressure. The real concern with this is not necessarily the actual duct static pressure but if each zone is receiving enough

supply air. A forced reduction in supply air flowrate will result in a cooling coil load reduction but will also result in thermal zone temperature increases during cooling season. The air supplied to thermal zones not only removes heat but is also responsible for maintaining indoor air quality (IAQ) [38]. The supply air contains some ratio of fresh outdoor air mixed with return air from all of the zones. As supply air enters the zone, the air contaminants become diluted to acceptable levels. This is the primary reason that minimum supply air flowrates for each zone exist. Reducing the supply air flowrate by too much may result in undesirable levels of contaminants like carbon dioxide or volatile organic compounds.

In order to determine which constraint should be released, certain assumptions were made about the operating conditions in which EDR control would be implemented. First, EDR control is not a control method that would run at all times. It would only be implemented for relatively short periods during which it was deemed that load management outweighed human comfort and IAQ requirements. Next, the thermal comfort condition outweighs the IAQ conditions during this time. This operation could make the zone temperature even hotter if the supply air temperature is not maintained. Supplying warm or hot air to the zone would not remove enough heat to keep the room conditions bearable. Additionally, if the IAQ requirements were to be maintained, even more heat would enter the system as the fan power is increased.

Therefore, the constraints that must be met for EDR operation are to precisely maintain the supply air temperature and cooling coil load. Due to the nature of heat exchangers, the supply air temperature could be controlled in more than one way. If all operating conditions are held the same, then increasing the chiller water flowrate will decrease the supply air temperature. Alternatively, a decrease in supply air flowrate will result in a decrease in supply air temperature.

The supply air temperature in this case is regulated by adjusting the supply air fan speed and in turn the supply air flowrate. A PI control loop is used to eliminate the operating error and maintain the temperature at 55°F.

The cooling coil load is then regulated by the chiller water control valve which alters the chiller water flow rate. By increasing the chiller water flowrate, the cooling coil load can increase. More heat can be removed from the air as more cold chiller water flows through the cooling coil. Again, the cooling coil load is not directly measured but can be calculated from measured values as shown in Equation 4.1. The heat removed from the air must enter the chiller water. The sensible heat transfer rate of the chiller water can be used because there is no phase change.

$$q_{cc} = \dot{m}_{cw} c_{p,cw} (T_{cw,in} - T_{cw,out}) = \dot{m}_{sa} (i_{sa,out} - i_{sa,in}) \quad (4.1)$$

The chiller water measurements are also generally simpler to take and fewer are required. The only points that must be measured are the entering CHW temperature, the exiting CHW temperature, and the CHW flowrate. If the air side were to be used to additional measurements would be required to calculate the enthalpy. This could be the wet-bulb temperature or relative humidity. Each additional measurement offers more opportunity for sensor error to affect the calculation. The cooling coil load used by the control sequence is calculated from the chiller water conditions. Both control sequences are shown in Figure 4-1.

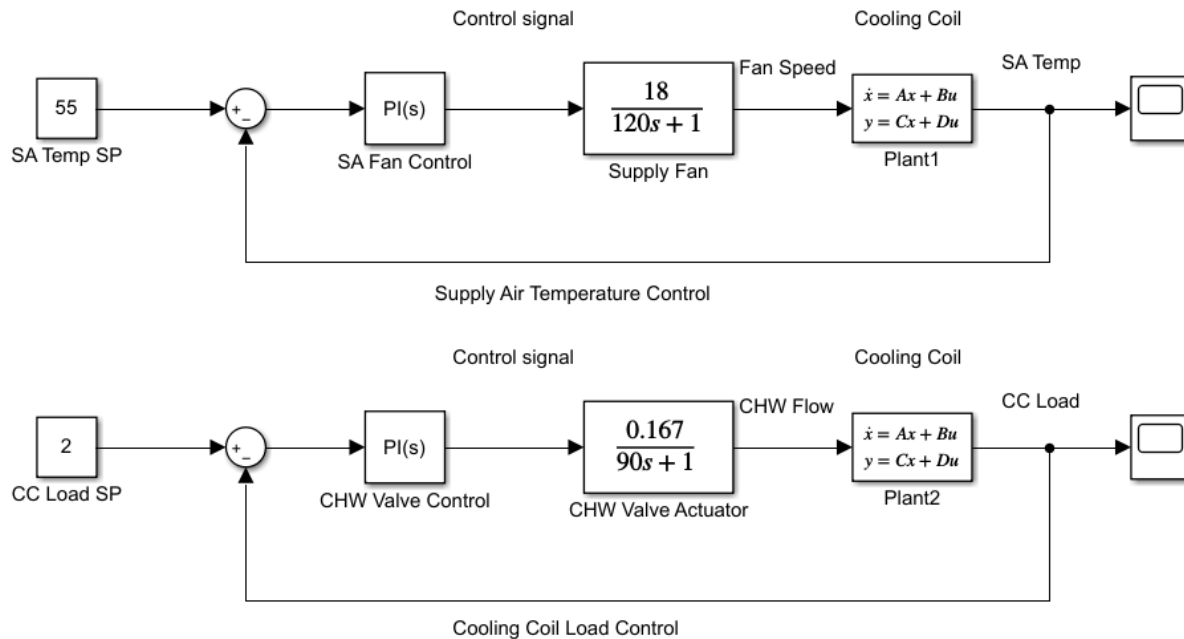


Figure 4-1: EDR Control Sequences

For EDR control, the control sequences in the AHU are adjusted based on the previously discussed strategy. All operations external to the AHU remain the same as during normal operation. This primarily covers the terminal box operation and thermal zone temperature setpoints. The zone temperature setpoints remain constant when EDR control is initiated. During this time, less supply air is available, so the zone temperatures are expected to increase. The terminal box dampers are then expected to open further to offset the zone temperature increase. At some point all terminal boxes will open fully if the cooling coil load is sufficiently limited. Each zone will essentially be fighting for the limited supply air. On a physical system, this behavior may result in zones nearest the AHU receiving the most supply air. The expected system behavior is that the cooling coil load will be controlled precisely, but there will be no way to prioritize the temperature of specific zones.

4.2 Simulation and result analysis

Both methods of cooling coil load management were simulated allowing for direct comparison under more precise operating conditions.

In the simulation, to find suitable setpoints that would offer a fair comparison between control methods, the system was first allowed to operate normally through peak hours. The mean cooling coil load during this time was measured and recorded. Next, the cooling coil load was reduced by some amount, approximately 50% in the experimental case, by implementing EDR control during peak hours in another day. Due to the reduced cooling coil output, all zone temperatures should exceed the respective setpoint. The maximum temperature for each zone during this time was recorded to be used as the new reset setpoint temperature. Each zone reset setpoint will be the maximum temperature from that specific zone. Zone reset setpoints in this scenario will be unique unless conditions result in multiple zones reaching the same maximum temperature.

All simulations were conducted for a simulation time of three days. The simulation begins with time zero equal to midnight. The graphics in this section will highlight the simulation results from Days 2 and 3. At this point, the transient effects due to the initial conditions have settled. The operating conditions at the start of Day 2 are determined by the model and are not user inputs. This is important because a physical system does not just reset at certain points but is dependent on previous conditions.

The simulation conditions are of a hot summer day. The outdoor air temperature follows a sinusoidal pattern with a period of 24 hours to represent a day. The outdoor temperature ranges from 90°F to 110°F. The hottest point in the day is set to occur at 3 PM. This outdoor

temperature can be viewed in Figure 4-2 as the orange line. These outdoor temperatures may not be very common in many locations but using them allows the system behavior to be approximated in extreme conditions. This figure also contains the temperature response of Zone A over the timespan and an indication of the peak hour time. The peak hour time is used to signal when the setpoint will reset. The time of peak hours is from 2PM to 7PM and follows the schedule of Oklahoma Gas and Electric Corp, a local electricity provider. The peak temperature occurs shortly after the onset of peak hours as in real systems.

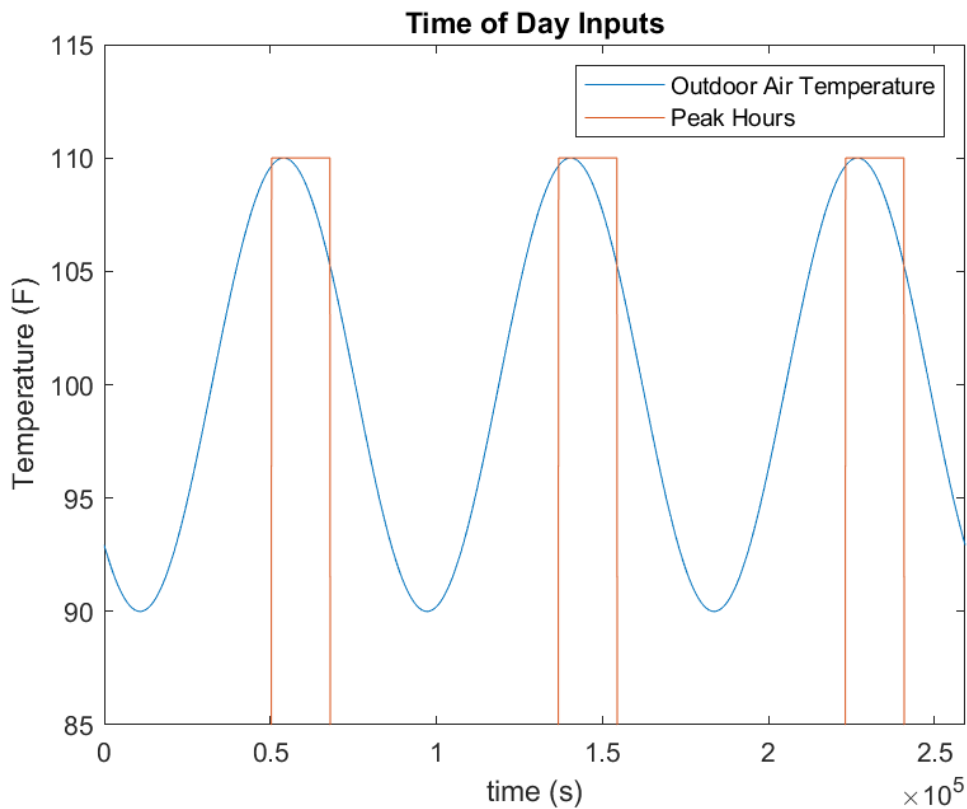


Figure 4-2: Simulation Inputs based on Time of Day

As a reminder, the simulated model consists of three thermal zones with identical thermal envelope structures. To provide slight variety in the system, the maximum flow rate of each terminal box is unique. These flowrate values can be seen in Table 4-1. The temperature dynamics of each zone can be made distinct by providing each zone with its own maximum

flowrate. For example, a zone with a lower maximum flowrate than another and the same terminal box damper dynamics may cool down more slowly after the setpoint reset. This increases the realism of the model as most physical systems have some variations between zones.

Table 4-1: Simulation maximum zone flowrate

| Zone Label | Maximum Supply Air Flowrate |
|-------------------|------------------------------------|
| Zone A | 500 cfm |
| Zone B | 600 cfm |
| Zone C | 700 cfm |

An additional constraint was added to the VAV system to increase the accuracy of the behavior of the full model. The supply air entering all thermal zones must be equal to that supplied by the supply air fan. Consider a scenario in which the supply fan is at a partial speed and the thermal zones are each in need of cooling, it is likely that the zones do not receive enough cold air to maintain the desired zone temperature. For example, if each of three zones has an airflow rate setpoint of 500 cfm but the total supply airflow rate is only 750 cfm, then all zones cannot be satisfied. The behavior under these conditions in a physical system would depend on the physics of the airflow and the pressure drop would be affected by numerous parameters such as the air velocity, duct size and material, and distance from the AHU to the zone among other factors.

It is possible for this assumption to be untrue on a physical system for very short time periods (seconds) due to the compressibility of air in the ducts. However, it is reasonable to assume the sum of all zone airflow rates is equal to the supply airflow rate due to the inherently slow dynamics of buildings. Additionally, the air supplied to the zones is only used for heat

transfer. The building pressurization and change in air mass are not considered so those dynamics are irrelevant to the outcomes of this work.

The total zone airflow constraint will be addressed by proportionally distributing the available supply air flow rate from the fan to each zone. First, the total desired airflow rate is calculated using Equation 4.2 as the sum of desired flow rates from all zones. The supply air fan tries to meet this total desired flow rate by using a PI control loop. The air entering a specific zone is based on the proportion of desired airflow for that zone compared to the total desired airflow rate. The modeled zone actually receives this proportion of the available, actual airflow from the fan. The procedure for determining flow rate into each zone is given by the following Equations 4.2-4.4 where $Q_{tot,des}$ is the total desired flowrate for all zones, $Q_{i,des}$ is the desired flow rate for a specific zone i , α_i is the proportion of desired flow rate for zone i to the total, $Q_{tot,act}$ is the total actual flowrate available from the supply air fan, and $Q_{i,act}$ is the actual amount of air entering zone i .

$$Q_{tot,des} = \sum_{i=1}^N Q_{i,des} \quad (4.2)$$

$$\alpha_i = \frac{Q_{i,des}}{Q_{tot,des}} \quad (4.3)$$

$$Q_{i,act} = \alpha * Q_{tot,act} \quad (4.4)$$

The reset temperature setpoints were determined from the EDR control temperature response. The cooling coil load was directly controlled and limited to a lower magnitude for the duration of the peak hours. The peak temperature reached during this time was recorded and used as the reset temperature setpoint. The simulated average cooling coil load during peak

hours and normal operation was found to be 3.1 tons. This is with all zones prioritizing comfort and maintaining the zone temperature at 72°F.

The cooling coil load during EDR control was set to 2 tons. This is approximately 65% of the mean cooling coil load throughout normal operation peak hours. The EDR control temperature of all zones is given by Figure 4-3. It can be noted that the temperature response of each zone is unique as a result of the distinct maximum airflow rates. Since the airflow allowed into each zone is determined proportionally, it follows that the zone with the largest maximum flowrate will remain the most comfortable. This can be seen with the temperature of Zone C maintained closest to the setpoint and Zone A being the least effective.

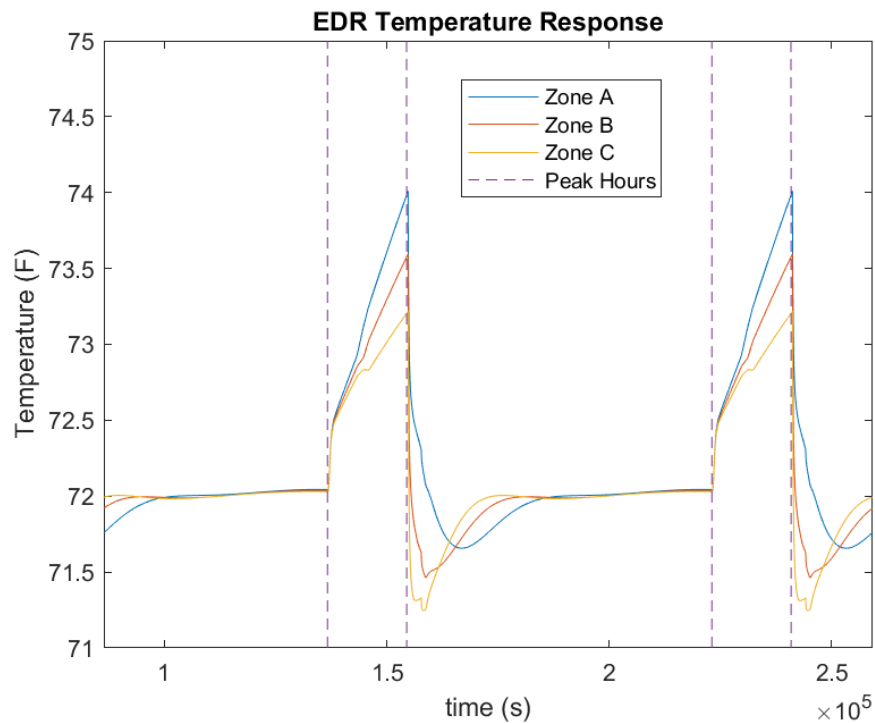


Figure 4-3: Energy Demand Response Simulation Temperatures

Again, the maximum temperature reached for each zone during this time will be used for the setpoint reset temperature. The new setpoint for each zone is given in Table 4-2.

Table 4-2: Simulation Zone Temperature Setpoints

| Zone Label | Normal Temperature Setpoint | Reset Temperature Setpoint |
|------------|-----------------------------|----------------------------|
| Zone A | 72.0 °F | 74.0 °F |
| Zone B | 72.0 °F | 73.6 °F |
| Zone C | 72.0 °F | 73.2 °F |

The system under each operating condition begins with all zone temperature setpoints at the normal operating value of 72°F. During peak hours of setpoint reset operation, the setpoint of each zone is reset to its respective value. From Figure 4-4, it can be seen that the zone temperature follows the setpoint as desired.

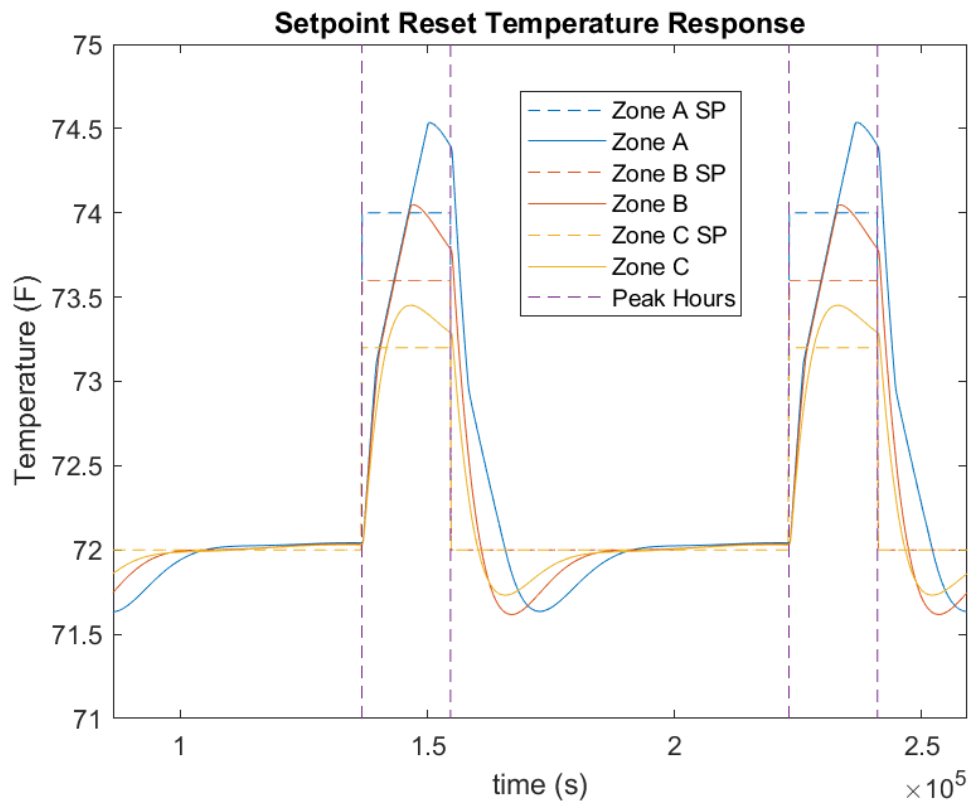


Figure 4-4: Setpoint Reset Simulation Temperatures

The zone temperature reaches the setpoint if sufficient time is given after a disturbance. When the setpoint increases, the zone temperature takes some time to reach the new setpoint. The temperature overshoots the setpoint by a small amount due to the slow dynamics of the

damper and system. When the setpoint is increased, the damper will slowly close allowing the temperature to increase. Once the new setpoint is reached, it takes time for the damper to open up and increase the flow rate again. The setpoint is reverted to the original value at the end of peak hours. At this point, the system slightly overcools the zone. This is again caused by the slow dynamics of the system.

The temperature response of both methods compared in Figure 4-5, which includes the temperature response of Zones A and C over the simulated time. Zone B was excluded to reduce clutter.

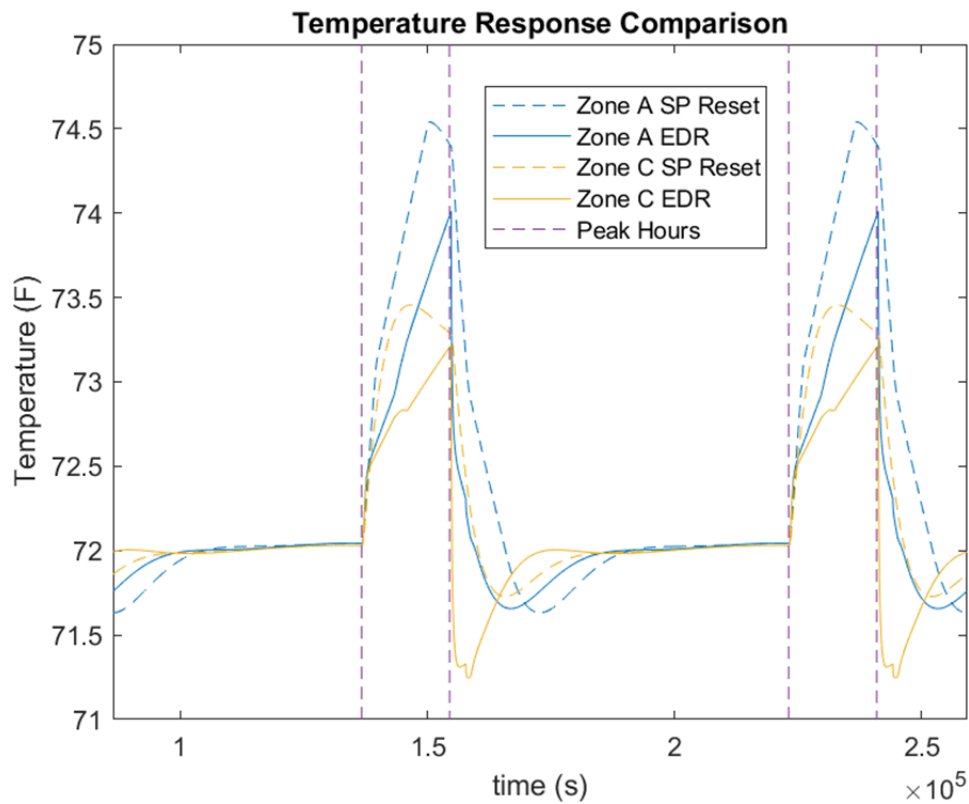


Figure 4-5: Setpoint Reset, EDR Temperature Comparison

The temperature of each zone increases quickly at the onset of peak hours for all control methods. The temperature is then maintained if and when the zone temperatures reach the reset setpoint during that operation. The temperature seems to increase at a steadier rate during EDR

control. This is because each zone desires an increased flowrate, where the flowrate changes in the SP reset operation. The temperature responses of all zones meet expectations with the SP reset having more control over the compromised temperature. One noteworthy behavior is that zones overcool by some amount when the control is released back to normal operation. This is especially prominent in Zone C with EDR control. This behavior is caused by the high flow setpoint to maintain the temperature at the setpoint of 72°F. Once the EDR control is released and the supply air fan output increases, the zone will receive the maximum allowable air flow and result in that overcooling. The desired and actual flowrates into the zones can be seen in Figure A- 1 and Figure A- 2 in the Appendix.

The cooling coil load is the main consideration of these strategies along with the temperature responses. There are multiple factors of the load that must be considered. First, is the load maintained to acceptable levels during peak hours? Is the peak load acceptable? The cooling coil load for both control methods is given by Figure 4-6.

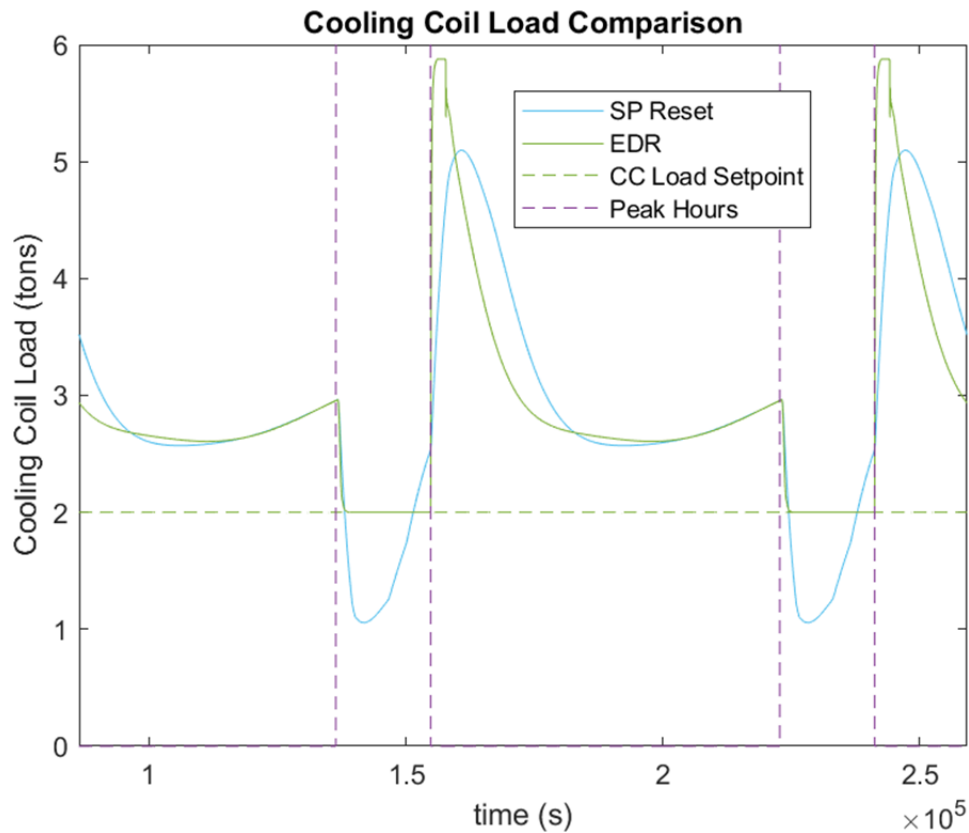


Figure 4-6: SP Reset, EDR Cooling Coil Load Comparison

Due to the varying setpoints of all thermal zones and other system dynamics, it is expected that the cooling coil load will not be constant. It will also not be a smooth transition between operating conditions. The abrupt setpoint adjustments will cause sharp changes in cooling coil load, and EDR control is expected to quickly take control of the load. During peak hours of the setpoint reset, the cooling coil load drops dramatically to 1.06 tons. However, the load does not remain below the desired maximum setpoint of 2 tons. The cooling coil load reaches 2.54 tons by the end of peak hours. This may not seem like much of a difference but could be critical in some circumstance. The excess load could also increase drastically if the outdoor air temperature increases or internal gains change, requiring more airflow into a zone. After peak hours end, the cooling coil load increases to 5.10 tons as all zones are cooled back to the normal setpoint. The supply air flowrate may reach its maximum during this period. This

behavior may be acceptable as the peak does occur after peak hours. Some variation in the cooling coil load throughout the day can also be noted. This can be explained by the outdoor air temperature. The outdoor air temperature is reduced at night, resulting in less heat transfer through the envelope and less airflow required.

The cooling coil load during EDR control is precisely controlled at 2 tons for the duration of peak hours. The most notable cooling coil load behavior is the large peak after peak hours when normal operation is reinstated. The cooling coil load reaches a peak of 5.9 tons. The cause of this is the same as the cause of the zone overcooling in these conditions. When EDR operation ends, the supply airflow rate increases because of the fan speed increasing, but the terminal box cannot close fast enough to prevent over supplying the air and overcooling the zone. During normal operation, the cooling coil loads of both control methods are similar as expected.

Both the setpoint reset and EDR control are valid means in reducing the cooling coil load for a period of time based on the simulation. The simulation environment is very useful for testing a variety of scenarios but will also result in some simplifications that may not be indicative of the physical system. For this reason, these control strategies are also verified through experimentation.

4.3 Experimental result comparison

The load control strategy experiments were conducted on the Engineering Laboratory Building. All experimental tests were conducted on days with similar operating conditions. The tests were conducted during the summer so that cooling operation would be guaranteed. Summer is a low occupancy period for this building, which will reduce unmeasured environmental impacts. People will not be entering and exiting zones causing shifts in the internal

gains. The temperature dynamics of the zones will be fairly predictable and primarily affected by the outdoor air temperature and the HVAC operation.

The new zone temperature setpoint values were determined in conjunction with the Energy Demand Response Control test. In that test, the cooling coil load was limited and allowed to run for two hours. the maximum zone temperature during the time period was recorded for each individual zone. This maximum temperature was used as the new zone temperature setpoint for the experimental setpoint reset test. This procedure was completed to ensure the different control strategies were tested under comparable conditions. The maximum zone temperature is an important factor to hold constant because it is strongly correlated to occupant comfort. The setpoint values for normal operation and during the reset are recorded in Table 4-3.

Table 4-3: Zone Temperature Setpoints for Reset Test

| Zone | Normal Temperature Setpoint | Reset Temperature Setpoint |
|-------------|------------------------------------|-----------------------------------|
| A | 74 °F | 78.1°F |
| B | 71°F | 73°F |
| C | 72°F | 75.5°F |
| D | 73°F | 74°F |
| E | 70°F | 75.1°F |
| F | 69°F | 76.5°F |
| G | 71°F | 72°F |

The experimental test for zone temperature setpoint resets was started at approximately 3:30 PM. Data was collected while the system was in normal operation as a baseline. The zone temperature setpoints were each set to the new reset temperature setpoints. The system was allowed to operate for 2 hours with higher temperature setpoint values. Each setpoint was then set back to the original value. During this test, the outdoor air temperature ranged between 90-

84 °F. Figure 4-7 is used to indicate the temperature response of all zones in the building and the outdoor air temperature.

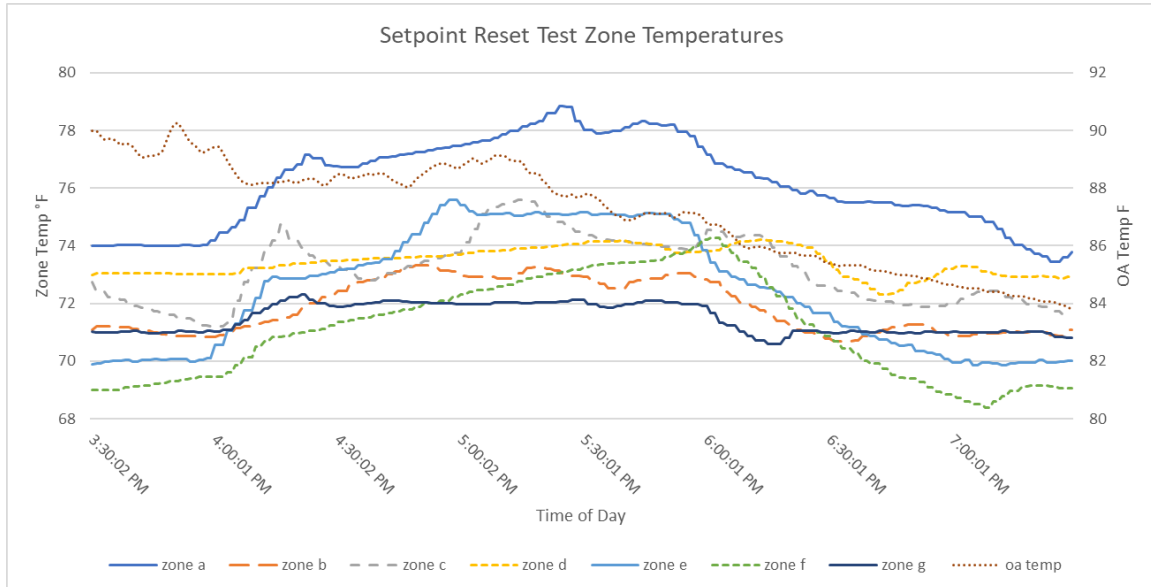


Figure 4-7: Zone Temperature Reset Test

The energy demand response tests were conducted during an afternoon in cooling season to allow for proper comparison to other control strategies. The system was allowed to operate under normal conditions to begin with. EDR control was then initiated for approximately two hours before the system was reverted back to standard operation. The control operation changes were made at the AHU level. All operations downstream of the AHU remained the same, including zone temperature setpoints. The setpoints were held at the starting values because it is often the case that zones have unique setpoints in physical buildings. The setpoints are the same as those given in

Table 4-3.

Energy demand response control was active from 4:08PM to 5:58PM. The cooling coil load was limited to 1.1 tons during this time. this cooling coil load setpoint was determined from

the mean cooling coil load during the setpoint reset test. This provided sufficient time for the zone temperatures to respond. The outdoor air temperature during the test ranged from 90°F to 82°F, which is similar to the outdoor conditions of the setpoint reset test. The temperature response of all zones is shown in Figure 4-8.

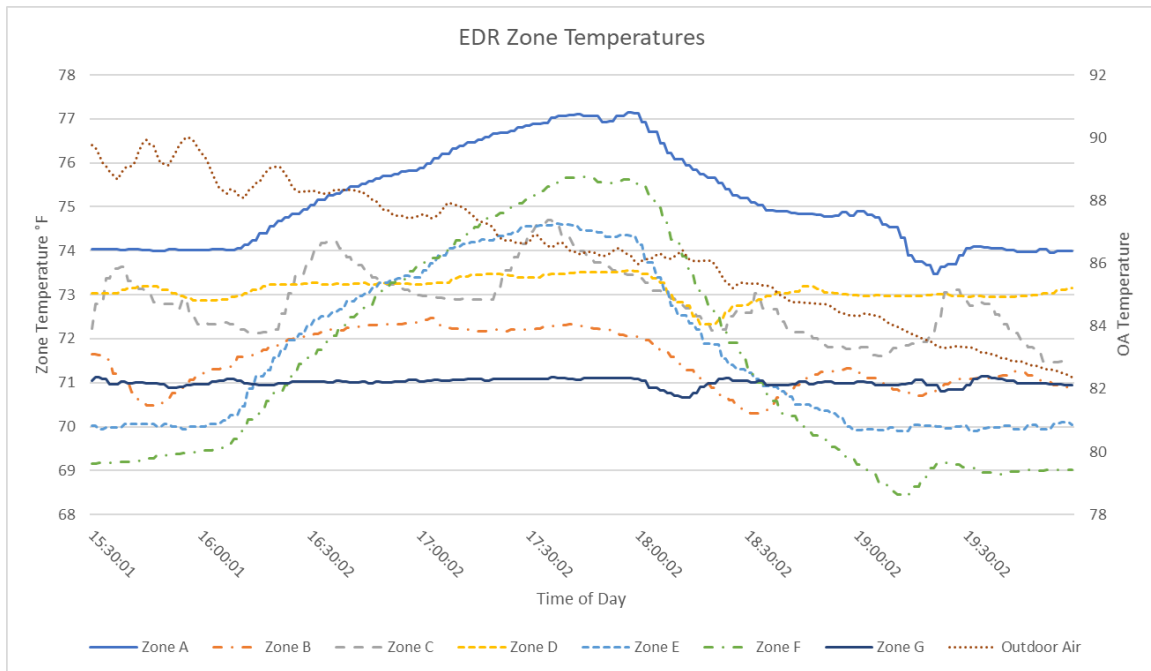


Figure 4-8: Energy Demand Response Control, Experimental Temperature Response

A couple of observations can be made from this temperature response as a sort of reality check. When EDR control is activated, the zone temperatures are expected to increase. This can be seen in almost every zone, with the exception of Zone G. This behavior is not necessarily an error. Zone G does have an exterior wall as shown in the floor plan which would imply heat transfer through the envelope and a rising zone temperature. This is true, but it should also be noted that the exterior windows in Zone G have been removed and closed in. Zone G was also unoccupied during this time. The combination of low heat transfer through the envelope and low or no internal gains allows the temperature to be maintained for the most part. Alternatively,

Zone F could be considered which was also unoccupied during this time. Zone F has a west facing wall with a significant amount of window coverage. This increase in heat transfer into the zone cause the temperature to increase further where other conditions would be the same. overall, the system behaves as expected during this time. when the cooling coil load is forced to reduce, the zone temperatures rise.

Although the load profiles of the EDR test and setpoint reset test were very similar, the temperature responses showed some variation. During the setpoint reset test, most zones reached a higher temperature than during the EDR test, all except for zone F. All maximum zone temperatures for both test methods are recorded in Table 4-4. This observation can be explained by the control methods and slow dynamics of the terminal boxes.

Table 4-4: Maximum zone temperature experimental results

| Zone | Maximum EDR Temperature | Maximum SP Reset Temperature |
|-------------|--------------------------------|-------------------------------------|
| A | 77.1°F | 78.8°F |
| B | 72.5°F | 73.3°F |
| C | 74.7°F | 75.6°F |
| D | 73.5°F | 74.2°F |
| E | 74.6°F | 75.6°F |
| F | 75.7°F | 74.3°F |
| G | 71.2°F | 72.3°F |

When the setpoint is reset, the terminal box dampers will begin to close up so that the new setpoint can be attained. The damper will not open again until the zone temperature exceeds the setpoint. At this point, the cooling rate into the zone is so small that the temperature continues increasing. Alternatively, when EDR control is initiated the supply air flowrate is greatly reduced immediately. This will cause the zone temperature to immediately increase but at a steady rate.

Not all zone temperatures increased at the same rate. Figure 4-9 and Figure 4-10 show the temperature response of Zone E and Zone F, which are representative of all zone behaviors. Figure 4-9 shows the temperature response of Zone F where the temperature during the EDR test exceeds the temperature of the setpoint reset. The temperature response of Zone E is given by Figure 4-10. In Zone E, the setpoint reset temperature exceeds the temperature reached during the EDR test. These temperature responses indicate that each load control type may not result in the exact same behavior, even if the test conditions are very similar.

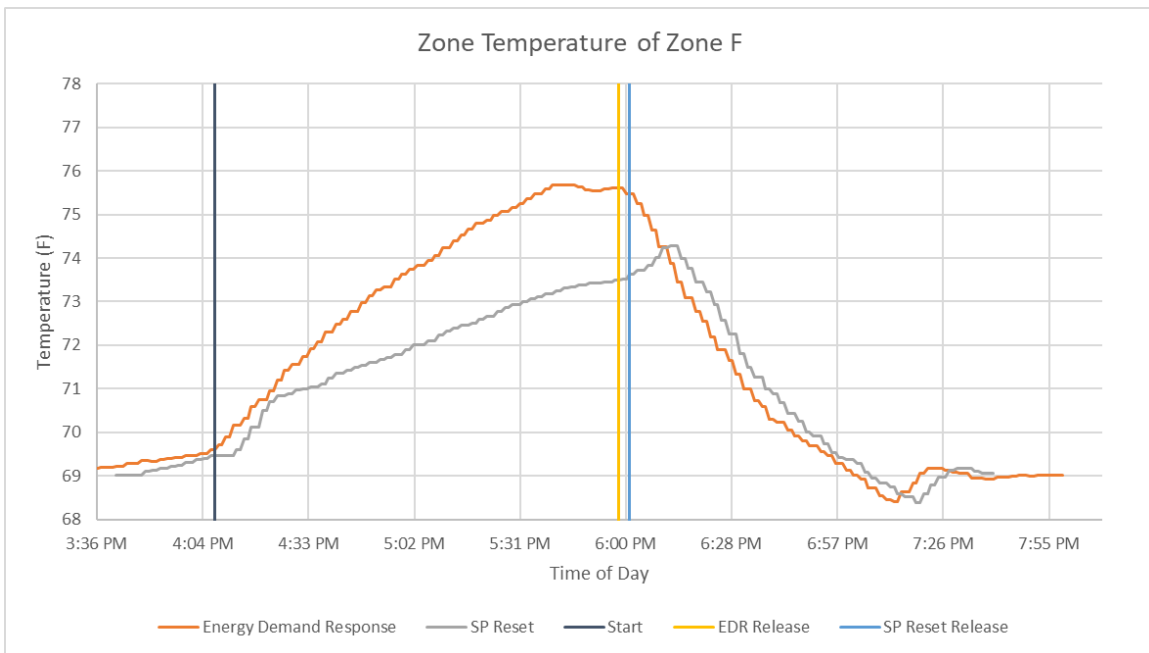


Figure 4-9: EDR and Setpoint Reset Temperature Response Comparison for Zone F

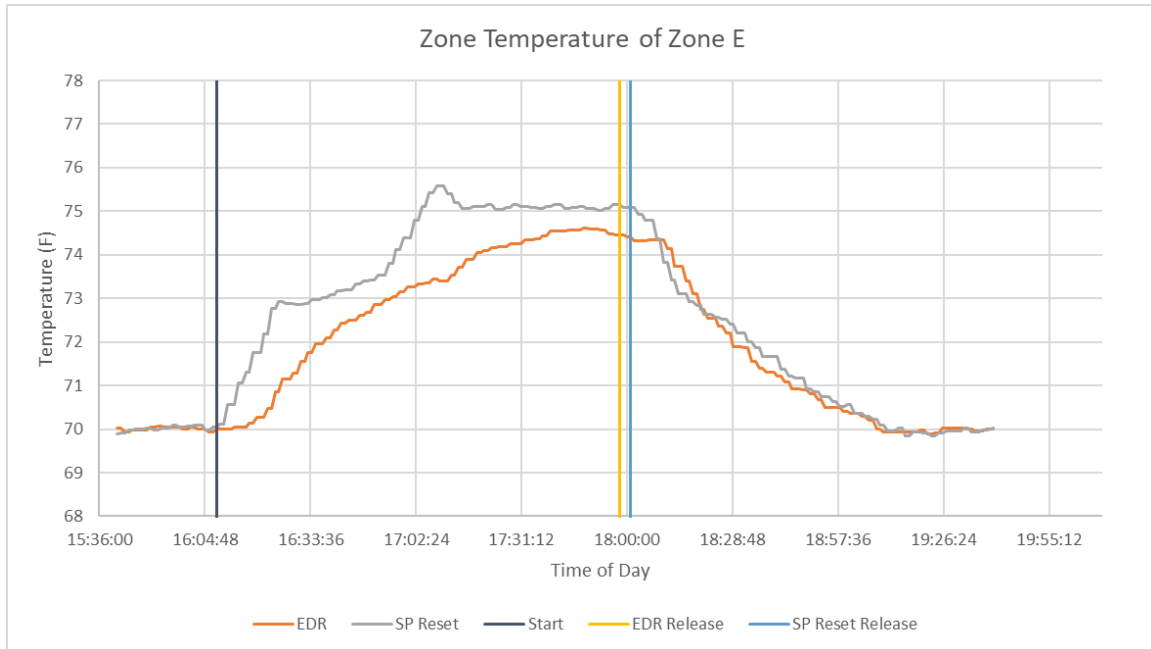


Figure 4-10: EDR and Setpoint Reset Temperature Response Comparison for Zone E

The cooling coil load cannot be directly measured easily in an experimental setup; however, it can be calculated based on parameters that are known. The cooling coil load is based on the total heat transfer rate, not just the sensible heat or just the latent heat. In order to find the total heat transfer rate on the air side, the flowrate and enthalpy difference would be required. This requirement is due to the dehumidification of the air that may occur during wet cooling. The air enthalpy calculation requires additional measurements like the wet bulb temperature. In order to reduce the number of conversions and decrease the complexity, the cooling coil load is calculated based on the chiller water. This can be done based on the chiller water flowrate and the temperature difference between the chiller water entering and exiting the cooling coil. All heat removed from the air must enter the chiller water so the cooling coil load can be simplified because there is no phase change in the chiller water. This relationship is demonstrated in Equation 4.2.

$$\dot{q}_{cc} = \dot{m}_{cw} c_{p,cw} (T_{cw,out} - T_{cw,in}) \quad (4.2)$$

The cooling coil load profile for both sets of experimental tests is given by Figure 4-11. The start time of the EDR test matches that given by the x axis. The SP reset results were shifted slightly so that the start times of both tests are aligned. The desired cooling coil load for these tests was 1.1 tons. This cooling coil load is significantly reduced from normal operation but not so much so that the system is essentially not in operation.

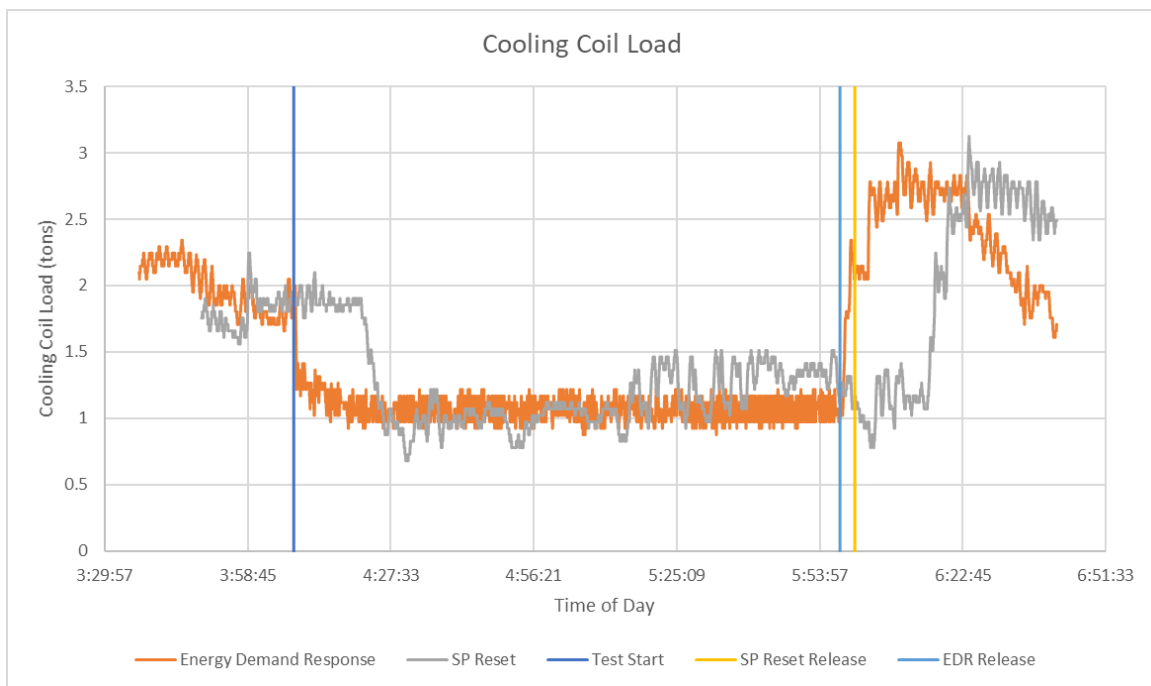


Figure 4-11: Experimental Cooling Coil Load Profile

Based on Figure 4-11, a few notable observations can be made. First, with regards to the SP reset test, it can be seen that after the zone temperature setpoints are increased, the cooling coil load remains unchanged for a period of time. This can be explained by the slow dynamic response of many components in the system. Once the setpoint is reset, the PI loop controlling the temperature will signal the terminal box damper to close. The PI controller may take some time to adjust the output to achieve a sufficient reduction in airflow. Dynamics are also

introduced by the damper actuator which can take as much as five minutes to fully close. The cooling coil load finally begins to reduce as the dampers close and the supply airflow rate reduces. The cooling coil load reduces below 1 ton. From this point to approximately 5:00 PM, the cooling coil load stays near 1 ton with slight variation. This is close to the ideal behavior, where the load is consistent and lower than standard operation. The minimum load is primarily dictated by the minimum supply air flowrate of all terminal boxes. The airflow rate cannot fall below the minimum, so the cooling coil load also approaches a minimum value.

After 5:00 PM, the load begins to increase to above 1 ton. This deviation is a negative behavior of this control strategy; however, it is expected based on the system operating constraints. When the setpoint is reset, the airflow rate for each terminal box will reduce to minimum or near minimum resulting in the smallest cooling coil load. As the zones begin to heat up and reach the reset setpoint, the terminal box dampers will be opened to maintain this new temperature. It can now be observed that a higher zone temperature setpoint does result in a reduced cooling coil load. However, the load is not consistent or precise. It varies from 0.7 tons up to 1.5 tons. This variation could cause issues in some scenarios if the load must be strictly controlled for any reason.

The zone temperature reset strategy does allow for the load to be reduced, significantly so in some circumstances. The major advantage to this method is that the zones can still be prioritized. It was not exactly done in this scenario, but the setpoint values could be chosen to favor the comfort of certain zones. However, a tradeoff of this method is that the cooling coil load cannot be guaranteed. The load drops dramatically directly after the setpoint reset but then

begins to increase before the end of peak hours. The setpoint reset provides a compromise between zone prioritization and precise load control but may not suffice if strict load limits exist.

With respect to the EDR operation, the cooling coil load quickly reaches the cooling coil load setpoint of 1.1 tons. This cooling coil load responds rapidly due to the fact that the system response time for EDR operation is determined primarily by the supply air fan and chiller water valve. Both of these devices have a time constant in terms of seconds where the terminal box time constant is more in terms of minutes. Once the setpoint is reached, the cooling coil load remains at 1.1 ± 0.15 tons. It may be possible to reduce the load variation through different control parameters but is satisfactory for this test. Once EDR control is released, the cooling coil load increases quickly and has a very similar profile to the SP reset results.

The simulated results and the experimental results both offer insights into both the setpoint reset method and EDR control. First, both control strategies result in a reduced cooling coil load. Each strategy also brings about unique tradeoffs. EDR control provides precise load control but does not allow for any prioritization between zones. Resetting the zone setpoints allows for some prioritization between zones but does not allow for precise load control. sometimes the load will be less than desired and will be greater at other times. Now it must be determined if the benefits of both strategies can be achieved simultaneously. How can the cooling coil load be precisely controlled while still prioritizing some zones?

Chapter 5 Integration of Transactive Control and Coordination

There are multiple ways that the lack of prioritization could be addressed, but this would generally mean the load could not be precisely controlled. In order to address this requirement, transactive control and coordination (TCC) was used in conjunction with energy demand response control. TCC is a control strategy that has been developed by Pacific Northwest National Laboratory (PNNL). The foundational idea of TCC is that the entire system acts as a transactive market. To put it very basically, multiple users that desire some commodity will place a bid for that commodity to the market. The market will then distribute the commodity based on the bids and availability. In the case of this work, the commodity will be cooling coil energy or could be taken down further to the amount of cold air supplied by the AHU. This process is done repeatedly in what will be referred to as bid cycles. With each new bid cycle, a new bid is placed to the market, and the market returns a new cleared amount [41, 42].

5.1 Overview of Transactive Control and Coordination Operation

TCC is used to distribute the resources based on multiple factors including the resource availability, resource demand, and the level to which each user wants or needs the resource. It is important to note that bid price and transactions are do not necessarily require the use or transfer of money. In this work, the bids have not been quantified in terms of monetary cost but are instead based on a more abstract measure of need or desire. For example, a room that has workers may need more cool air than an empty conference room.

TCC markets utilizes two-way communication between multiple agents that each act on their own behalf and communicate with the market agent. The most basic TCC system will consist of multiple bidding agents and a single market agent. This simple market as an air market can be

seen in Figure 5-1. Each VAV agent acts as a bidding agent with the Air Market as the market agent. The VAV agents must submit a bid price and a bid quantity to the market. The bid price could be a monetary amount or the severity of need for the device that the agent represents. A zone that is either more important or less comfortable may have a greater need than other zones. The bid quantity will be the amount of energy or cool air that the agent is requesting. For example, an agent representing a large thermal zone may require more cool air just to maintain the temperature. The market agent will create a demand curve from all bids and a market curve from the cost and benefit of using the cool air. Finally, the market agent produces a clear price from both curves which is then sent to all bidding agents. Once the bidding cycle completes, the process will be repeated [41, 42].

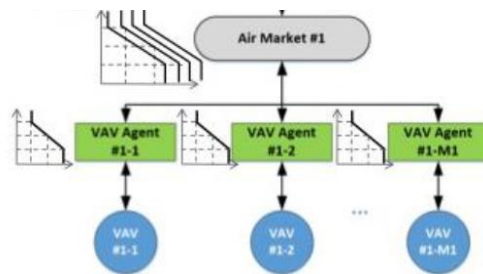


Figure 5-1: Illustration of single commodity market inside a commercial building [41]

TCC markets can be made in varying degrees of complexity. There may even be multiple market agents. These market agents may be in the same level bidding for the same resource or in different levels. Market agents may also need to act as bidding agents in complex systems with multiple levels of resource distribution. An example of a complex transactive market for a commercial building (or buildings) is shown in Figure 5-2. The resource used in a specific layer is given on the left side of the figure from air to cooling energy (BTU) to electricity. In this set up, there are multiple AHUs. Each AHU acts as a market for all zones that are served by that specific

AHU. Each AHU then bids for an amount of chilled water from the chiller that serves it. All chillers and electricity consuming devices bid for electricity from the top-level electricity market [41].

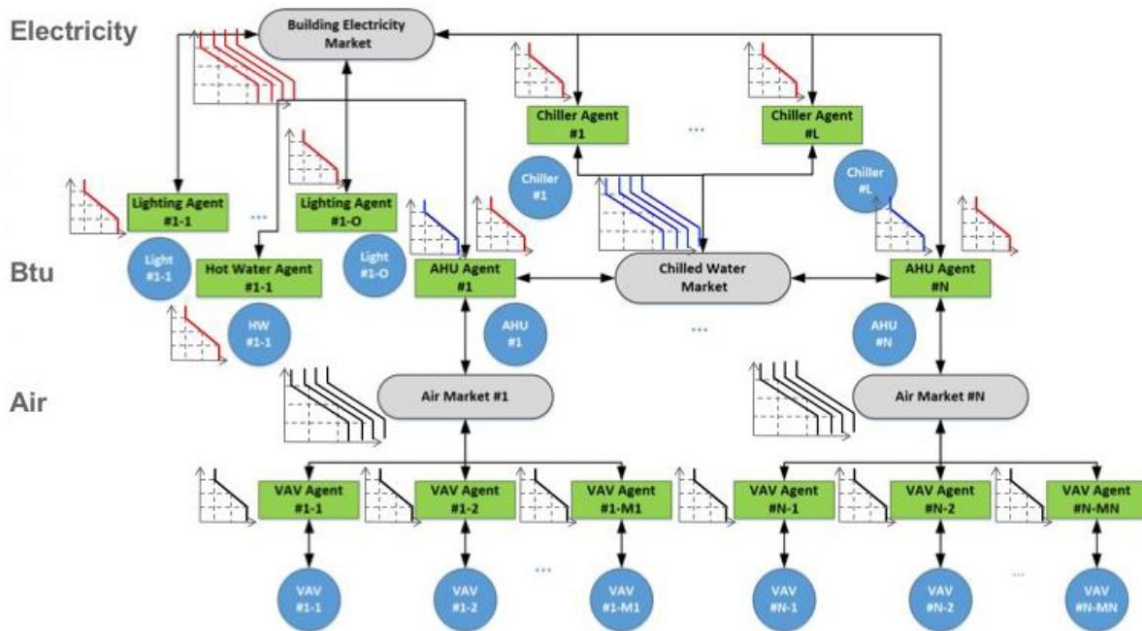


Figure 5-2: Illustration of multiple commodity markets inside a commercial building [41]

5.2 Application of TCC in EDR Control

In order for a simple TCC system with a single market to work for the EDR operation, there must be a strategy to determine the bid price, the bid quantity, and a cleared amount for each zone to use. The bidding agents for this work each represent a thermal zone.

5.2.1 Bid Pricing

The bid price strategy will be introduced first. The bid price is tied to the need of that bid agent so a zone with a greater need will submit a larger bid price. The need in this work is based solely on the zone temperature which could be correlated to occupant comfort levels. No zones are inherently more important than the others. There is not a way to directly quantify human comfort, but generalizations can be made for the sake of determining the bid price. The main

assertion is that during cooling season, the occupants prefer the zone to be cooler. Therefore, if the zone temperature is currently very hot then the occupant will be willing to bid a higher amount. A low zone temperature would indicate that the occupants are satisfied+ The bid determined from a linear curve made from acceptable comfort conditions of that zone and allowable bidding range [42, 43]. This bid price curve is given by Figure 5-3.

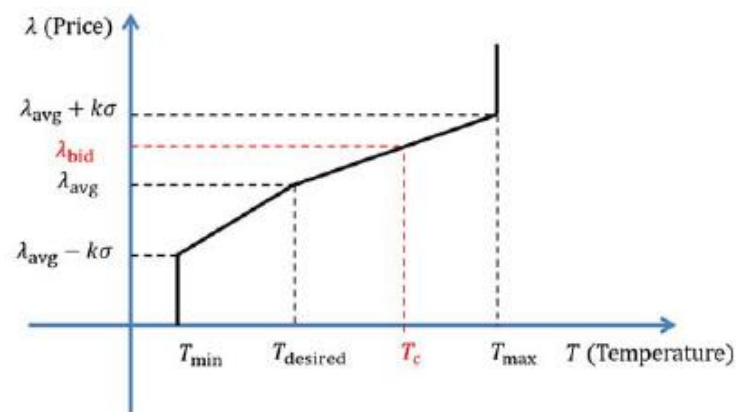


Figure 5-3: Bid Price Curve [42]

Table 5-1:TCC Bidding Parameters

| Parameter | Definition |
|-----------------|--|
| T_{min} | Minimum allowable zone temperature |
| T_{max} | Maximum allowable zone temperature |
| $T_{desired}$ | Desired zone temperature |
| T_c | Current zone temperature |
| λ_{avg} | Average historical bid Price |
| σ | Standard deviation of historical bid price |
| K | User-defined preference factor |

The temperature points would be set by the user. The minimum and maximum temperatures are the ranges of the comfort conditions for that zone, and $T_{desired}$ is the ideal temperature set by the user. For example, the user may want the zone temperature to be 75°F

but willing to let the zone reach 80°F if necessary. λ_{avg} is the average of historical bid prices sent to the market. The user defined value “K” is an important value defined by the user [42]. This indicates the user’s preference between the desire to reduce energy consumption and to remain as close as possible to the desired set point. A smaller K value will maximize the energy savings. A large K value will maximize the comfort of the zone [41]. Finally, the bid price can be determined with this curve based on the current room temperature. If the current temperature is at or above the maximum comfortable temperature, then that agent will bid its maximum amount. Similarly, the agent will bid the average when the temperature is at the desired condition.

This method was simulated using the existing EDR model while trying to maintain the zones at the setpoint of 72°F. The comfort bounds are set at 68°F and 78°F. The average bid price was assumed to be 10 with the variation due to user preference and standard deviation at ± 5 . The cooling coil load is limited to 2 tons during peak hours. The zone temperature and calculated bid price are given in Figure 5-4. From this figure, it can be seen that the bid price increases as the zone temperature increases above the desired point as anticipated.

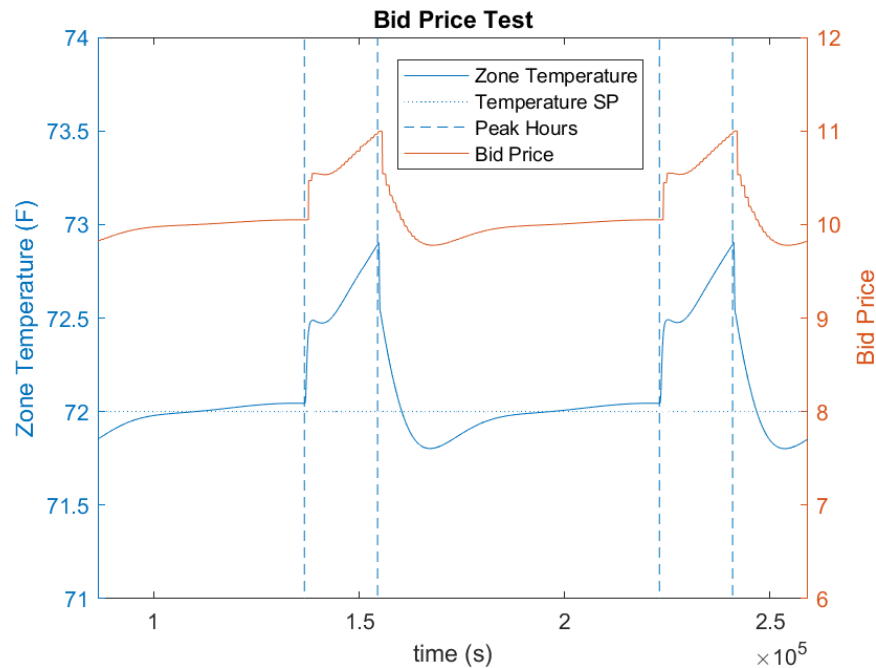


Figure 5-4: Bid Pricing Test

It should be noted that each zone can have its own K value and temperature points. This provides another layer of prioritizing certain zones. An occupied office may need to maintain the temperature between 73-77°F, and a storage room could range between 78-88°F. In this scenario, each room would have its own desired temperature and comfort conditions. Not only are the comfort conditions different, but the range is also unique. One could have the range set at 4°F while the other, less critical one has a range of 10°F. These parameters allow for a variety of methods to prioritize certain zones. Additionally, bid pricing is not an exact method and a range of methods may be used to quantify the bid. The ideal relationship between temperature and bid price may not be linear. However, the method given is sufficient to demonstrate the TCC operation.

5.2.2 Bid Quantity

The bidding agents must submit a bid quantity along with the bid price. The bid quantity is how much of the resource is desired by that zone [42]. In this case the resource is energy from

the cooling coil in BTU. First it is necessary to decide what the quantity of energy must achieve. The energy from the cooling coil will, of course, be used to remove heat from the zones but could be done to different extents. Should the bid quantity only maintain the current temperature? Should it be the energy required to reduce the zone temperature to the minimum comfort condition or the desired temperature? The desired temperature is considered the ideal case, so the bid quantity will be the amount of energy needed for the zone temperature to reach the desired temperature.

There are numerous ways to create a bid quantity in practice. It could be chosen by using machine learning to forecast the needed quantity for the next cycle, but a physics based model would be preferred for this work. A model like the 3R3C building model with the required inputs could be used to estimate the building behavior. However, this would require significant knowledge of the building to find appropriate R and C values. There are ways to predict the R and C values based on measurements from the building dynamics as done by Wang [13]. A true physics based model was not used in the end. The primary reason that this method was not used is that a 3R3C model was already used to represent the building dynamics in the simulation. This could result in an improbably accurate bid quantity calculation. Instead, a new strategy was developed.

The basic foundation of the strategy relies on the assumption that the cooling load of the current bid cycle will be the same as the previous cycle. The new bid quantity consists of two basic parts. First, the new bid quantity must negate the heat gains in the cycle. The next component of the bid quantity is the energy required for the current zone temperature to reach the desired temperature. This strategy was also selected because it utilizes measurements that

are commonly available on physical commercial systems, like the zone temperature and supply air flowrate.

First, the zone can be treated as a control volume. The difference between the heat gains and bid quantity can be determined from the zone temperature error with respect to the desired temperature. Since the gains for the next cycle are not known yet, the gains calculated from the previous cycle are used to determine the bid quantity for the current cycle. This assumption for heat gains between cycles remaining nearly constant holds true for most times. The exception is when internal gains increase dramatically between cycles, but this would be difficult to capture in most models. These relationships can be seen in Equations 5.1 and 5.2, where P indicates an amount of energy in BTU.

$$P_{gain} - P_{bid} = C_a (T_{des} - T_i) \quad (5.1)$$

$$P_{bid} [Btu] = P_{gain} + C_a(T_i - T_{des}) \quad (5.2)$$

The zone heat gains, P_{gain} , are not immediately available. However, it can be calculated by using a technique similar to that used in the 3R3C model. The rate of change of the average zone air temperature can be found from the heat transfer into or out of the zone. This relationship is given by Equation 5.3.

$$C_a \frac{dT_a}{dt} = q_{gain} - q_c \quad (5.3)$$

This allows for the system dynamics to be determined at an instance in time but not for the entire bidding cycle. The system can be integrated with respect to time in order to find the heat gains over a period of time. The temperature change in the zone over the entire bidding cycle is a function of the total amount of heat entering and the total heat exiting the zone during

that time. The temperature difference at the start of the cycle and end of the cycle are known, both in the simulation and on physical systems.

$$C_a(T_{r,i} - T_{r,i-1}) = \sum_{i=t-1}^t q_{gain,i} - \sum_{i=t-1}^t q_{cool,i} \quad (5.4)$$

The heat removed from the zone through cooling is not directly known but is calculable from commonly measured values. It is assumed that heat is removed only through air conditioning. The heat removed through air conditioning can be calculated as a function of the supply air mass flowrate and enthalpy difference of the room air and supply air. These values are not directly measured, but the relationship can be simplified when using only sensible heat. The supply air temperature, room air temperature, and supply air flowrate are all measured. The cooling rate relationship is given in Equation 5.5.

$$q_c = \dot{m}_{sa}(i_{rm} - i_{sa}) \approx Q_{sa}c_{p,sa}\rho_{sa}(T_{rm} - T_{sa}) \quad (5.5)$$

This relationship can then be inserted into Equation 5.4, yielding Equation 5.6. Since the specific heat and density do not change by a large amount, they are assumed to be constant.

$$C_a(T_i - T_{i-1}) = \sum_{i=t-1}^t q_{gain,i} - c_{p,a}\rho_a \sum_{i=t-1}^t (T_{r,i} - T_{sa,i})Q_{sa,i} \quad (5.6)$$

The heat gains into the zone over the bid cycle causing this temperature change is equal to the gains required for the bid quantity calculation. Combining Equations 5.6 and 5.7, gives the relationship Equation 5.8.

$$P_{gain} = \sum_{i=t-1}^t q_{gain,i} \quad (5.7)$$

$$P_{gain} = C_a(T_i - T_{i-1}) + c_{p,a}\rho_a \sum_{i=t-1}^t (T_{r,i} - T_{sa,i})Q_{sa,i} \quad (5.8)$$

Again, the bid quantity consists of the expected heat gains during the cycle and the energy required to reach the desired temperature. The bid quantity as a function of known parameters is given by Equation 5.10.

$$P_{bid} = P_{gain} + C_a(T_i - T_{des}) \quad (5.9)$$

$$P_{bid} = C_a(T_{r,i} - T_{r,i-1}) + C_a(T_{r,i} - T_{des}) + c_{p,a}\rho_a \sum_{i=t-1}^t (T_{r,i} - T_{sa,i})Q_{sa,i} \quad (5.10)$$

The bid quantity in this form consists of three basic parts. First, the new bid quantity must negate the heat gains in the cycle, which is determined by the required amount of cooling in the previous cycle. The bid quantity should be able to negate the rate of change of temperature in the zone. If the zone temperature is rising quickly, then the bid quantity should be increased to prevent the temperature rise. The third component of the bid quantity is the energy required for the zone temperature to reach the desired temperature. Each of these terms contributes to finding an accurate bid quantity.

This method of choosing a bid quantity is not perfect; however, it does show promise when the heat gains between bid cycles change slowly. To improve accuracy, a scheduling parameter could be built into the bidding formula. This would be for times when gains are expected to change significantly between cycles such as an unoccupied period to an occupied period.

This method was tested on a simulated zone operating under normal conditions. The setpoint of the zone was maintained at 72°F with the average outdoor air temperature at 100°F. The zone had an internal gain of 1 Btu/second which was increased to 1.5 Btu/second at the time

150,000s. The bid quantity, actual required energy, and error are given in Figure 5-5. It can be noted that the error remains within 3% after the internal gain disturbance.

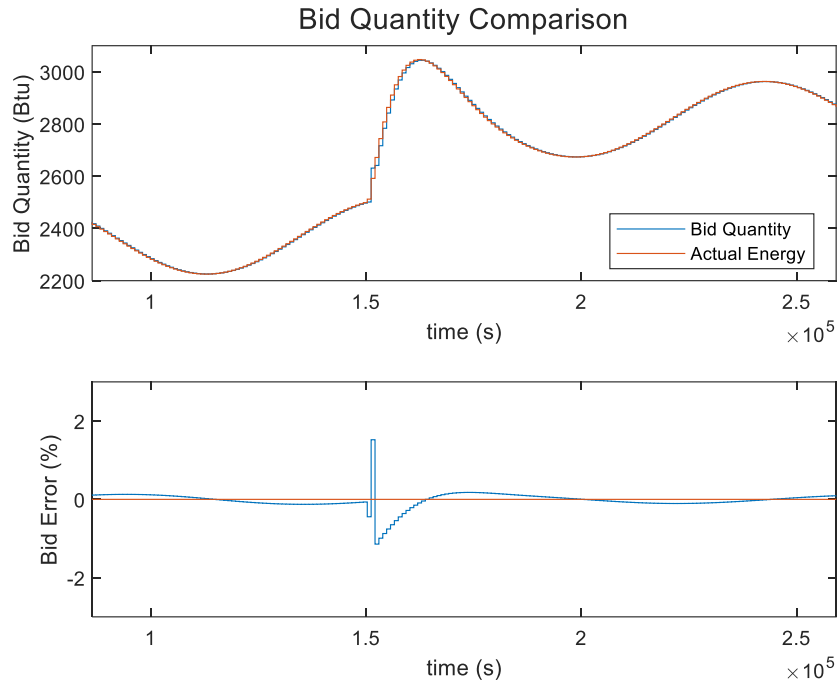


Figure 5-5: Bid Quantity Comparison

This method of determining the bid quantity provides sufficiently accurate results for the TCC market. The bid quantity follows the trend of the required energy to maintain the zone temperature.

5.2.3 TCC Market Agent

The basic operation of the market agent is to take inputs from all of the zones and produces an output that will result in limiting the distribution of the desired resource. The inputs to the market are the bid price and bid quantity from each zone served by that market. The output is what is known as a cleared price for all zones to use.

The market agent must first aggregate the bid prices and bid quantities from all bidding agents. The bid price and bid quantity are treated as pairs, with each pair representing one

bidding agent. The market sorts all bid pairs in terms of decreasing price. This can be seen in Figure 5-6 as the green curve. The y-axis is the bid price, and the x-axis is the resource to be distributed, power in the case of this graph. Bid 1 represents the bid pair with the highest bid price which is shown by the vertical height of the bid. Each succeeding bid pair has a lower bid price. The power of each bid is plotted as the width of the specific bid. The quantity at each bid in the market is the sum of all preceding bids. For example, the quantity of Bid 3 in the market will be the sum of Bids 1, 2, and 3.

λ_{base} and λ_{cap} are the minimum and maximum allowed cleared prices, respectively. P_{uc} is the power of the uncontrollable loads. These are loads that use the resource of the market but whose operation cannot be compromised. If an electricity market is considered, uncontrollable loads could include lighting, computers, or any other required electrical devices. The uncontrollable loads are given a bid price of λ_{cap} because they are treated as a priority by the market. P_{lim} is the maximum power limit that should be allowed by the market.

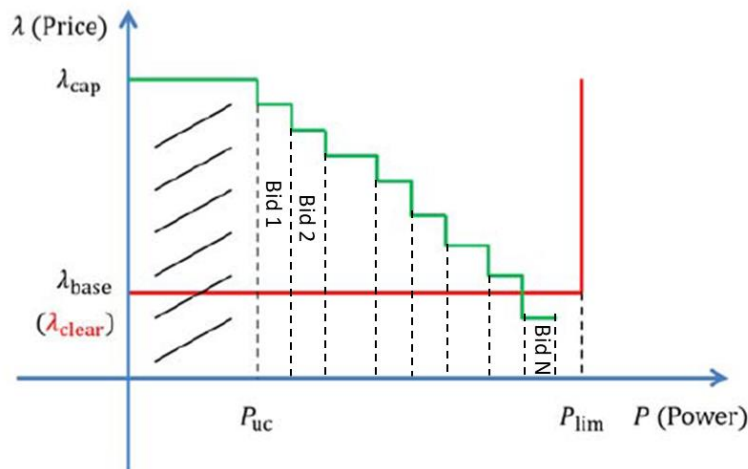


Figure 5-6: TCC Uncongested Sample Market Agent [42]

The power limit P_{lim} is used to create the demand curve, given by the red line. The cleared price is determined by the intersection point of the market curve and demand curve. The market in Figure 5-6 is known as an uncongested market. An uncongested market occurs when the total bid quantities do not exceed the power limit. In this case, the cleared price λ_{clear} will be equal to the base price λ_{base} . An uncongested market will generally only occur when the power is not a concern or when all bidding agents are already satisfied.

The other market condition is known as a congested market. This occurs when the bid quantities exceed the power limit, as shown in Figure 5-7. The cleared price is still the intersection point of the demand and market curves. Now, this intersection point is located above the base price. The cleared price must be between the base price and cap.

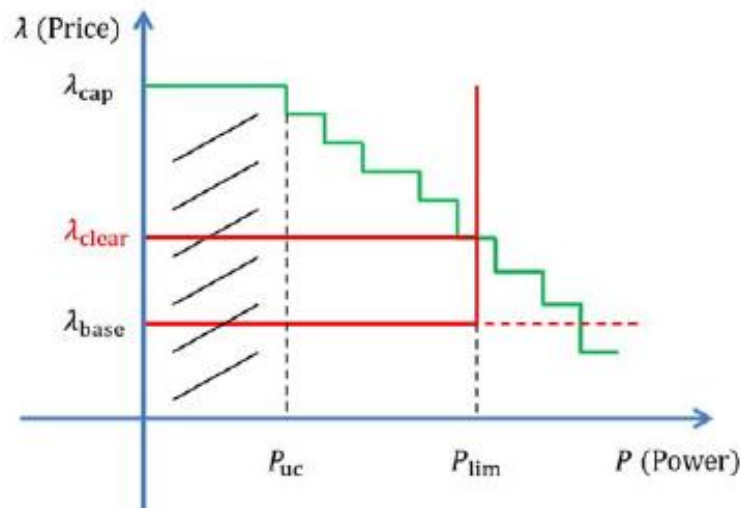


Figure 5-7: TCC Congested Market Agent [42]

Generally, the power limit and cleared price have an inverse relationship. As the power limit decreases, the cleared price increases. The demand curve in this scenario is only indicated by the power limit, but it could be possible to construct the demand curve differently. For example, there may be a quadratic relationship between power and price for the demand curve.

This could be done as complexity increases and multiple markets with different resources are used as in Hao et Al. [44] and Chandra et Al. [45].

5.2.4 TCC Operation

The cleared price is sent to all bidding agents from the market agent. Each bidding agent receives the same cleared price. The bidding agent is responsible for adjusting the resource consumption of its zone or device by using the original bidding curve.

The bidding agent takes in the cleared price to determine a new setpoint for the next bidding cycle. This operation can be seen in Figure 5-8. A higher cleared price will result in a higher setpoint. If the cleared price happens to equal the average historical bid, then the new setpoint will be the desired temperature. If the cleared price is above the maximum, $\lambda_{avg} + k\sigma$, then the new setpoint will be the user defined maximum comfort condition. Additionally, the new setpoint will be the minimum temperature if the cleared price is below $\lambda_{avg} - k\sigma$.

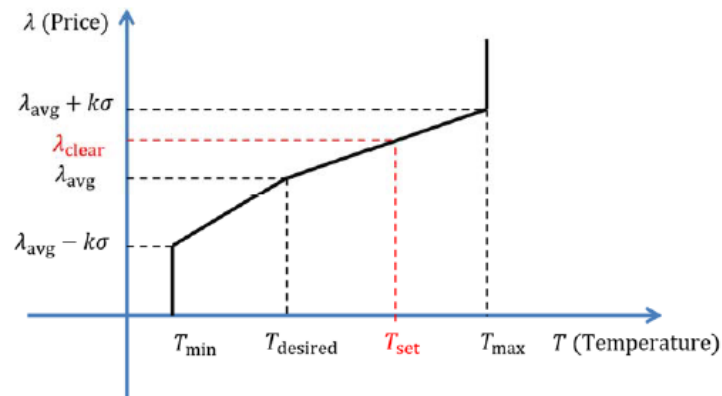


Figure 5-8: Cleared price at bidding agent [42]

As a reminder, the cleared price will increase as the power limit at the market decreases. A higher cleared price will result in higher setpoints for the new cycle at the bidding agent level. The power consumption at the market level (cooling coil) is regulated by adjusting the setpoints

of each of the zones. TCC allows the load to be broadly affected but will not directly control the load as EDR does. This is why TCC is used in conjunction with EDR control. The EDR setpoint and TCC market power limit are set to the same value. EDR control directly controls the cooling coil load and TCC is used to distribute the available cool air.

The TCC market follows a simple sequence of operations. First, all bidding agents produce a bid price and bid quantity. These bids are then all sent to the market agent. The market collects and sorts all of the bids to create a market curve. A demand curve is created in the market agent based on the user specified power limit. The market determines a cleared price from the market and demand curves. Each bidding agent determines a new setpoint from the original bidding curve and the cleared price. This sequence of operation is illustrated in Figure 5-9.

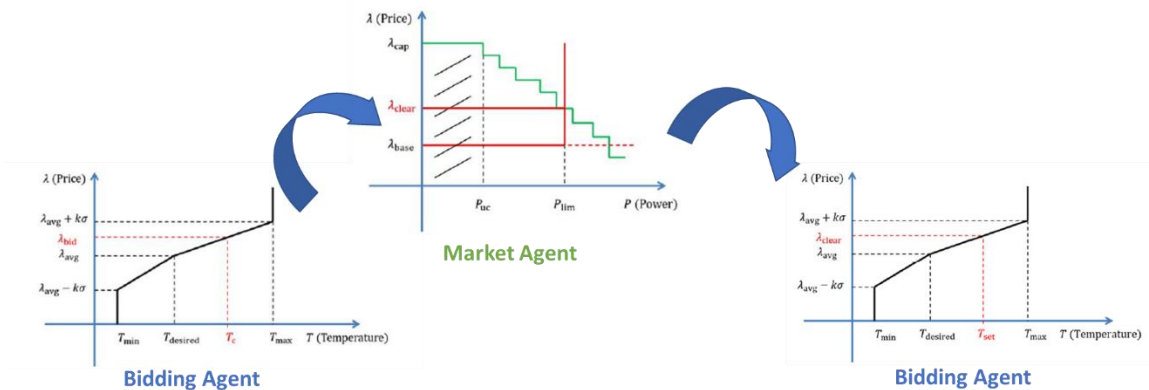


Figure 5-9: TCC Market operation [42]

The final parameter is the bidding cycle time or the amount of time between consecutive bids. This is also the time between setpoint changes in the zones. The bid cycle is defined by the user and can be set at virtually any duration. Changing the bid cycle will not affect the actual sequence of operations, but it can change the behavior of the system. A long bidding cycle time will result in the zone setpoints changing less often and make the system less dynamic overall. A

long bidding cycle time may also increase the accuracy of the bid quantity. Small variations in the zone heat gains would be outweighed by the normal operation during the cycle. However, if there is a large heat gain variation then it could take a considerable amount of time for the bidding agent to increase the bid quantity to an appropriate level. A short bidding cycle will be able to adjust to heat variations more quickly but will also result in a very dynamic setpoint.

5.3 Simulation results of EDR+TCC and EDR Comparison

The desired operation with this control strategy is to precisely control the cooling coil load while giving priority to certain zones. EDR is used for precise control of the cooling coil load. This is combined with TCC to give priority to certain zones. The combination of these two control strategies will be denoted as EDR+TCC.

The system with TCC was simulated under the same conditions as with the previous strategies. The simulation was of a hot summer day with the outdoor air temperature varying between 90-110°F. The temperature setpoint was the same for all zones at 72°F. Each zone has a different maximum supply air flowrate. Zone A has the smallest maximum flowrate at 500 cfm followed by Zones B and C at 600 and 700 cfm.

In order to compare the results to EDR control operation, each zone was given a different priority. Zone A reached the highest temperature in the EDR results, so it was assigned the highest priority. Zone C was assigned the lowest priority. The priority was adjusted through the user defined 'k' value, given in Table 5-2. The user defined comfort conditions were the same for each zone. The desired temperature was 72°F. The acceptable temperature range was between 68-78°F. the historical average bid price was set to 10 with a standard deviation of 0.5.

Table 5-2: TCC Simulation K values

| Location | K |
|----------|---|
| Zone A | 9 |
| Zone B | 6 |
| Zone C | 3 |

The system was allowed to operate normally throughout the simulation except during peak hours. EDR+TCC was enabled at the start of peak hours and disabled at the end of peak hours. The cooling coil load setpoint during peak hours was 2 tons. The bidding cycle time was set to 15 minutes. The temperature response of all zones is given by Figure 5-10.

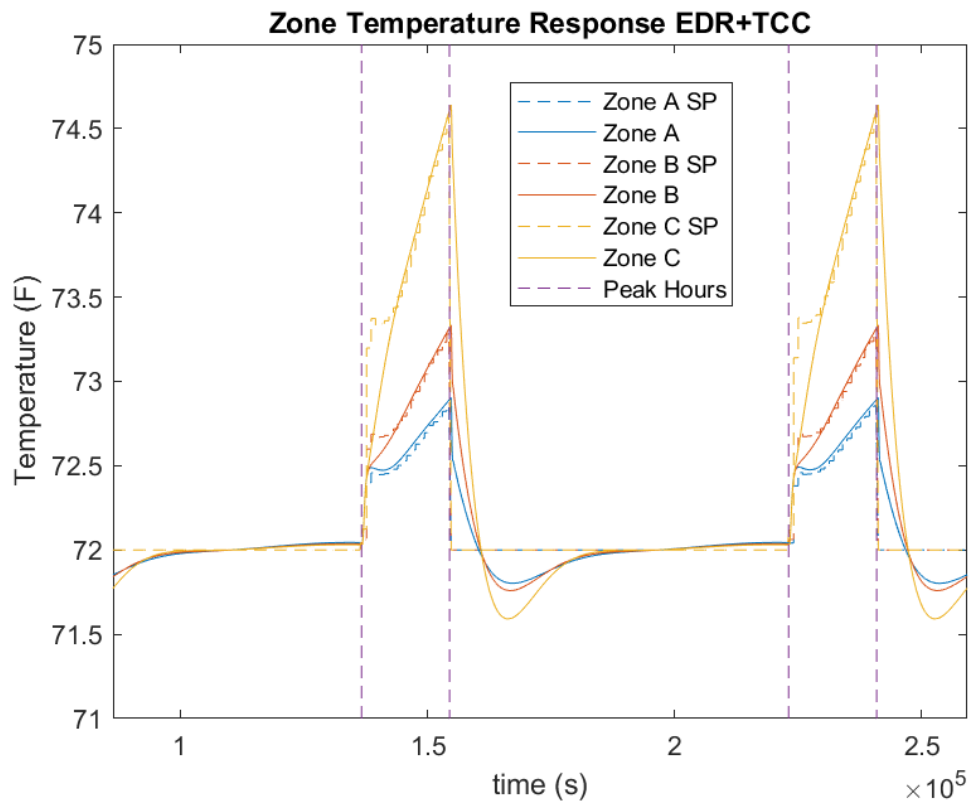


Figure 5-10: EDR+TCC Temperature Response of all Zones

Based on this response, the system appears to behave as desired. The temperature of Zone A is lower than all other zones. Zone C, the lowest priority zone, is warmer than the others. each zone follows the respective setpoint during and out of peak hours. All temperatures being

maintained at the setpoint, even if the setpoint has increased, indicates that the cooling coil load is sufficient. If the cooling coil load were too small then, the temperature would not be maintained. This could happen under the given conditions if the EDR+TCC operating duration was extended.

The temperature response of EDR+TCC is compared to EDR only in Figure 5-11. From this, it can be seen that zone with the smallest available flowrate reaches the highest temperature with EDR control. This behavior is avoided by prioritizing this zone with EDR+TCC operation. Zone C does reach an even higher temperature in this operation, but that is acceptable because the temperature remained within the user-define comfort bounds.

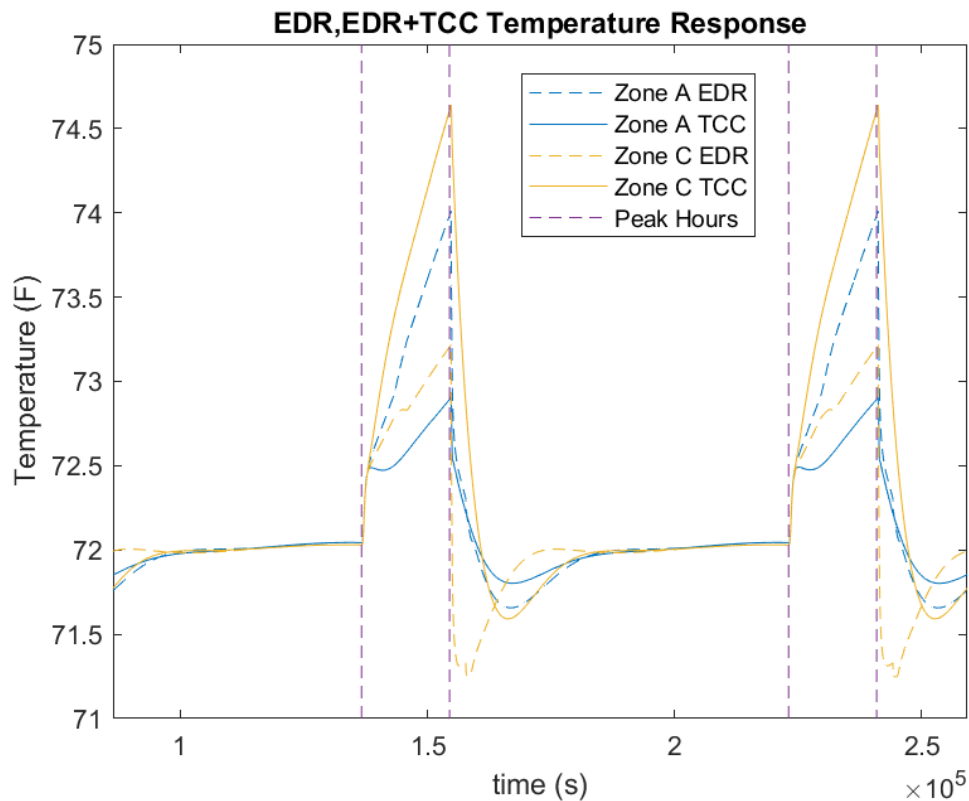


Figure 5-11: EDR+TCC and EDR Temperature Comparison

It can also be seen that the extent of overcooling in EDR is reduced in EDR+TCC operation. This can be explained by the desired supply air flowrate of each zone being regulated by the PI

control loop. During EDR control, the temperature setpoint is held constant even though the temperature is increasing. This temperature error over an extended time results in the supply air flow setpoint increasing to the maximum value. At the end of peak hours, each zone will receive the maximum amount of supply air overcooling the zone and resulting in a large cooling coil load.

During EDR+TCC operation, the supply airflow setpoint is continuously changing to maintain the new temperature setpoint. The supply airflow setpoint will only reach its maximum if the zone temperature cannot be maintained. At the end of peak hours, the zone setpoints will revert from the TCC setpoint back to the desired temperature. The supply airflow setpoint remains within reasonable values because there is not an extended period of temperature error.

The final consideration is the cooling coil load. It is expected to be precisely maintained because EDR control is still in use. The cooling coil load of all three control methods is given by Figure 5-12.

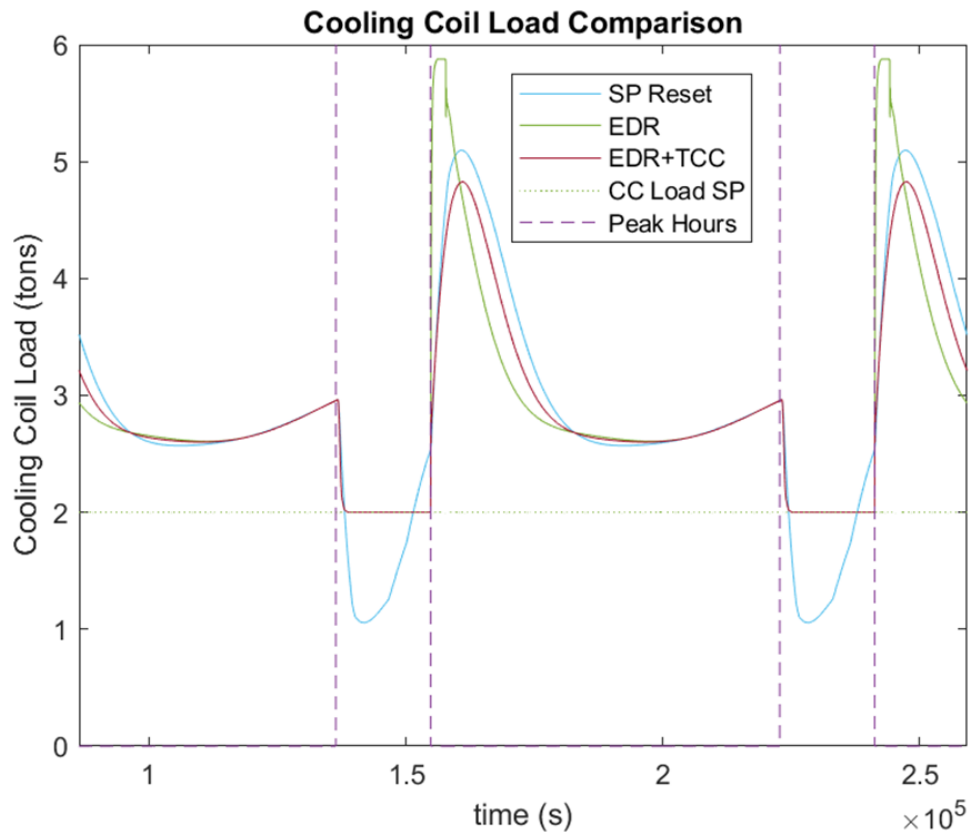


Figure 5-12: EDR+TCC Cooling Coil Load Comparison

All three control strategies result in a reduced cooling coil load while active. EDR+TCC operation results in precisely controlled cooling coil load and a reasonable peak load of 4.8 tons when released. This shows a significant improvement over the peak load of 5.87 tons in EDR control. The load profile of each control method is unique, but the total heat transfer is very similar, as given in Table 5-3.

Table 5-3: 3-day cooling coil load

| Method | 3-Day Cooling Coil Heat Transfer |
|----------|----------------------------------|
| SP Reset | 2.564 MMBTU |
| EDR | 2.596 MMBTU |
| EDR+TCC | 2.581 MMBTU |

EDR+TCC shows the ability to prioritize the temperature of certain zones. It also results in precise control of the cooling coil load. A single test case was covered in this section to highlight

the benefits of EDR+TCC compared to only EDR; however, this only touches the surface of EDR+TCC operation. A series of additional test cases were simulated and included in Chapter 5.4.

5.4 Simulation Results Under Different Scenarios of EDR+TCC Operation

EDR+TCC accomplishes the goals of precise load control and zone prioritization. A simple case is detailed in the previous section where all zones have similar operating and desired conditions. The only distinction between the zones was the prioritization. The given scenario may be very likely to occur with common desired conditions, but TCC offers much more customization. Multiple zones do not need to have the same comfort conditions or desired temperature. One zone could have a desired temperature of 72°F while another is at 68°F. The comfort ranges could also shift or be smaller or larger. For example, the range could be 65-85°F instead of 68-78°F.

The system was simulated under a variety of user preferences to capture a wider range of behaviors. The series of tests are defined in Table 5-4. Table entries are to compare the given parameter between all zones. A table entry of “same” indicates that that parameter is the same for all zones. The priority indicates which zone is prioritized by the use-defined value ‘k’. The tests can be broken down into three categories, show by different colors in Table 5-4. Category 1 has varied maximum supply air flow rates between zones. Category 2 has unique desired temperatures, both during peak hours and normal operation. Category 3 has distinct comfort bands between the zones.

Table 5-4:EDR+TCC Test Conditions

| Parameter Comparison Between Zones | | | | |
|---|------------------------|------------------------|---------------------|--------------------|
| Scenario | T_{des} | Max supply flow | Comfort Band | Priority |
| 1 | same | unique | same | High flow zone |
| 2 | unique | same | same | High temp zone |
| 3 | unique | same | same | Low temp zone |
| 4 | same | same | unique | small comfort band |
| 5 | same | same | unique | large comfort band |
| 6 | same | same | unique | none |

5.4.1 Category 1 – Maximum Supply Airflow Switch from the lowest to highest priority zone

Category 1 is a continuation of the original EDR+TCC test case. Each zone has a different maximum supply air flowrate. All zones have the same desired temperature and comfort band. The cooling coil load during peak hours is limited to 2 tons. The original case prioritized the zone with the lowest flow rate. Scenario 1 prioritizes the zone with the highest flow rate. The pertinent testing conditions are provided in Table 5-5.

Table 5-5: EDR+TCC Category 1 Test Conditions

| | T_{des} | Comfort Band | Max supply flow | K |
|-------------------|------------------------|---------------------|------------------------|----------|
| Original | | | | |
| Zone A | 72°F | 68-78°F | 500 cfm | 9 |
| Zone B | 72°F | 68-78°F | 600 cfm | 6 |
| Zone C | 72°F | 68-78°F | 700 cfm | 3 |
| Scenario 1 | | | | |
| Zone A | 72°F | 68-78°F | 500 cfm | 3 |
| Zone B | 72°F | 68-78°F | 600 cfm | 6 |
| Zone C | 72°F | 68-78°F | 700 cfm | 9 |

A one-day section of both scenarios is given by Figure 5-13. It can be seen that the temperature is maintained lower in whichever zone is prioritized. The temperatures follow a very

similar pattern based on the respective priority level. The highest priority zone is initially maintained well, then increases gradually through the remainder of peak hours. The temperature of the lowest priority zone increases quickly at the onset of peak hours. The zone temperatures of specific priority levels are approximately equal regardless of the maximum supply air flowrate.

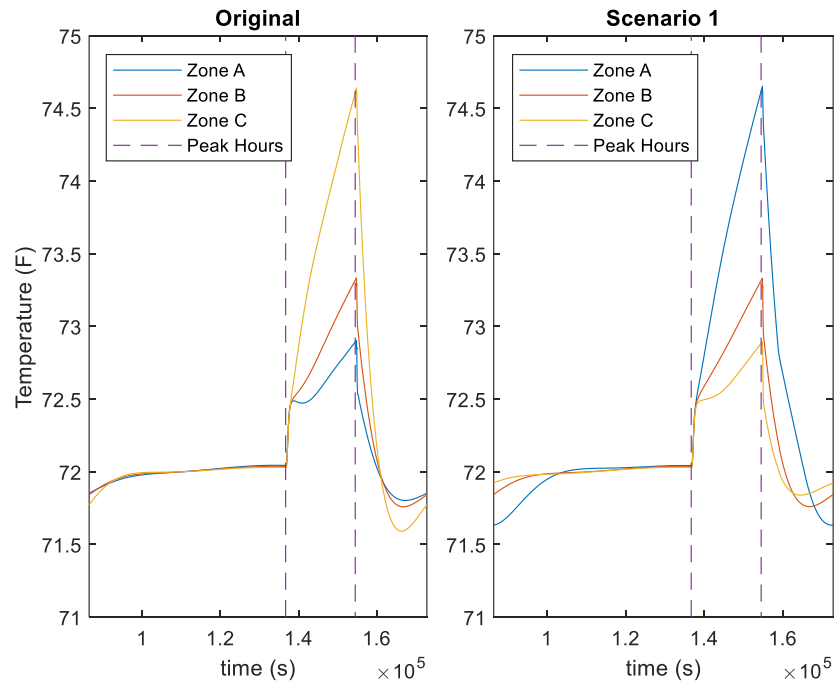


Figure 5-13: EDR+TCC Category 1 Temperature Response

5.4.2 Category 2 – Different Desired Temperature for Different Zones

Category 2 tests were constructed to see the system behavior when each zone has a unique desired temperature. Other conditions were held constant to highlight the effects of assigning unique desired temperatures. The maximum supply air flowrate was adjusted to 600 cfm for each zone. All zones were given the same comfort band size, which was calculated as the desired temperature plus or minus 4°F. There are two considerations for prioritization given these test conditions. The zone with the highest desired temperature could be prioritized, or the

zone with the lowest desired temperature could be prioritized. The pertinent test parameters are provided in Table 5-6.

Table 5-6: EDR+TCC Category 2 Test Conditions

| | $T_{des} \pm$ Comfort Band | K |
|-------------------|----------------------------|---|
| Scenario 2 | | |
| Zone A | 75±4°F | 9 |
| Zone B | 72±4°F | 6 |
| Zone C | 69±4°F | 3 |
| Scenario 3 | | |
| Zone A | 75±4°F | 3 |
| Zone B | 72±4°F | 6 |
| Zone C | 69±4°F | 9 |

The temperature response of all zones for Scenarios 2 and 3 is given in Figure 5-14. The temperature of the highest priority zone remains closest to the respective setpoint floating approximately 1°F regardless of the desired temperature. The lowest priority zone temperature increases by approximately 3°F.

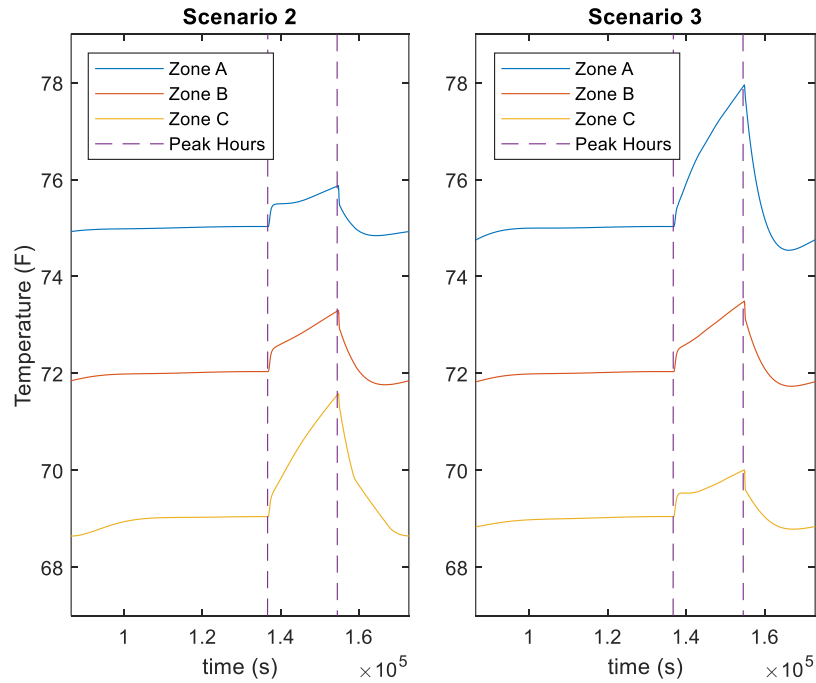


Figure 5-14: EDR+TCC Category 2 Temperature Response

It may appear that the temperature response of a certain priority zone is similar regardless of the desired temperature of the prioritized zone; however, there are small variation between the scenarios. For example, when the low temperature zone is prioritized, other zone temperatures increase by a greater amount than when the higher temperature zone is prioritized. Consider Zone B which has the same priority in each scenario. The temperature float of Zone B reaches 1.3°F when the Zone A is prioritized and 1.5°F when Zone C is prioritized. This result is sensible because it will require more energy to maintain a zone at a low temperature. Important Category 2 results are summarized in Table 5-7.

Table 5-7:EDR+TCC Category 2 Results

| | $T_{des} \pm$ Comfort Band | Peak Temperature | Temperature Float |
|-------------------|----------------------------|------------------|-------------------|
| Scenario 2 | | | |
| Zone A | 75±4°F | 75.9°F | 0.9°F |
| Zone B | 72±4°F | 73.3°F | 1.3°F |
| Zone C | 69±4°F | 71.6°F | 2.6°F |
| Scenario 3 | | | |
| Zone A | 75±4°F | 78.0°F | 3.0°F |
| Zone B | 72±4°F | 73.5°F | 1.5°F |
| Zone C | 69±4°F | 70.0°F | 1.0°F |

5.4.3 Category 3 – Different Comfort Bands for Different Zones

Category 3 tests were constructed to consider the system response if each zone has the same identical temperature but unique comfort band ranges. The desired temperature is at the center of the comfort band. the comfort bands range in size from ±3°F to ±7°F. Other conditions such as the maximum supply air flowrate were held constant. Relevant test parameters are given in Table 5-8.

Table 5-8: EDR+TCC Category 3 Test Conditions

| | $T_{des} \pm$ Comfort Band | K |
|-------------------|----------------------------|---|
| Scenario 4 | | |
| Zone A | 72±3°F | 9 |
| Zone B | 72±5°F | 6 |
| Zone C | 72±7°F | 3 |
| Scenario 5 | | |
| Zone A | 72±3°F | 3 |
| Zone B | 72±5°F | 6 |
| Zone C | 72±7°F | 9 |
| Scenario 6 | | |
| Zone A | 72±3°F | 6 |
| Zone B | 72±5°F | 6 |
| Zone C | 72±7°F | 6 |

Category 3 temperature responses are given by Figure 5-15. The two primary factors that affect a specific zone temperature compared to the other zones are the comfort band size and priority level. Generally, the effects of the comfort band size outweigh the effects of the priority level. Zone A has the smallest comfort band and results in a smaller temperature float than other zones except when it is the lowest priority. Even when Zone A is the lowest priority, the temperature float is very similar to the higher priority zones. The root cause of this behavior can be explained by the bidding curve. If the comfort band is small, then even a slight increase in temperature can significantly impact the bid price. Conversely, a large comfort band causes a zone temperature increase to have low impact on the bid price. Category 3 temperature results are given in

Table 5-9.

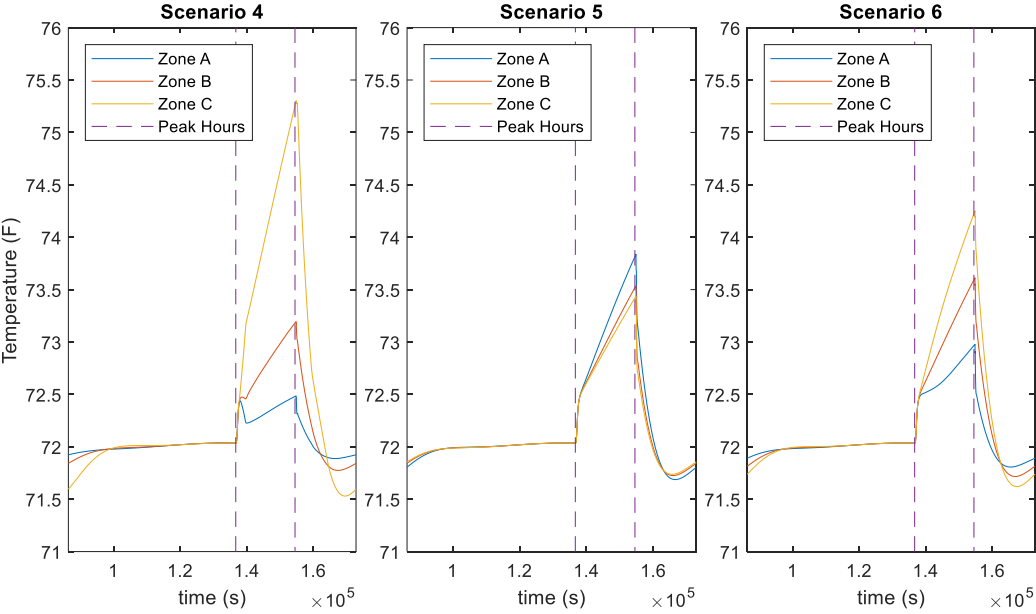


Figure 5-15: EDR+TCC Category 3 Temperature Response

Table 5-9: EDR+TCC Category 3 Results

| | $T_{des} \pm \text{Comfort Band}$ | Peak Temperature | Temperature Float |
|-------------------|-----------------------------------|------------------|-------------------|
| Scenario 4 | | | |
| Zone A | 72±3°F | 72.5°F | 0.5°F |
| Zone B | 72±5°F | 73.2°F | 1.2°F |
| Zone C | 72±7°F | 75.3°F | 3.3°F |
| Scenario 5 | | | |
| Zone A | 72±3°F | 73.8°F | 1.8°F |
| Zone B | 72±5°F | 73.5°F | 1.5°F |
| Zone C | 72±7°F | 73.4°F | 1.4°F |
| Scenario 6 | | | |
| Zone A | 72±3°F | 73.0°F | 1°F |
| Zone B | 72±5°F | 73.6°F | 1.6°F |
| Zone C | 72±7°F | 74.3°F | 2.3°F |

EDR+TCC control offers numerous methods to prioritize certain zones or devices. The scenarios presented in this chapter only cover some of the control conditions that are likely to occur. In practice, combinations of the presented scenarios are likely to occur. The process of choosing appropriate control parameters, like an appropriate comfort band and priority level, presents new topics to study.

Chapter 6 Concluding Remarks

The state-of-the-art method to reduce the cooling coil load is to reset the zone temperature setpoints to a higher value. This method does indeed reduce the cooling coil load but has some undesired behavior. The cooling coil load is not controlled precisely. The transient response results in a sharp cooling load decrease followed by a less intense steady state response. The setpoint reset does allow for some prioritization between zones by adjusting the setpoints individually.

Energy demand response control is able to precisely control the cooling coil load within 0.1 tons (add a percentage would be better too) in the experimental test. The cooling coil load in experimental tests is reduced very quickly compared to the setpoint reset test. This could be very beneficial in scenarios when the load must be reduced immediately such as during a grid emergency. The faster cooling coil load response reduces the need for scheduling in advance. Scheduling is still preferred especially if a precooling strategy is to be used. The main drawback of EDR control is that there is no way to prioritize specific zones. All terminal box dampers will open fully allowing the supply air to be distributed based on physical properties of the system.

Energy Demand Response control combined with Transactive Control and Coordination addresses the deficiencies of the previous control strategies. EDR control precisely controls the cooling coil load, and TCC provides a way to prioritize certain zones. It was noted that the peak cooling coil load upon the control release was reduced from the EDR control response. Transactive control allows the user to specify the desired temperature, an acceptable temperature range for comfort, and a preference between energy savings and cost savings.

6.1 Future Work

The first plan for future work is to integrate a virtual flow meter, as proposed by Song et Al., into EDR control. The virtual flow meter would calculate the chiller water flowrate from values that are measured more commonly. The water flowrate could be determined by the system characteristic curve, the differential pressure across the chiller water control valve, and the valve position [46]. This would eliminate the need to install a physical flow meter and make EDR control implementation easier to roll out.

6.1.1 Scale up EDR+TCC

The implementation of EDR+TCC can be scaled up to a higher system level. EDR+TCC is currently only designed up to the AHU level. This can be taken even further with the creation of additional markets. All AHUs in a building would bid for chilled water from a chiller market. The chiller would bid from the electricity market at the highest level [41, 44]. The AHU would also bid at the electricity market for electric components like the fan. Lower level market limits would calculate the market limit based on the cleared price from upper level markets.

6.1.2 Validate EDR+TCC Experimentally

EDR+TCC control was simulated under numerous conditions but was not validated experimentally. Experimental results would increase trust in the results. EDR+TCC operation was not tested experimentally due to the limitations of the experimental test bed control system. The test bed uses a control system common to commercial HVAC systems which provides a good comparison to actual commercial system, but also has certain drawbacks for research purposes. The system is designed to be cost effective and only needs to meet the basic control needs. The common operations include simple control loops, scheduling, basic mathematics, but it cannot

handle complex calculations and sorting as needed by TCC. The leading idea is to transmit the necessary data from the control system to a secondary device like a raspberry pi. The secondary device would be responsible for performing the calculations of the bidding agents and the market agents. It would then return the new zone temperature setpoints to the building control system. This process would repeat each bidding cycle. The transmission could be accomplished through standard protocols like Lon talk, BACnet, or Modbus.

6.1.3 Investigate Limitations of EDR+TCC

Further work needs to be conducted to investigate the limitations of EDR+TCC. Observations from the simulation provide insights to areas to examine. TCC tends to work better as the number devices or zones increase. This creates a more stable market and makes the system steadier.

TCC only may not sufficiently limit the power if the desired reduction is too great. Once the zones reach the maximum comfort bound, the temperature must be maintained regardless of the load. EDR+TCC will strictly limit the cooling coil load but may not maintain the comfort conditions. This condition could be explored to find which condition should be the top priority.

Successful operation of TCC requires that the market is competitive. The market may become non-competitive if all zones are satisfied. If the zones are satisfied, then the bid prices will be low. A sufficient amount of low bid prices will result in a low clear price. A low clear price will cause low temperature setpoints because of the bidding curve. These low setpoints will then increase the cooling coil load. The market cannot function and results in too high of a load if it is not competitive. Introducing EDR to a sufficient extent forces the market to be competitive because the load is strictly controlled.

The results from this study and areas of future study make energy demand response control, alone and combined with TCC, a promising subject to study further.

References

- [1] U.S Energy Information Administration, "Monthly Energy Review," March 2021. [Online]. Available: <https://www.eia.gov/energyexplained/electricity/use-of-electricity.php#:~:text=Electricity%20is%20an%20essential%20part,machinery%2C%20and%20public%20transportation%20systems>. [Accessed May 2021].
- [2] California ISO, "Flexible Resources Help Renewables - Fast Facts," Folsom, 2016.
- [3] P. Denholm, M. O'Connell , G. Brinkman and J. Jorgenson, "Overgeneration from Solar Energy in California: A Field Guide to the Duck Chart," Golden, CO, 2015.
- [4] California ISO, "CAISO time-of-use periods analysis," 2016.
- [5] OGE Energy Corp., "Smart Hours," [Online]. Available: https://www.oge.com/wps/portal/oge/save-energy/smarthours!/ut/p/z1/IZFNC4JAEIZ_SwevzqQm1m1tY_OgsEK0vYSFrYK6opZ_PyEvQfYxp5nheedlZoBDDLxK7rlulxWSTHUR26eLI1uHA-1LbMPJpK9vWSMLXRmGhCNAK7RNTQPvSEla4v6u6Wto2MA_0vPFG2DxKd0twjo3LV_1ONEEPzVfxLgn8dHwEeL6Qu8Am9W_Gbi. [Accessed 07 2021].
- [6] U.S. Energy Information Administration, "Annual Energy Outlook," February 2021. [Online].
- [7] N. Motegi, M. A. Piette, D. S. Watson, S. Kliccote and P. Xu, "Introduction to Commercial Building Control Strategies and Techniques for Demand Response," Lawrence Berkeley National Laboratory, Berkely, CA, 2007.
- [8] M. Neukomm, V. Nubbe and R. Fares, "Grid-interactive Efficient Buildings Technical Report Series Overview of Research Challenges and Gaps," U.S. Department of Energy Office of Energy Efficiency and Renewable Energy, 2019.
- [9] K.-h. Lee and J. E. Braun, "Reducing Peak Cooling Loads through Model-Based Control of Zone Temperature Setpoints," in *Proceedings of the 2007 American Control Conference*, New York City, NY, 2007.
- [10] M. Cai, S. Ramdasalli, M. Pipattanasomporn, S. Rahman, A. Malekpour and S. Kothandaraman, "Impact of HVAC Set Point Adjustment on Energy Savings and Peak Load Reductions in Buildings," in *2018 IEEE International Smart Cities Conference (ISC2)*, Kansas City, MO, 2018.
- [11] S. Kiliccote, M. A. Piette and D. Hansen, "Advanced Controls and Communications for Demand Response and Energy Efficiency in Commercial Buildings," in *Second Carnegie*

Mellon Conference in Electric Power Systems: Monitoring, Sensing, Software and Its Valuation for the Changing Electric Power Industry, Pittsburgh, PA, 2006.

- [12] R. Yin, E. C. Kara, Y. Li, N. DeForest, K. Wang, T. Yong and M. Stadler, "Quantifying flexibility of commercial and residential loads for demand response using setpoint changes," *Applied Energy*, vol. 177, pp. 149-164, 2016.
- [13] J. Wang, *Design and Analysis of Building Thermal Model for Grid-Interactive Efficient Operations*, Norman, OK: University of Oklahoma, 2020.
- [14] M. M. Hossain, T. Zhang and O. Ardakanian, "Identifying grey-box thermal models with Bayesian neural networks," *Energy and Buildings*, vol. 238, p. 110836, 2021.
- [15] G. P. Henze, G. S. Pavlak, A. R. Florita, R. H. Dodier and A. I. Hirsch, "An Energy Signal Tool for Decision Support in Building Energy Systems," National Renewable Energy Laboratory, Golden, 2014.
- [16] P. Xu , P. Haves, M. A. Piette and J. Braun, "Peak Demand Reduction from Pre-Cooling with Zone Temperature Reset in an Office Building," in *2004 ACEEE Summer Study on Energy Efficiency in Buildings*, Pacific Grove, CA, 2004.
- [17] K. R. Keener and J. E. Braun, "Application of building precooling to reduce peak cooling requirements," in *ASHRAE Transactions*, Philadelphia, PA, 1997.
- [18] J. E. Braun, T. M. Lawrence, C. J. Klaassen and J. M. House, "Demonstration of Load Shifting and Peak Load Reduction with Control of Building Thermal Mass," in *ACCEE Summer Studies on Energy Efficiency in Buildings*, Pacific Grove, 2002.
- [19] E. Biyik and A. Kahraman, "A predictive control strategy for optimal management of peak load, thermal comfort, energy storage and renewables in multi-zone buildings," *Journal of Building Engineering*, vol. 25, p. 100826, 2019.
- [20] J. Wang, C. Y. Tang and L. Song, "Design and analysis of optimal pre-cooling in residential buildings," *Energy and Buildings*, vol. 216, 2020.
- [21] R. Martyr, J. Moriarty and C. Beck, "Optimal control of a commercial building's thermostatic load for off-peak demand response," *Journal of Building Performance Simulation*, vol. 12, no. 5, pp. 580-594, 2019.
- [22] J. E. Braun, "Reducing Energy Costs and Peak Electrical Demand Through Optimal Control of Building Thermal Storage," *ASHRAE Transactions*, vol. 96, no. 2, p. 876, 1990.

- [23] S. Aghniaey and T. M. Lawrence, "The impact of increased cooling setpoint temperature during demand response events on occupant thermal comfort in commercial buildings: A review," *Energy & Buildings*, vol. 173, pp. 19-27, 2018.
- [24] American Society of Heating, Refrigerating, and Air-Conditioning Engineers, Inc., *ANSI/ASHRAE Standard 55-2010 Thermal Environmental Conditions for Human Occupancy*, Atlanta, GA, 2010.
- [25] A. C. Roussac, J. Steinfeld and R. de Dear, "A preliminary evaluation of two strategies for raising indoor air temperature setpoints in office buildings," *Architectural Science Review*, vol. 54, no. 2, pp. 148-156, 2011.
- [26] J. A. Candanedo, V. R. Dehkordi, A. Saberi-Derakhtenjani and A. K. Athienitis, "Near-optimal transition between temperature setpoints for peak loadreduction in small buildings," *Energy and Buildings*, vol. 87, pp. 123-133, 2015.
- [27] F. C. McQuiston, J. D. Parker and J. D. Spitler, *Heating, Ventilation, and Air Conditioning Analysis and Design*, 5th ed., Hoboken, NJ: John Wiley & Sons, 2005.
- [28] K. M. Lunsford, *Increasing Heat Exchanger Performance*, Bryan: Bryan Research and Engineering, Inc., 2006.
- [29] X. Wang, K. Kim, C. Lee and J. Kim, "Prediction of Air Filter Efficiency and Pressure Drop in Air Filtration Media Using a Stochastic Simulation," *Fibers and Polymers*, vol. 9, no. 1, pp. 34-38, 2008.
- [30] N. Nassif , "The impact of air filter pressure drop on the performance of typical air-conditioning systems," *Building Simulations*, vol. 5, pp. 345-350, 2012.
- [31] U.S. Department of Energy, *Guide to Determining Climate Regions by County*, 2015.
- [32] Invensys Building Systems, *Workplace Tech Tool 4.0 Engineering Guide*, Loves Park, IL, 2003.
- [33] O. T. Ogunsola, L. Song and G. Wang, "Development and validation of a time-series model for real-time thermal load estimation," *Energy and Buildings*, vol. 76, pp. 440-449, 2014.
- [34] F. P. Incropera , D. P. Dewitt, T. L. Bergman and S. A. Lavine, *Fundamentals of Heat and Mass Transfer*, 6th ed., Hoboken, NJ: John Wiley & Sons, 2007.
- [35] J. W. Nilsson and S. A. Riedel, *Electric Circuits*, 10 ed., Upper Saddle River, NJ: Pearson, 2015.

- [36] O. T. Ogunsola and L. Song, "Review and Evaluation of Using R-C Thermal Modeling of Cooling Load Prediction for HVAC System Control Purpose," in *Proceedings of the ASME 2012 International Mechanical Engineering Congress & Exposition*, Houston, 2012.
- [37] K. Ogata, *Modern Control Engineering*, 3 ed., Upper Saddle River, NJ: Prentice Hall, 1997.
- [38] American Society of Heating, Refrigeration, and Air-Conditioning Engineers, inc., *ANSI/ASHRAE Standard 62.1-2019 Ventilation for Acceptable Indoor Air Quality*, Atlanta, GA: ASHRAE, 2019.
- [39] X. Zhou, *Dynamic Modeling of Chilled Water Cooling Coils*, West Lafayette, IN: Purdue University, 2005.
- [40] American Society of Refrigeration, Heating, and Air-Conditioning Engineers, Inc., *ANSI/ASHRAE Standard 90.1-2013 Energy Standards for Buildings Except Low-Rise Residential Buildings*, Atlanta, GA: ASHRAE, 2013.
- [41] Brambley, Michael R; Katipamula, Srinivas; Pacific Northwest National Laboratory, "Transactive Control and Coordination for Residential and Commercial Grid-interactive Efficient Buildings," in *2020 Summer Study on Energy Efficiency in Buildings*, 2020.
- [42] J. Lian, L. Marinovici, W. Zhang, K. Kalsi, Y. Sun and S. Widergren, "Part I: Theoretical Underpinnings of Payoff Functions, Control Decisions, Information Privacy, and Solution Concepts," Richland, WA, 2017.
- [43] S. Katipamula, D. P. Chassin, D. D. Hatley, R. G. Pratt and D. J. Hammerstrom, "Transactive Controls: A Market-Based GridWise(TM) Controls for Building Systems," Pacific Northwest National Laboratory, Richland, 2006.
- [44] H. Hao, C. D. Corbin, K. Kalsi and R. G. Pratt, "Transactive Control of Commercial Buildings," *IEEE Transactions on Power Systems*, vol. 32, pp. 774-783, 2017.
- [45] R. Chandra, G. N. B. Yadav and S. K. Panda, "Transactive Control of Air-Conditioning Systems in Buildings for Demand Response," in *2020 IEEE PES Innovative Smart Grid Technologies Europe (ISGT-Europe)*, Virtual, 2020.
- [46] L. Song, G. Wang and M. R. Brambley, "Uncertainty analysis for a virtual flow meter using an air-handling unit chilled water valve," *HVAC&R Research*, vol. 19, pp. 335-345, 2013.

Appendix

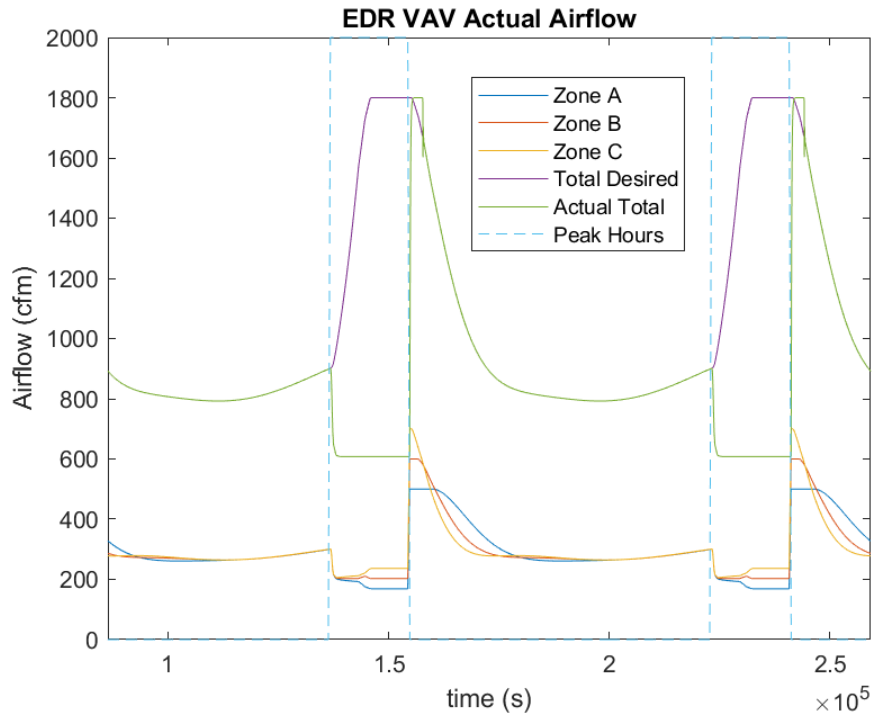


Figure A- 1: Energy Demand Response Actual Airflow

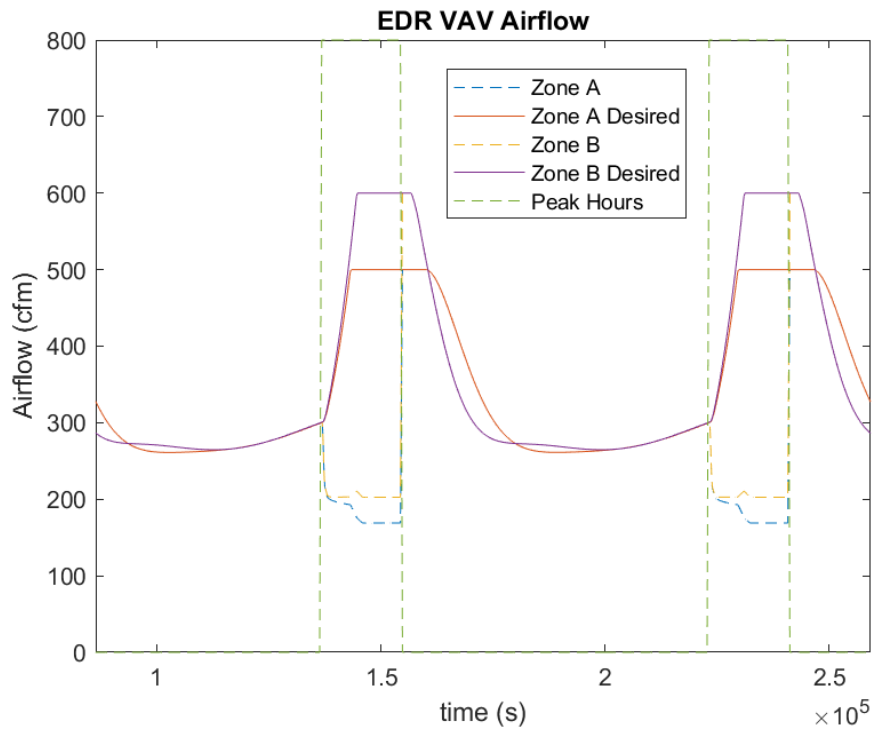


Figure A- 2: Energy Demand Response Airflow Comparison